Retrospective Theses and Dissertations

Iowa State University Capstones, Theses and Dissertations

1982

Kinetic and mechanistic studies of the reactions of selected aliphatic radicals with metal complexes and the decomposition of organoperoxy cobalt complexes

Jwu-Ting Chen
Iowa State University

Follow this and additional works at: https://lib.dr.iastate.edu/rtd

Part of the Inorganic Chemistry Commons

Recommended Citation

Chen, Jwu-Ting, "Kinetic and mechanistic studies of the reactions of selected aliphatic radicals with metal complexes and the decomposition of organoperoxy cobalt complexes " (1982). *Retrospective Theses and Dissertations*. 8337.
https://lib.dr.iastate.edu/rtd/8337

INFORMATION TO USERS

This reproduction was made from a copy of a document sent to us for microfilming. While the most advanced technology has been used to photograph and reproduce this document, the quality of the reproduction is heavily dependent upon the quality of the material submitted.

The following explanation of techniques is provided to help clarify markings or notations which may appear on this reproduction.

1. The sign or "target" for pages apparently lacking from the document photographed is "Missing Page(s)". If it was possible to obtain the missing page(s) or section, they are spliced into the film along with adjacent pages. This may have necessitated cutting through an image and duplicating adjacent pages to assure complete continuity.

2. When an image on the film is obliterated with a round black mark, it is an indication of either blurred copy because of movement during exposure, duplicate copy, or copyrighted materials that should not have been filmed. For blurred pages, a good image of the page can be found in the adjacent frame. If copyrighted materials were deleted, a target note will appear listing the pages in the adjacent frame.

3. When a map, drawing or chart, etc., is part of the material being photographed, a definite method of "sectioning" the material has been followed. It is customary to begin filming at the upper left hand corner of a large sheet and to continue from left to right in equal sections with small overlaps. If necessary, sectioning is continued again—beginning below the first row and continuing on until complete.

4. For illustrations that cannot be satisfactorily reproduced by xerographic means, photographic prints can be purchased at additional cost and inserted into your xerographic copy. These prints are available upon request from the Dissertations Customer Services Department.

5. Some pages in any document may have indistinct print. In all cases the best available copy has been filmed.

.

8307740

Chen, Jwu-Ting

KINETIC AND MECHANISTIC STUDIES OF THE REACTIONS OF
SELECTED ALIPHATIC RADICALS WITH METAL COMPLEXES AND THE
DECOMPOSITION OF ORGANOPEROXY COBALT COMPLEXES

Iowa State University   PH.D.   1982

University
Microfilms
International 300 N. Zeeb Road, Ann Arbor, MI 48106

PLEASE NOTE:

In all cases this material has been filmed in the best possible way from the available copy. Problems encountered with this document have been identified here with a check mark __√__ .

1.   Glossy photographs or pages _____

2.   Colored illustrations, paper or print _____

3.   Photographs with dark background _____

4.   Illustrations are poor copy _____

5.   Pages with black marks, not original copy _____

6.   Print shows through as there is text on both sides of page _____

7.   Indistinct, broken or small print on several pages __✓__

8.   Print exceeds margin requirements _____

9.   Tightly bound copy with print lost in spine _____

10.   Computer printout pages with indistinct print _____

11.   Page(s) _____ lacking when material received, and not available from school or author.

12.   Page(s) _____ seem to be missing in numbering only as text follows.

13.   Two pages numbered _____. Text follows.

14.   Curling and wrinkled pages _____

15.   Other_____

Kinetic and mechanistic studies of the reactions of

selected aliphatic radicals with metal complexes and

the decomposition of organoperoxy cobalt complexes

by

Jwu-Ting Chen

A Dissertation Submitted to the

Graduate Faculty in Partial Fulfillment of the

Requirements for the Degree of

DOCTOR OF PHILOSOPHY

Department: Chemistry
Major: Inorganic Chemistry

Approved:

In Charge of Major Work

For the Major Department

For the Graduate' College

Iowa State University
Ames, Iowa

1982

TABLE OF CONTENTS

GENERAL INTRODUCTION

The increasing usage of transition metal species in homogeneous catalysis in industrial chemical processes has stimulated the growth of the twin fields of organometallic chemistry and catalysis of organic reactions (1, 2, 3). Among the fundamental research interests in these areas has been the investigation of metal-carbon bond reactivity to understand its basic chemistry. The kinetic and mechanistic studies of metal-carbon bond chemistry, therefore, is one of the indispensable aspects. The objective of this dissertation is to study the kinetics and the mechanisms of some reactions pertaining to organochromium and organocobalt complexes and related compounds.

This thesis consists of two independent parts. The first chapter deals with the reactions of selected α-substituted carbon-centered radicals, which are produced by an organochromium complex undergoing homolytic cleavage of its metal-carbon bond, with vanadium(II) ion and with a macrocyclic cobalt(II) complex. The second chapter presents a study of the decomposition of organoperoxycobaloxime complexes in acidic aqueous media; the latter work has been published in 1981 (4).

PART I. REDUCTION OF SELECTED ALIPHATIC RADICALS BY

THE VANADIUM(II) ION AND BY A MACROCYCLIC

COBALT(II) COMPLEX — A KINETIC STUDY

BY A NOVEL METHOD OF CHEMICAL COMPETITION

INTRODUCTION

Background

Organic free radicals have long been considered as important reactive intermediates in organic chemistry. Today, their importance in a variety of metal-catalyzed organic reactions as well as the reactions of organometals is well-recognized (1). Many catalytic reactions undergoing chain processes or homolytic (one-equivalent) pathways rely on these metastable paramagnetic transients for facile reactions. Further interest in the study in organic radicals may be attributed to the increase of chemical sophistication, which makes possible the direct observation, characterization, and even isolation of these transient species of short-life time.

Over the last decade, one of the widely used techniques to generate various aliphatic free radicals has been pulse radiolysis (5). The radiolysis of water caused by impinging a pulse of high-energy electrons onto it can be summarized by Reaction I-1, where

$$4.0\ H_2O \xrightarrow{\quad\quad} 2.6\ e_{aq}^- + 2.6\ \dot{O}H + 0.6\ H\cdot + 2.6H^+ + 0.4\ H_2$$
$$+ 0.7\ H_2O_2 \tag{I-1}$$
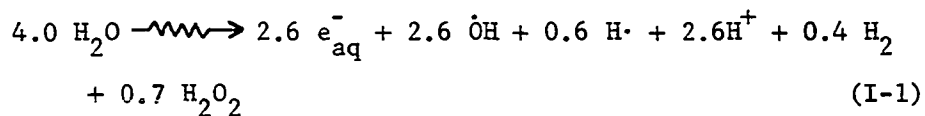
the coefficients express the units of molecules of each species destroyed or formed per 100 eV of energy absorbed by the water, and are called G-values. In nitrous oxide saturated solution, $[N_2O] \sim 2 \times 10^{-2} M$, at pH $\geq$ 3, the hydrated electrons are transformed into hydroxyl radicals in a yield of ca. 90%, and the rest into hydrogen atoms.

$$e_{aq}^- + N_2O \xrightarrow{H^+} N_2 + \cdot OH \quad k = 8.7 \times 10^9 M^{-1}s^{-1} \qquad (I-2)$$

$$e_{aq}^- + H^+ \longrightarrow H\cdot \quad k = 2.3 \times 10^{10}M^{-1}s^{-1} \qquad (I-3)$$
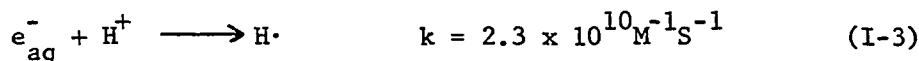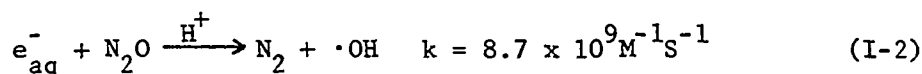
In the presence of the selected organic solutes having at least modest

solubility ($\geq \sim 0.1M$), the generation of particular carbon-centered

radicals may occur via hydrogen atom abstraction from the substrate upon

the reaction with hydroxyl radicals or hydrogen atoms. One example is

the 2-hydroxy-2-propyl radical[1] derived from 2-propanol.

$$(CH_3)_2CHOH + \cdot OH/H\cdot \longrightarrow \cdot C(CH_3)_2OH + H_2O/H_2 \qquad (I-4)$$
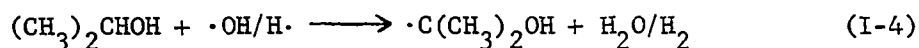
This method produces a "spur" of radical at a concentration, typically

$10^{-5}M$, to permit direct detection. This concentration is high enough

that the radical is largely subject to fast self-reactions, which generally

are dimerization and/or disproportionation. Only the latter one occurs

in the case of $\cdot C(CH_3)_2OH$, however, with the rate constant $1.4 \times 10^9 M^{-1}s^{-1}$

(6).

$$2 \cdot C(CH_3)_2OH \longrightarrow (CH_3)_2CHOH + (CH_3)_2CO \qquad (I-5)$$
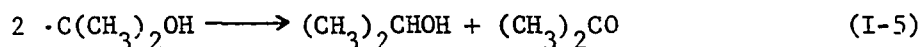
Because this radical is subject to rapid self-reaction, direct kinetic

determinations are limited to substrates which react with it quite

rapidly. In practice, the techniques of radiation chemistry applied

to aliphatic radicals are limited to reactions which have $k > 3 \times 10^6 M^{-1}s^{-1}$

(7).

---

[1]Referred to by Chemical Abstracts as 1-hydroxy-1-methylethyl
radical.

New Application of Organochromium Complexes

With this point in mind, a chemical method was used to provide a ready source of the carbon-centered radical in acidic solution based on the pentaaquo-(organo)chromium(III) cations, $(H_2O)_5CrR^{2+}$, in which R represents alkyls, aralkyls, haloalkyls, hydroxyalkyls, and alkoxyalkyls, etc. This class of complexes has recently been reviewed (8). A particular one shown below, $(H_2O)_5CrC(CH_3)_2OH^{2+}$,
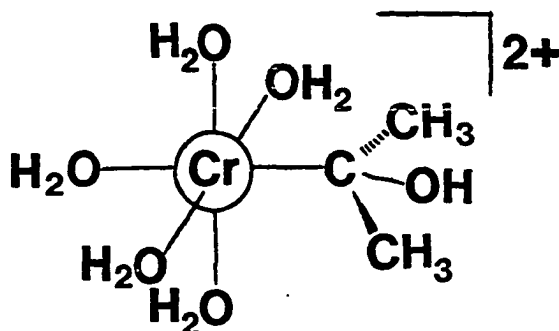
produces the aforementioned 2-hydroxy-2-propyl radical. It is now used for illustrating the chemistry of organochromium complexes, not only because it shows typical behavior in its homologous series, but also because it is the main reagent of this study owing to its unique kinetic character (9).

The $(H_2O)_5CrC(CH_3)_2OH^{2+}$ complex is metastable and is subject to decomposition by two parallel routes simultaneously. One of them, called acidolysis, is a reaction consisting of heterolytic cleavage of the chromium-carbon bond (10).

$$(H_2O)_5CrC(CH_3)_2OH^{2+} + H_3O^+ \longrightarrow Cr(H_2O)_6^{3+} + (CH_3)_2CHOH$$

$$(I-6)$$
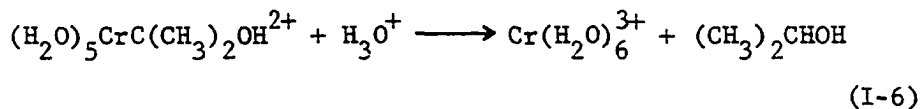
It follows the rate law

$$-\frac{d[CrC(CH_3)_2OH^{2+}]}{dt} = k_A[CrC(CH_3)_2OH^{2+}] \qquad (I-7)$$

with a rate constant k_A given by

$$k_A = k_{1A} + k_{2A}[H^+] \qquad (I-8)$$

where $k_{1A} = (3.31 \pm 0.10) \times 10^{-3}s^{-1}$ and $k_{2A} = (4.91 \pm 0.71) \times 10^{-3}M^{-1}s^{-1}$ at 25.0°C, $\mu = 1.0M$ (7). The acidolysis may be understood as an electrophilic process with the pH-independent pathway occurring by intramolecular proton transfer

$$(H_2O)_5CrC(CH_3)_2OH^{2+} \longrightarrow \left[\begin{array}{c} HO\cdots\cdots H \quad 2+ \\ | \quad \vdots \\ (H_2O)_4Cr\cdots\cdots C(CH_3)_2OH \end{array} \right]^{\ddagger} \xrightarrow{H_2O} \begin{array}{c} (H_2O)_5CrOH^{2+} \\ + (CH_3)_2CHOH \end{array}$$

$$(I-9)$$
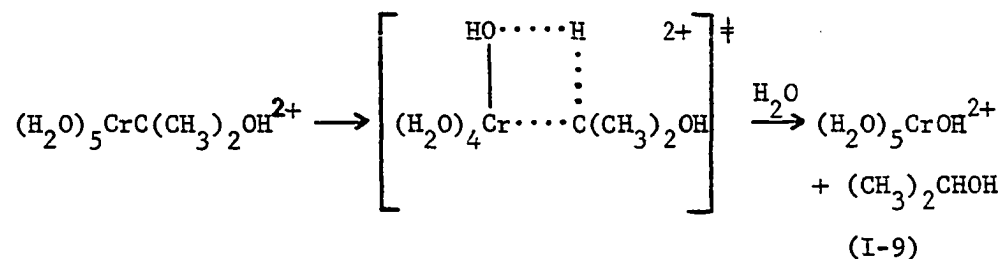
and the pH-dependent pathway using H_3O^+ as the attacking electrophile

$$(H_2O)_5CrC(CH_3)_2OH^{2+} \xrightarrow{H_3O^+} \left[\begin{array}{c} H\cdots OH_2 \quad 3+ \\ \vdots \\ (H_2O)_5Cr\cdots\cdots C(CH_3)_2OH \end{array} \right]^{\ddagger} \xrightarrow{H_2O} \begin{array}{c} Cr(H_2O)_6^{3+} \\ + (CH_3)_2CHOH \end{array}$$

$$(I-10)$$
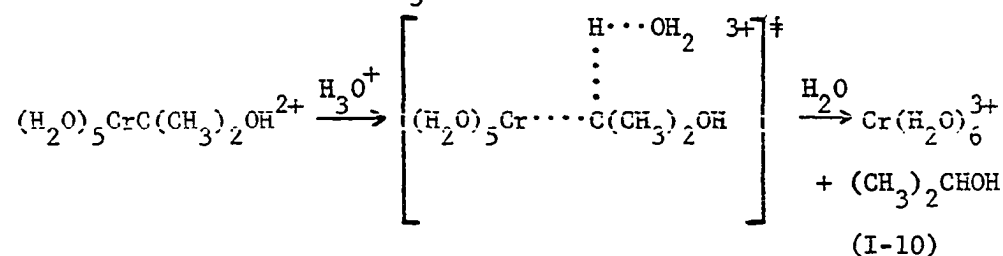
Another route leading to the decomposition of $(H_2O)_5CrC(CH_3)_2OH^{2+}$ is a process with the homolytic dissociation of the chromium-carbon bond as the rate-limiting step. Homolysis, actually the reverse of the reaction used for its preparation, produces chromium(II) ion and the 2-hydroxy-2-propyl radical:

$$(H_2O)_5CrC(CH_3)_2OH^{2+} + H_2O \rightleftharpoons Cr(H_2O)_6^{2+} + \cdot C(CH_3)_2OH \quad (I-11)$$
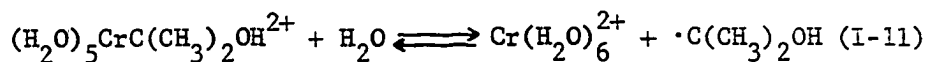
The homolytic decomposition pathway may be totally suppressed by the recombination reaction with the presence of only a small amount of Cr^{2+}, typically $\sim 10^{-4}$M. This amount of Cr^{2+} often remains from the preparation of the complex, or it can accumulate from the homolysis itself, but usually Cr^{2+} is deliberately added to the solution. The homolysis is brought to completion on the other hand when any one of certain oxidizing agents is present. Such a reagent can be $Co(NH_3)_5X^{2+}$ (X = F, Cl, Br), VO^{2+}, H_2O_2, etc., which scavenges Cr^{2+} and/or $\cdot C(CH_3)_2OH$. Such an oxidizing agent must not react with the organochromium complex itself.

As a consequence, this system of organochromium constitutes a chemical kinetic switch: the addition of Cr^{2+} shuts the homolysis off and leaves the acidolysis to proceed alone; on the other hand, the addition of an oxidizing scavenger turns on the homolysis to occur along with the acidolysis. This is depicted in Figure I-1 by a step-function plot (7).

A new application of the reversibility of homolytic dissociation of $(H_2O)_5CrC(CH_3)_2OH^{2+}$ was recently adopted for the studies of competitive kinetics. This complex provides a facile source to generate a low concentration of the $\cdot C(CH_3)_2OH$ radical at a controlled rate. Under these conditions, Reaction I-5 does not prevail. If a certain substrate S, whose reactivity toward Cr^{2+} is negligible, reacts with $\cdot C(CH_3)_2OH$, the scheme based on the chemical generation of the radical is thus the following
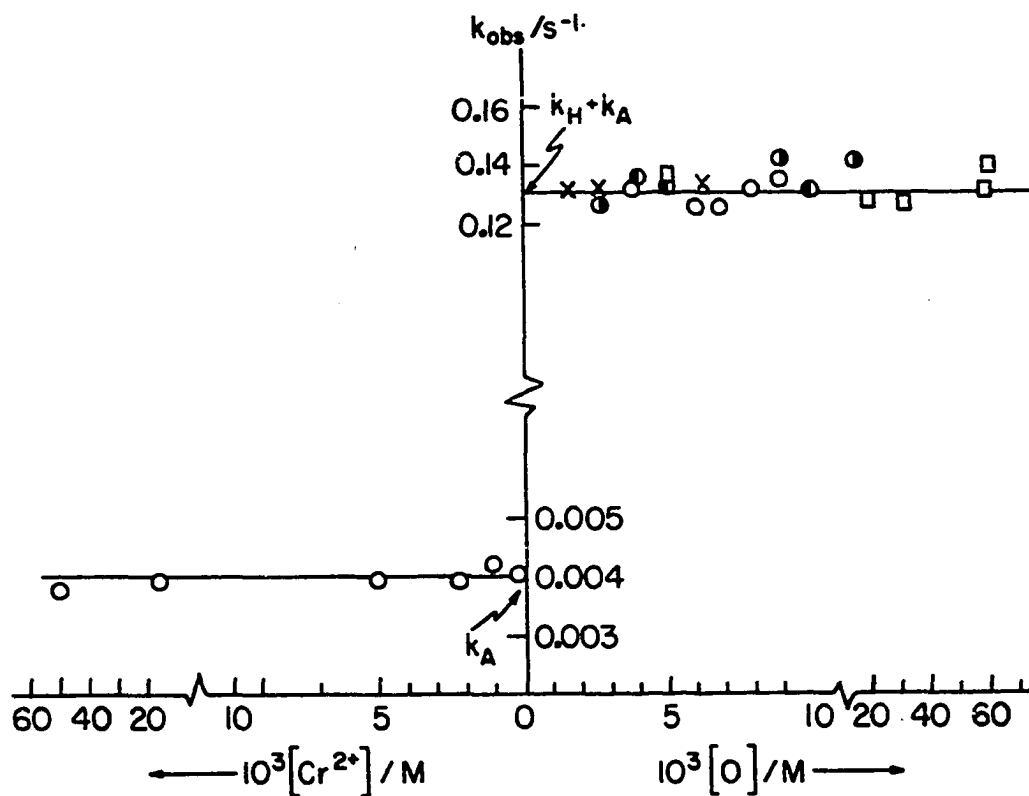
Figure I-1. Illustrating the jump in rate constant for decomposition of $(H_2O)_5CrC(CH_3)_2OH^{2+}$ from solutions containing added Cr^{2+} (left, where only acidolysis is important), to experiments (right) containing various oxidizing scavengers for Cr^{2+} and $\cdot C(CH_3)_2OH$. The latter include points for $Co(NH_3)_5F^{2+}$ (◑), $Co(NH_3)_5Cl^{2+}$ (○), $Co(NH_3)_5Br^{2+}$ (◉), VO^{2+} (◻), and H_2O_2 (X).

Scheme I-1

$$CrC(CH_3)_2OH^{2+} \underset{k_{Cr}}{\overset{k_H}{\rightleftharpoons}} Cr^{2+} + \cdot C(CH_3)_2OH \qquad (I-12)$$

$$S + \cdot C(CH_3)_2OH \xrightarrow{k_S} Product(s) \qquad (I-13)$$
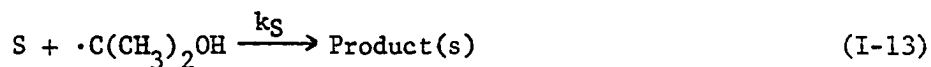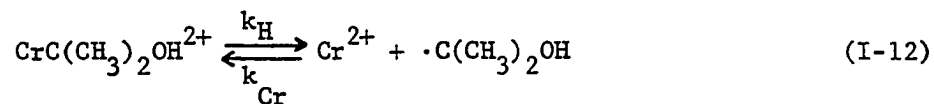
With the steady-state approximation for $[\cdot C(CH_3)_2OH]$, the analysis of the net rate of loss of $(H_2O)_5CrC(CH_3)_2OH^{2+}$ affords the value of $(k_Hk_S)/k_{Cr}$. Since the values of k_H and k_{Cr} for this specific organo-chromium complex have been independently measured, the desired rate constant, k_S, for the bimolecular Reaction I-13 can be evaluated.

New Chemistry of Selected Radicals Based on the Competitive
Kinetics of the Organochromium Complexes

The 2-hydroxy-2-propyl radical has been extensively investigated using radiation techniques (11) and has been long known to be a strong reducing agent (12, 13).

$$\cdot C(CH_3)_2OH = (CH_3)_2CO + H^+ + e^- \qquad E^o = 1.2V \ (14) \qquad (I-14)$$
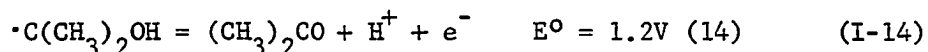
Its chemistry, however, exhibits fascinating diversity. Recently, the kinetics of the reduction of $Co(NH_3)_6^{3+}$ and related complexes by $\cdot C(CH_3)_2OH$ has been studied. In acidic solutions, they are too slow to be measured by pulse radiolysis. With the new method of chemical competition, the rate constant for $Co(NH_3)_6^{3+}$ was found to be $4.1 \times 10^5 M^{-1}s^{-1}$ (7).

Another class of reactions involving the same radical includes the

coupling reactions with benzylcobaloxime or alkylcobaloximes. They

yield the coupled products, $PhCH_2C(CH_3)_2OH$ and $RC(CH_3)_2OH$, respectively.

The kinetics of these reactions were also studied with a modified

competitive method (15, 16).

In addition, the $\cdot C(CH_3)_2OH$ radical also acts as an oxidizing

agent. Almost all reactions of this category involve strongly reducing

metal ions or complexes, and are believed to occur via metal-carbon bond

formation. One of them, which has been demonstrated before, is its

reaction with labile Cr^{2+}. The chromium(II) ion is oxidized by

$\cdot(CH_3)_2OH$ to yield a metastable organochromium(III) intermediate which

ultimately decomposes with the assistance of acid to the thermodynamic

products Cr^{3+} and $(CH_3)_2CHOH$. This reaction, termed acidolysis, has

been discussed previously, Equations I-6 to I-10.

$$Cr^{2+} + \cdot C(CH_3)_2OH \rightleftharpoons Cr^{III} - C(CH_3)_2OH \xrightarrow{H^+} Cr^{3+} + (CH_3)_2CHOH$$

$$(I-15)$$
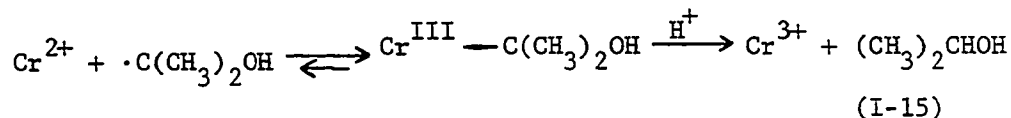
Several other reducing species considered to react with $\cdot C(CH_3)_2OH$ in

the same fashion are Fe^{2+} (17), Ni^+ (18), Zn^+ (19), Cd^+ (20), Pb^+ (21),

and possibly Cu^+ (22).

One of the themes in this chapter is to investigate the chemistry

between $\cdot C(CH_3)_2OH$ and V^{2+}. The vanadium(II) ion is strongly reducing

$(E^O = -0.26V$ vs. NHE). But V^{2+} is a d^3 substitution-inert species,

hence, the displacement of the H_2O coordinated to V^{2+} by $\cdot C(CH_3)_2OH$

to form $(H_2O)_5VC(CH_3)_2OH^{2+}$ is disfavored. The analogous reaction of

$V(H_2O)_6^{2+}$ with methyl radical has been explored by Gold and Wood recently

(23). The discovery of methane as the major product, although in a

low yield ($\sim$ 25%), suggested the oxidation of $V(H_2O)_6^{2+}$ by $\cdot CH_3$. The occurrence of a seven-coordinate organovanadium intermediate was proposed; however, no evidence was obtained to support it. Another related system is the rapid reductive coupling of aralkyl halides by $V^{II}(Py)_4Cl_2$, in which the intervention of [R-V(III)] species was also mentioned, but still without direct detection (24).

The kinetic inhibition technique affords a useful method to determine the rate constant of the bimolecular reaction between $V(H_2O)_6^{2+}$ and $\cdot C(CH_3)_2OH$. The isotope effect was also examined by conducting the kinetic experiments in D_2O. The deuterated V^{2+} also provided information about the organic product by GC-MS analysis. The inorganic product resulting from the reaction of $V(H_2O)_6^{2+}$ and $\cdot C(CH_3)_2OH$ was kinetically analyzed. The analogous reaction between $V(H_2O)_6^{2+}$ and 1-ethoxyethyl radical, $\cdot CH(CH_3)OC_2H_5$ was studied in the same manner by using the $CrCH(CH_3)OC_2H_5^{2+}$ complex. This system provides a more definitive product analysis and an opportune comparison for the reactivity of radicals. With all these more detailed studies, further insight into the mechanisms of this kind of reactions may be gained.

Organocobalt(III) complexes have been attracting considerable research interest since vitamin B_{12} was found to contain a cobalt-carbon bond. Many of these compounds containing multidentate (often tetradentate, sometimes pentadentate) nitrogen-coordinated macrocyclic ligands have been made and found to be stable (25). Among a variety of their synthetic routes, there is one which is similar to the formation of organochromium, in which organocobalt is formed by capture of a free

radical by a macrocyclic cobalt(II) complex (26, 27).

Some other organocobalt(III) complexes, such as α-substituted alkylcobalt compounds, are extremely unstable, so that they can only exist as transients. These complexes are nowadays of interest for their possible roles as intermediates in the Fischer-Tropsch processes (28). Elroi and Meyerstein have reported the studies of the formation and the decomposition for a series of α-substituted organocobalt(III) complexes of the macrocyclic ligand $Me_6[14]dieneN_4$ by pulse radiolysis (27). Their formation rates from $Co^{II}(Me_6[14]dieneN_4)^{2+}$ and free radicals have been measured. The formation of the 2-hydroxy-2-propyl complex, however, occurred too slowly and the rate constant could only be estimated as $\leq 1 \times 10^7 M^{-1}s^{-1}$. Tait, Hoffman and Hayon studied the similar chemistry by the similar techniques (29) and found that the $Co^{II}(Me_4[14]1,3,8,10-tetraeneN_4)^{2+}$ complex was reduced by $\cdot C(CH_3)_2OH$ to give the Co(I) complex with a rate constant $5.5 \times 10^9 M^{-1}s^{-1}$. No attempt was made to monitor the organocobalt(III) transient. The rates of reduction of $Co^{II}(Me_6[14]4,11-dieneN_4)^{2+}$ and $Co^{II}(Me_6[14]4,14-dieneN_4)^{2+}$ by the same radical were not measurable by pulse radiolysis because of their sluggishness ($< 10^7 M^{-1}s^{-1}$).

The investigation of the reactions of $Co^{II}([14]aneN_4)^{2+}$, which is illustrated below, with both $\cdot C(CH_3)_2OH$ and $\cdot CH(CH_3)OC_2H_5$ radicals constituted the second theme of this chapter. Accurate determinations of their rate constants, again, were made by the competitive kinetic method. Product analyses and the examination for the organocobalt(III) intermediates were also studied to seek further understanding of their reaction mechanisms.

$$\left[\begin{array}{c} \text{structure} \end{array} \right]^{2+}$$
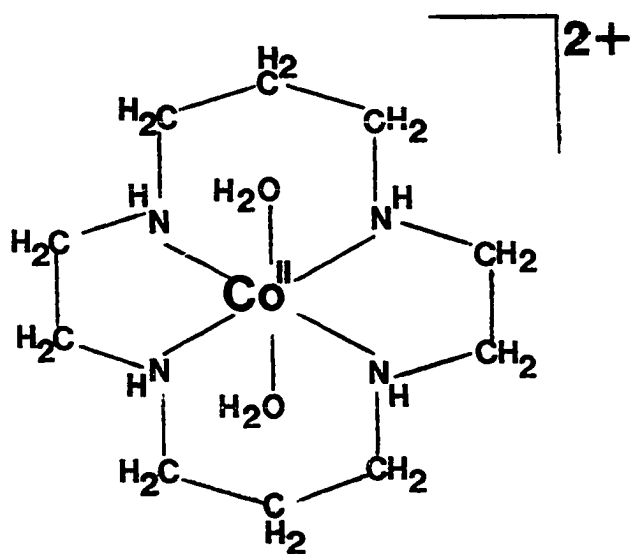
EXPERIMENTAL

Materials

Pentaaquo(organo)chromium(III) complex solution

Almost all the pentaaquo(organo)chromium(III) complexes are formed through the capture of a carbon-centered radical by a chromium(II) ion (8).

$$Cr(H_2O)_6^{2+} + \cdot R \longrightarrow (H_2O)_5Cr\text{-}R^{2+} + H_2O \qquad (I\text{-}16)$$
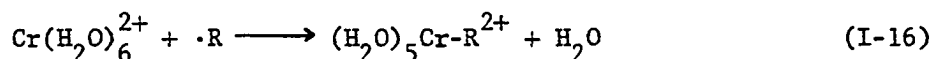
Any method which suitably supplies free radicals is employable for the preparation of $(H_2O)_5CrR^{2+}$ complexes. Two chemical methods have been used in this study, as follows.

"The modified Fenton's reagent" method   The reaction between Cr^{2+} and H_2O_2, which produces the $\cdot OH$ radical in a similar way to Fenton's reagent (30), may be carried out in a chosen solute to generate the desired organic radical. It hence provides the most versatile method of making various $(H_2O)_5CrR^{2+}$ complexes according to Equations I-17 to I-19

$$Cr^{2+} + H_2O_2 \xrightarrow{\ H^+\ } Cr^{3+} + H_2O + \cdot OH \qquad (I\text{-}17)$$

$$\cdot OH + RH \longrightarrow \cdot R + H_2O \qquad (I\text{-}18)$$

$$Cr^{2+} + \cdot R \longrightarrow Cr\text{-}R^{2+} \qquad (I\text{-}19)$$
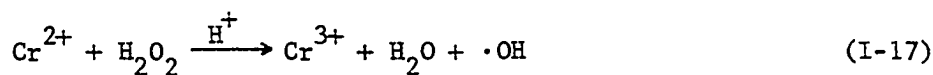
For example, $CrC(CH_3)_2OH^{2+}$ and $CrCH(CH_3)OC_2H_5^{2+}$ may be acquired by conducting this reaction in 0.01M perchloric acid with the presence of 2-propanol at 1M or diethyl ether at the saturated concentration

($\sim$ 0.5M), respectively.

The 2-hydroxy-2-propyl complex is so unstable that it has to be made and studied in situ or used immediately after the preparation. The yield of $CrC(CH_3)_2OH^{2+}$ has never exceeded 70% of the theoretical, because of the concurrence of several side reactions. The reaction of Cr^{2+} and H_2O_2 consists of a one-electron redox pathway which is of major importance ($\sim$ 90%), producing $\cdot OH$ as Equation I-17, and a direct two-electron pathway (31). The hydroxyl radical can abstract hydrogen atom from the α-carbon, the β-carbon and the hydroxyl group of 2-propanol to give respective radicals with the relative yields shown (6)

$$\cdot OH + (CH_3)_2CHOH \begin{cases} \xrightarrow{85.5\%} \cdot C(CH_3)_2OH + H_2O & \text{(I-20)} \\ \xrightarrow{13.3\%} \cdot CH_2CH(CH_3)OH + H_2O & \text{(I-21)} \\ \xrightarrow{1.2\%} \cdot OCH(CH_3)_2 + H_2O & \text{(I-22)} \end{cases}$$
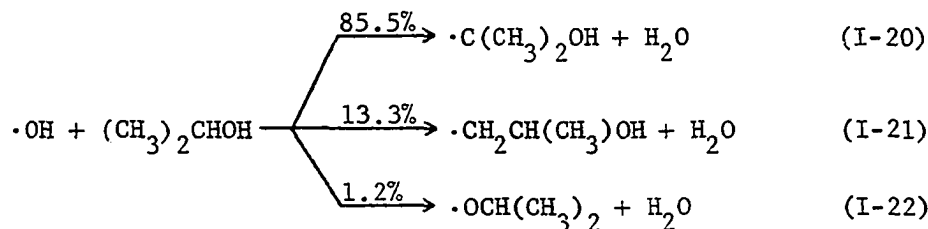
The small amount of the oxygen-centered radical is negligible. With the presence of at least another equivalent of Cr^{2+}, the other two carbon-centered radicals couple with Cr^{2+} to form the corresponding organochromium complexes. The β-substituted complex is extremely unstable in acidic solution, however, and decomposes to Cr^{3+} and propene within the time of mixing (32,33), leaving $CrC(CH_3)_2OH^{2+}$ in the solution as the major product.

This preparation also requires a large concentration of 2-propanol, such that [2-propanol]/[Cr^{2+}] > 50, to minimize the competition of Cr^{2+} reacting with $\cdot OH$ according to Equation I-23, k_{23} being 4.8 x $10^9 M^{-1}s^{-1}$ (34), which is comparable to that of Equation I-20, being $k_{19} =$

$2.2 \times 10^9 M^{-1}s^{-1}$ (34).

$$Cr^{2+} + \cdot OH \xrightarrow{k_{23}} CrOH^{2+} \qquad\qquad (I-23)$$

The $CrCH(CH_3)OC_2H_5$ complex is stable enough to be chromatographed on a Sephadex C-25 column anaerobically with slightly acidic 0.25M of $NaClO_4$. The isolated organochromium solution can be kept at -10°C for about two weeks under a nitrogen atmosphere.

Reactions of chromium(II) and organic halides   The benzyl-chromium(III) complex has been prepared by the reduction of benzyl bromide with chromium(II) ion (35, 36). The overall process consists of two steps, bromine atom transfer followed by the capture of benzyl radical:

$$Cr^{2+} + PhCH_2Br \longrightarrow CrBr^{2+} + PhCH_2\cdot \qquad\qquad (I-24)$$

$$Cr^{2+} + PhCh_2\cdot \longrightarrow PhCH_2Cr^{2+} \qquad\qquad (I-25)$$
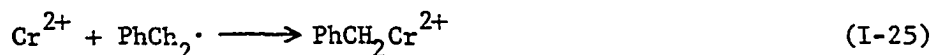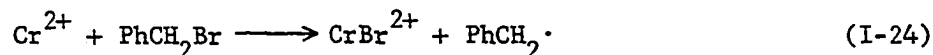
The reaction may be done by injecting two equivalents of Cr^{2+} into one equivalent of $PhCH_2Br$ dissolved in aqueous acetone. The resulting benzylchromium ion can also be purified by column chromatography.

(1,4,8,11-tetraazacyclotetradecane)cobalt(II) perchlorate solution (37)

The macrocyclic complex, $(H_2O)_2Co([14]aneN_4)^{2+}$ or cobalt(II)-(cyclam), can be made by mixing equimolar quantities of Co^{2+}, [14]aneN$_4$, and $HClO_4$ under a nitrogen atmosphere. No attempt at isolation of this complex was made because of its extreme oxygen sensitivity. Its concentration was determined spectrophotometrically at λ_{max} 465 mm ($\epsilon = 22$ $M^{-1}cm^{-1}$). The maximum concentration of this solution throughout this study was 0.05M.

The perchlorate solution of Co^{2+} was obtained by chromatographing $CoCl_2$ on a Dowex 50W-X8 ion-exchange column. The [14]aneN$_4$ ligand was purchased from Strem Chemicals, Inc.

Vanadium(II) perchlorate solution

Solutions of vanadium(II) were prepared by the reduction of vanadyl ion with zinc amalgam in an acidic aqueous solution. Two moles of hydrogen ion are also required to reduce one mole of VO^{2+} ion. The $VO(ClO_4)_2$ solution was made from $VOSO_4$ by the ion-exchange technique. Its concentration was spectrophotometrically measured at λ_{max} 760 nm (ϵ = 17.2 M^{-1}cm^{-1}) and used as that for V^{2+} solution. The concentration of H^+ was determined by titration of the eluent from ion exchange with standard base.

A solution of VO^{2+} was concentrated twice in D_2O to 1/4 of the original volume to give > 99% of deuteration. The reduction of this solution formed $V(D_2O)_6^{2+}$.

Chromium(II) perchlorate solution

Solutions of Cr^{2+} were prepared by the reduction of chromium(III) perchlorate with zinc amalgam in acid.

Miscellaneous

2,3-dimethyl-2-butyl hydroperoxide   The oxidation of 2,3-dimethyl-2-butanol by H_2O_2 in acid gives the hydroperoxide (38)

$$\text{>}\!\!\!+\!\!\text{OH} + H_2O_2 \longrightarrow \text{>}\!\!\!+\!\!\text{OOH} + H_2O \qquad \qquad (I-26)$$
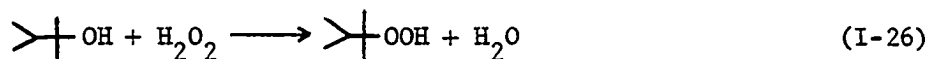
Essentially the same method was used to prepare 1-phenyl-2-methyl-2-propyl hydroperoxide ($PhCH_2C(CH_3)_2OOH$) (39).

Methods

Characterization

Inorganic reagents   All of the solutions of the metal ions or complexes were characterized with UV-visible spectroscopy and showed values consistent with the literature data (Table I-1).

Analysis

Inorganic product   In the reaction of $CrC(CH_3)_2OH^{2+}$ with V^{2+}, the product, V^{3+} ion, was analyzed by studying its reduction by Cr^{2+}. A solution of $CrC(CH_3)_2OH^{2+}$ was made first by mixing 0.0354M H_2O_2, 0.0708M Cr^{2+}, 1M 2-propanol and 0.0615M $HClO_4$ in a total volume of 5 mL. Immediately after the preparation, 3 mL of this organochromium solution was transferred into 7 mL of 0.179M V^{2+} solution containing 0.65M H^+. The mixture was allowed to react at 25.0°C for 3 minutes (~ 5 half-lives). Then, 9 mL of the resulting solution was added into a 5 cm cylindric cell which had 5 mL of 0.0853M Cr^{2+} and 1.330M $HClO_4$. This solution was monitored at λ 408 mm at 25.0°C. Both the absorbance change and the reaction rate were determined and compared to the calculated values known to apply to V^{3+}.

Separation of organic products   Organic products were separated from aqueous or semi-aqueous reaction solutions first, then identified. Two separation methods were chosen according to the solubility of the organic products in water.

Table I-1. The UV-visible spectroscopic data for some inorganic reagents

Compound	Solvent	Absorption λ_{max}/nm (ϵ/M^{-1}cm^{-1})		λ_{sh}/nm (ϵ/M^{-1}cm^{-1})	Reference
$(H_2O)_5CrC(CH_3)_2OH^{2+}$	H_2O/2-propanol	407(700)	311(2500)		32, 40
$(H_2O)_5CrCH(CH_3)OC_2H_5^{2+}$	H_2O	396(468)	290(2270)		32, 40
V^{2+}	H_2O	850(3.22)	558(4.44)	364($\sim$ 2)	41, 42
V^{3+}	H_2O^a	586(5.47)	396(8.07)		41, 42, 43
VO^{2+}	H_2O	760(17.2)			43
$(H_2O)_2Co([14]aneN_4)^{2+}$	H_2O	465(22)	316(16.5)^b		44

^{a}[H^+] = 0.8M.

^{b}This absorption sometimes appears as a shoulder.

Owing to the miscibility of 2-propanol and acetone with water, their extraction is almost impossible. An XAD-4 resin which has a strong affinity for organic material was used for the separation (45). A column packed with a 1 cm x 20 cm XAD-4 sorbent bed was washed with methanol, then followed by distilled water several times. Acetone or 2-propanol at 10 mmol level in a 10 mL aqueous solution may be effectively sorbed on the column. The water phase was removed by aspiration. The organic components then were completely eluted off the column with 10 mL of chloroform or ether, and ready for analysis.

The less water soluble products such as acetaldehyde and diethyl ether were simply extracted with $CHCl_3$ directly from reacted solutions and analyzed.

GLC analysis   Acetone, diethyl ether, and acetaldehyde were identified on a 5% FFAP column, using a Perkin-Elmer 3920B instrument with a FID, by the comparison of the authentic reagents. On a non-polar capillary column, 2-propanol in chloroform could be detected with a Varian 3700 instrument. The column temperature was set at $50 \pm 10^{\circ}C$ and the samples were chromatographed isothermally to give better separation of the small volatile compounds from the solvent (chloroform), except that $180^{\circ}C$ was applied for the detection of pinacol.

HPLC analysis   Acetone was also directly detected in the reacted solutions without separation. The aqueous samples were injected into a micropak MCH-10 30 cm x 4 mm reversed phase column installed in a Varian 5060 HPLC instrument. The chromatography was done with an eluent of 90% H_2O-10% CH_3CN at a flow rate of 1 mL/min. with 48 atm pump pressure. It was detected with a UV-50 detector at λ 260 nm.

GC-MS analysis   The identification and quantification of 2-propanol and diethyl ether were also done with a Finnegan-90 GC-MS instrument equipped with a nonpolar capillary column by the Instrument Service group.

Kinetics

The conventional spectrophotometric method was employed for the investigation of the kinetics. The decomposition of the organochromium complexes was monitored with time by following the decrease in the absorbance at their maximum absorption wavelength. The immersion of the spectrophotometric cell in a water bath in a thermostated cell holder which was installed in the sample compartment of a Cary 219 spectrometer, maintained constant temperature throughout the course of the reactions. The ionic strength of the reaction solution was brought to a constant value by the addition of $LiClO_4$.

In a typical run for the reactions of $CrCH(CH_3)OC_2H_5^{2+}$, a mixture of the desired amount of Cr^{2+} and V^{2+} (or $Co^{II}([14]aneN_4)^{2+}$) with the required concentrations of $HClO_4$ and $LiClO_4$ in a 2 cm cuvette was deaerated with N_2 for 15 minutes and then thermostated for the same period. The reaction was initiated by the injection of a small amount of $CrCH(CH_3)OC_2H_5^{2+}$. The absorbance at λ 396 nm was recorded as a function of time.

The $CrC(CH_3)_2OH^{2+}$ complex was prepared in situ and the kinetic measurements were performed in solutions also containing 2-propanol. In a 2 cm cuvette, a solution containing 2-propanol, perchloric acid and lithium perchlorate was deaerated first. After introducing Cr^{2+}

into the cell, it was brought to 25.0°C in the cell holder. The injection of H_2O_2 with shaking the cell instantaneously produces yellow $CrC(CH_3)_2OH^{2+}$. The immediate addition of pre-thermostated V^{2+} or $Co([14]aneN_4)^{2+}$ initiated the reaction which was monitored at λ 311 nm or λ 407 nm.

The isotope effect for the reaction of $CrC(CH_3)_2OH^{2+}$ and V^{2+} was determined by using vanadium(II) in 92% D_2O for the kinetic studies. A small volume such as 0.5 mL of premade $CrC(CH_3)_2OH^{2+}$ ($\sim 5 \times 10^{-3}M$) with excess Cr^{2+} was injected into 5.50 mL of ca. 0.078M $V(D_2O)_6^{2+}$ solution at 25.0°C, and the reaction was monitored as before.

All of the kinetic runs were studied under pseudo-first-order conditions. The data were analyzed by a nonlinear least-squares program.

RESULTS

Product Analysis

The reaction of vanadium(II) with the 2-hydroxy-2-propyl radical

Organic products   The result of HPLC analysis for the reacted

solution was compared to that of authentic aqueous acetone and

no acetone was detected in the sample. The GLC analysis showed

that 2-propanol was the only significant organic species in the product

solution. One cannot arbitrarily conclude that 2-propanol is the product,

however, because that reaction itself was conducted in a solution con-

taining 2-propanol. In order to discern whether and how 2-propanol was

formed in the reaction, an experiment was carried out in D_2O.

A mixture of 0.521 mmol of H_2O_2, 1.04 mmol of Cr^{2+}, 10.06 mmol

of 2-propanol and 0.8 mmol of $HClO_4$, having a total volume of 10 mL,

was brought together to make $CrC(CH_3)_2OH^{2+}$. To maximize its yield,

the local concentration of 2-propanol during the mixing must be high

and those of Cr^{2+} and H_2O_2 must be low, so that $\cdot OH$ will predominantly

react with 2-propanol instead of Cr^{2+}; and H_2O_2 is used to initiate $\cdot OH$

instead of oxidizing $\cdot C(CH_3)_2OH$ or $CrC(CH_3)_2OH^{2+}$. This was done by

injecting acidic H_2O_2 and Cr^{2+} simultaneously into 2-propanol reagent

at a steadily controlled speed. The resulting brown color indicated a

good yield of $CrC(CH_3)_2OH^{2+}$. A volume of 3.4 mL $CrC(CH_3)_2OH^{2+}$ solution

was immediately transferred to 21.6 mL of V^{2+} solution (5.36 mmol)

in 99% D_2O with $[D_3O^+] = 0.1M$ under a nitrogen atmosphere. The reaction

was allowed to go for 10 minutes at 25.0°C. The solution was chromato-

graphed with XAD-4 column. The organic sample then was analyzed with GC-MS.

A blank was made with exactly the same procedure as above except that $CrC(CH_3)_2OH^{2+}$ was not transferred into V^{2+} until $CrC(CH_3)_2OH^{2+}$ had decomposed. Aqueous 2-propanol (0.14M) was also analyzed for the purpose of comparison.

The GC-MS results confirmed that 2-propanol was the only organic compound in the three samples. The blank and the solution containing authentic 2-propanol showed the same mass spectrum whose base peak was at m/e 45 due to $CH_3CH_2=OH$ ion. The real reaction system has essentially the same pattern of its mass spectrum except that the peak of m/e 46 is significantly greater than that in the former two. The relative contents of m/e 45 to 46 fragments for 2-propanol in those three solutions mentioned before are shown by the following data.

Table I-2. The relative contents of m/e 45 and m/e 46 fragments for 2-propanol

Samples	% relative	
	m/e 45	m/e 46
Authentic 2-propanol	96.32	3.39
Blank solution	96.59	2.63
Reaction solution	87.97	11.53

The extra amount of the m/e 46 fragment in the reaction solution may be contributed by $CH_3CD=\overset{+}{O}H$, $(CH_2D)CH=\overset{+}{O}H$, and/or $(CH_3)CH=\overset{+}{O}D$.

The last species believed to be formed by solvent exchange is negligible,

because the blank solution shows only the ^{13}C natural abundance for

m/e 46, whose intensity is the same as that found from aqueous 2-propanol

within the error, but no indication of deuterium exchange. The other

two fragments are resulted from the alcohols which are produced by the

way of Equations I-20 and I-21 followed by deuterium abstraction.

The maximum possible amount of these d_1-alcohols is 0.47 mmol limited

by Equation I-17, and then is 4.7% of the total 2-propanol. The relative

content of d_1-2-propanol observed is 8.9% which is a positive evidence

of the production of d_1-2-propanol but not a quantitative explanation

for its formation.

Inorganic product   The reaction solution was allowed to age

anaerobically and then chromatographed on a Sephadex C-25 ion-exchange

column, also anaerobically. The discovery of only V^{2+}, Cr^{3+} and

traces of $[(H_2O)_4CrOH]_2^{4+}$ implies that V^{2+} behaves as a catalyst in the

reaction. To know the primary product for V^{2+} turned out to be a

problem.

An assumption made is that if 2-propanol is indeed the only or-

ganic product of this reaction, the oxidation of V^{2+} to V^{3+} is ex-

pected. The V^{3+} ion can be eventually reduced back to V^{2+} by Cr^{2+}.

The direct analysis for V^{3+} is not feasible in the presence of large

amounts of V^{2+} and Cr^{3+} at low pH values (< 2). Fortunately, the

kinetics of the reduction of V^{3+} by Cr^{2+} has been studied by Espenson

(46); a kinetic method monitoring this redox reaction hence was de-

signed to prove the assumption.

The reaction between V^{3+} and Cr^{2+} ions follows the rate law of

Equation I-27 with k = 0.710 $M^{-1}s^{-1}$ at 25.0°C and 0.771M H^+:

$$- \frac{d[V^{3+}]}{dt} = k[Cr^{2+}][V^{3+}] \qquad\qquad (I-27)$$

A certain amount of acidic Cr^{2+} was deliberately added to the reacted

solution so that the reduction of V^{3+} by Cr^{2+} could obey the pseudo-

first-order kinetics. At the high concentration of hydrogen ion, this

reaction is slower than the homolysis of $CrC(CH_3)_2OH^{2+}$. It thus

could be studied after the radical reactions were completed.

With the known kinetic data for the preparation and the decomposition

of $CrC(CH_3)_2OH^{2+}$ and for the reaction between V^{2+} and $\cdot C(CH_3)_2OH$, the

instant concentrations of related species while immediately after the

addition of Cr^{2+} were calculated to be as follows, assuming the reaction

occurs as shown in Scheme I-1: $[Cr^{2+}] = 3.43 \times 10^{-2}M$, $[V^{3+}] = 3.8 \times 10^{-3}M$,

$[Cr^{3+}] = 9.84 \times 10^{-3}M$, $[V^{2+}] = 7.65 \times 10^{-2}M$, $[H^+] = 0.771M$, and [2-

propanol] = 0.19M. The apparent rate constant observed was $2.56 \times 10^{-2}s^{-1}$.

The second-order rate constant thus was determined to be 0.746 $M^{-1}s^{-1}$

which was in good agreement with the calculated value (0.710 $M^{-1}s^{-1}$)

with an error of only 5%.

The absorbance change at λ 408 nm for the reaction between V^{3+}

and Cr^{2+} was measured in a 5 cm quartz cell to be 0.17. Since the

ultimate concentrations of all the remaining species can be determined

by calculating the loss of V^{3+} and Cr^{2+}, and the gain of Cr^{3+} and V^{2+},

being $[Cr^{2+}] = 3.05 \times 10^{-2}M$; $[V^{3+}] = 0M$; $[Cr^{3+}] = 1.37 \times 10^{-2}M$; $[V^{2+}] =$

$8.03 \times 10^{-2}M$; $[H^+] = 0.771M$, the overall absorbance change at λ 408 nm

is 0.18 by using $\epsilon_{408} = 15.6 \ M^{-1}cm^{-1}$ (Cr^{3+}); 7.62 $M^{-1}cm^{-1}$ (V^{3+});

1.30 $M^{-1}cm^{-1}$ (V^{2+}); and 0 $M^{-1}cm^{-1}$ (Cr^{2+}). Again, it is consistent with

the experimental result with an error < 6%. The vanadium(III) ion

is confirmed to be primary product of the reaction of V^{2+} with $\cdot C(CH_3)_2OH$.

The reaction of vanadium(II) with the 1-ethoxyethyl radical

The reaction was conducted in an aqueous solution instead of a semi-aqueous solvent so that the product is the only organic species in the resulting solution and can be analyzed without interference by the organic co-solvent. The $CrCH(CH_3)OC_2H_5^{2+}$ complex reacts almost exclusively with V^{2+}, because its acidolysis is so slow as to offer but a small background.

A mixture prepared with 3 mL of $2.06 \times 10^{-2}M$ $CrCH(CH_3)OC_2H_5^{2+}$ in H_2O and 2.4 mL of 0.326M $V(D_2O)_6^{2+}$ and $9.25 \times 10^{-2}M$ $DClO_4$ in D_2O was left to react at 25.0°C under a nitrogen atmosphere for four hours. The solution at 45 mole-% deuterium then was extracted with three portions of distilled chloroform with a total volume of 5 mL. The organic extract was analyzed on GC and found to contain only diethyl ether. Its yield was 90% of the theoretical, determined by comparison to an authentic sample of diethyl ether. The GC-MS analysis was used to quantify the level of deuterium enrichment for both the product and the standard. The relative intensities for the major fragments whose identities could be $CH_3CH_2O^+$ (m/e 45), $CH_3CH_2OCH_2^+$ (m/e 59), the molecular ion (m/e 74) and their corresponding P + 1 species are shown in Table I-3. The relative contents of m/e 60 to m/e 59 and m/e 75 to m/e 74 for the authentic ether are 3.17/96.8 and 4.45/95.6, respectively, consistent with the natural abundance of ^{13}C, being (1.1/98.9) x (number of carbon atom in the fragment). The

Table I-3. The selected GC-MS data for the standard of $C_2H_5OC_2H_5$
and the product

| m/e | Ordinary $C_2H_5OC_2H_5$ | | Product | |
	Relative %	$(P + 1)/P^a$	Relative %	$(P + 1)/P$
45	79.77	97.8	91.78	96.6
46	$-^b$	$(2.2)^c$	3.20	3.37
59	100	96.8	100	93.1
60	3.27	3.17	7.44	6.92
74	60.17	95.6	66.03	92.6
75	2.80	4.45	5.31	7.44

[a] The relative content of fragment P + 1 vs. fragment P.

[b] The value is too small to be evaluated.

[c] The value is calculated according to the ^{13}C natural abundance.

analogous value for m/e 46 to m/e 45 is not available, but can be

reasonably estimated as 2.2/97.8, because the responsible fragment for

m/e 45 is CH_3CHO^+ containing two carbon atoms. The extra contents of

m/e 75, m/e 60, and m/e 46 for the product are 3.0/100, 3.75/100,

1.17/100, respectively. Since $\cdot CH(CH_3)OC_2H_5$ abstracts the deuterium

atom at the α-carbon to give $CH_3CHDOC_2H_5$ in the reaction, the molecular

ion ($CH_3CHDOC_2H_5^+$) and the fragments of m/e 60 ($CH_3CHDOCH_2^+$, $CH_3CH_2OCHD^+$)

ought to show full amount of deuteration of ether no matter how they

are formed. But the fragment of m/e 46 only show 50% of the deuteration

of ether, because either a C_2H_5 group can be lost from ether to give

CH_3CHDO^+ or a CH_3CHD group leaves to give $CH_3CH_2O^+$. Therefore, the

relative amount of the deuterated ether calculated from the extra

content of m/e 46 is 3.34/100. The average percentage of the α-deuterated

ether thus is $(3.3 \pm 0.3)\%$. With 45 mole-% deuterium in the reaction

solution, and the approximated ratio of $k_H/k_D \sim 6$ (a value determined

for the analogous reaction of $\cdot C(CH_3)_2OH$), a 12.5% level of deuteration

of ether was expected. The discrepancy could be caused by the H-D

exchange in the water coordinated to V^{2+} and solvent water, but this

point was not explored further since the quantitative (90%) production

of ether makes the point.

The reactions of $(H_2O)_2Co^{II}([14]aneN_4)^{2+}$ with radicals

The reactions of $Co([14]aneN_4)^{2+}$ with both $CrC(CH_3)_2OH^{2+}$ and

$CrCH(CH_3)OC_2H_5^{2+}$ have been studied in essentially the same manner as the

analogous reactions of V^{2+}. When the cobalt complex was added to a

solution of the $(H_2O)_5CrC(CH_3)_2OH^{2+}$ complex, a decrease in absorbance

was observed at each of the absorption maxima of CrR^{2+}. The final

spectra indicated no consumption of $Co([14]aneN_4)^{2+}$. Its absorption

in the visible region was distinctive and exceeded that of other species.

Addition of Cu^{2+} and Hg^{2+} to the reaction mixture resulted in a small

increase in absorbance throughout the visible spectrum. Most of the

absorbance changes occur at $\lambda \sim 570$ nm and $\lambda \sim 400$ nm, indicating that

the reaction responsible is the oxidation of Cr^{2+} to Cr^{3+} by Hg^{2+} or

Cu^{2+}. Based on the measured absorbance change at λ 570 nm and λ 408 nm,

Cr^{3+} was produced in a quantitative yield compared to the initial

$[CrC(CH_3)_2OH^{2+}]$ (47). It suggests that the chromium(II) ion results

from the homolysis of $CrC(CH_3)_2OH^{2+}$ in a quantitative yield.

The product solution of a mixture consisting of $CrCH(CH_3)OC_2H_5^{2+}$

$(9.78 \times 10^{-3}M)$ and $Co([14]aneN_4)^{2+}$ $(1.96 \times 10^{-2}M)$ was found to contain

acetaldehyde $(8.9 \times 10^{-3}M)$, in 91% yield. In the reaction of

$CrC(CH_3)_2OH^{2+}$, only acetone and no pinacol was found.

Organocobalt(III) intermediate   The spectral changes observed

during the reactions of $Co([14]aneN_4)^{2+}$ with $CrC(CH_3)_2OH^{2+}$ and

$CrCH(CH_3)OC_2H_5^{2+}$ indicated only the decomposition of the organochromium

complexes. The intermediates were detected spectrophotometrically. It was

thought that both $([14]aneN_4)CoC(CH_3)_2OH^{2+}$ and $([14]aneN_4)CoCH(CH_3)OC_2H_5^{2+}$,

possibly formed as intermediates, might be too unstable to be detected

by spectrophotometry. The reactions between $Co([14]aneN_4)^{2+}$ and $PhCH_2 \cdot$

or $(CH_3)_2CH\cdot$, which might give the more stable organocobalt complexes

thus were examined by two methods.

Espenson and Martin have reported that some cobalt(II) macrocyclic

complexes react with tert-alkyl hydroperoxides to yield organocobalt

products (26).

$$RC(CH_3)_2OOH + (Co^{II}) \longrightarrow RC(CH_3)_2O\cdot + (Co^{III})OH \qquad (I-28)$$

$$RC(CH_3)_2O\cdot \longrightarrow R\cdot + (CH_3)_2CO \qquad (I-29)$$

$$R\cdot + (Co^{II}) \longrightarrow R(Co^{III}) \qquad (I-30)$$
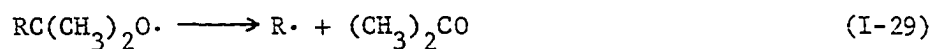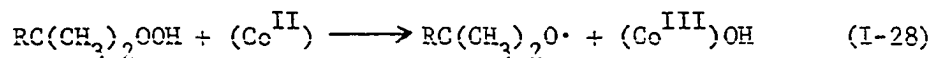
The mixing of $9 \times 10^{-3}M$ $PhCH_2C(CH_3)_2OOH$ and $2.09 \times 10^{-2}M$ $Co([14]aneN_4)^{2+}$

in 1:1 $H_2O\text{-}Bu^tOH$ mixture solvent with $[H^+] = 2.5 \times 10^{-2}M$ immediately

causes a formation of an orange species having a maximum absorption at

λ 524 nm and a shoulder at λ 380 nm. The absorbance change at λ 524 nm

was 0.69 in a 1 cm cell. If the reaction was assumed to be complete,

with all the reactants having been converted to products, the molar absorptivity at λ 524 nm could be evaluated as 76 $M^{-1}cm^{-1}$. This value is very close to that of $CH_3Co([14]aneN_4)OH_2^{2+}$ ($\varepsilon_{478\ nm} = 81\ M^{-1}cm^{-1}$ (48)). It is very reasonable to assign this cobalt product as $PhCH_2Co([14]aneN_4)OH_2^{2+}$ due to the known chemistry and the similarity of the spectral characteristic with $CH_3Co([14]aneN_4)^{2+}$. The complete UV-visible spectrum of $PhCH_2Co([14]aneN_4)^{2+}$ was never obtained, since it had decomposed during purification using column chromatography. The analogous reaction between $(CH_3)_2CHC(CH_3)_2OOH$ and $Co([14]aneN_4)^{2+}$ also produces a product with an absorption maximum at λ 526 nm ($\varepsilon \sim 85\ M^{-1}cm^{-1}$), which can be assigned as $(CH_3)_2CHCo([14]aneN_4)^{2+}$.

The $PhCH_2Co([14]aneN_4)^{2+}$ was also observed in the reaction between $PhCH_2Cr^{2+}$ and $Co([14]aneN_4)^{2+}$. The growth of the absorption at λ 530 nm occurred during the course of the slow homolysis of $PhCH_2Cr^{2+}$. Unfortunately, increasing cloudiness of the solution caused by the precipitation of $PhCH_2CH_2Ph$ made the measurement of a better-defined spectrum impossible. This species had also decomposed by the time of purification.

Kinetics

The reactions of vanadium(II) with radicals

The reaction of V^{2+} with $\cdot C(CH_3)_2OH$, based on the competitive inhibition of $CrC(CH_3)_2OH^{2+}$, may be written as below,

Scheme I-2

$$(H_2O)_5CrC(CH_3)_2OH \begin{array}{c} \xrightarrow{\text{H}^+,\ k_A} Cr^{3+} + (CH_3)_2CHOH \qquad (I\text{-}31) \\[2em] \underset{k_{Cr}}{\overset{k_H}{\rightleftarrows}} Cr^{2+} + \cdot C(CH_3)_2OH \qquad (I\text{-}32) \end{array}$$

$$V(H_2O)_6^{2+} + \cdot C(CH_3)_2OH \xrightarrow{k_V} (H_2O)_5VOH^{2+} + (CH_3)_2CHOH \qquad (I\text{-}33)$$
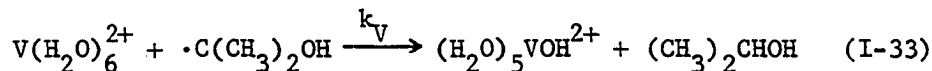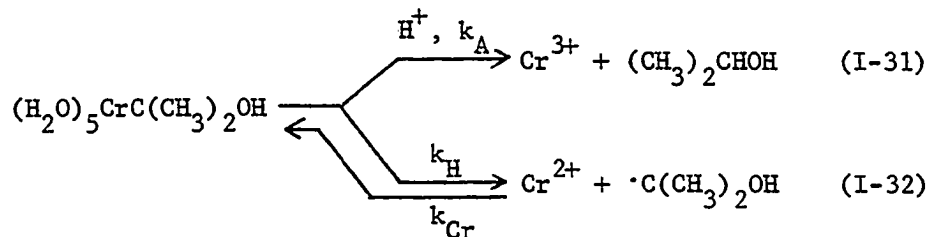
where k_A, k_H, k_{Cr}, k_V are the respective rate constants for acidolysis, homolysis, bimolecular recombination between Cr^{2+} and $\cdot C(CH_3)_2OH$ and the reaction being explored. Since $k_{Cr}[Cr^{2+}]$ and $k_V[V^{2+}]$ are much larger than k_H, $[\cdot C(CH_3)_2OH]$ remains quite low throughout the reaction. With the steady-state approximation for $[\cdot C(CH_3)_2OH]$, the decomposition of $CrC(CH_3)_2OH^{2+}$ is expressed as Equation I-34

$$- \frac{d[(H_2O)_5CrC(CH_3)_2OH^{2+}]}{dt} = \left(k_A + \frac{k_H}{1 + \dfrac{k_{Cr}[Cr^{2+}]}{k_V[V^{2+}]}} \right) [CrC(CH_3)_2OH^{2+}]$$

$$(I\text{-}34)$$

The reaction follows pseudo-first-order kinetics when $[Cr^{2+}]$ and $[V^{2+}]$ are in large excess over $[CrC(CH_3)_2OH^{2+}]$, and the apparent rate constant is formulated:

$$k_{obsd} = k_A + \frac{k_H}{1 + \dfrac{k_{Cr}[Cr^{2+}]}{k_V[V^{2+}]}} \qquad (I\text{-}35)$$

Depending on the value of the ratio $[Cr^{2+}]/[V^{2+}]$, k_{obsd} will vary in the range from k_A to $(k_A + k_H)$. The large difference in values of k_A ($\sim 8 \times 10^{-3} s^{-1}$ when pH > 0) and k_H (0.127 s^{-1}, at 25.0°C) for $CrC(CH_3)_2OH^{2+}$

allows a wide variation of k_{obsd}.

Rearrangement of Equation I-35 leads to a linear relationship between $(k_{obsd} - k_A)^{-1}$ and $[Cr^{2+}]/[V^{2+}]$.

$$\frac{1}{k_{obsd} - k_A} = \frac{1}{k_H} + (\frac{k_{Cr}}{k_H k_V})(\frac{[Cr^{2+}]}{[V^{2+}]}) \tag{I-36}$$

As a matter of fact, for the analogous reactions of the same organo-chromium under a given set of condition, the plots suggested by Equation I-36 have a common intercept k_H^{-1}. Among the conditions to be specified are temperature, the concentration of hydrogen ion, and ionic strength. At a given temperature, k_H is known to be independent of $[H^+]$ $(1.0 \times 10^{-3}M - 1.0M)$ and ionic strength $(0.1M-1.5M)$, whereas k_A varies with each but in a known manner, as shown in Table I-4.

Table I-4. The rate constants for acidolysis of $CrC(CH_3)_2OH^{2+}$ at $25.00 \pm 0.05°C$

Solvent	$[H^+]/M$	Ionic strength/M	k_A/s^{-1}
H_2O	0.20	1.5	$(4.56 \pm 0.01) \times 10^{-3}$
H_2O	0.50	1.5	$(7.04 \pm 0.24) \times 10^{-3}$
H_2O	1.00	1.5	$(1.02 \pm 0.05) \times 10^{-2}$
H_2O	0.20	1.0	4.30×10^{-3}[a]
H_2O	0.10	0.5	$(4.30 \pm 0.03) \times 10^{-3}$
H_2O	0.20	0.5	$(4.64 \pm 0.04) \times 10^{-3}$
92% D_2O	0.20	0.5	$(1.43 \pm 0.03) \times 10^{-3}$

[a] Calculated value from M. Shimura's data: $k_A = (3.31 \times 10^{-3} + 4.91 \times 10^{-3}[H^+])$ s^{-1} at $\mu = 1.0$ (7).

Figure I-2 illustrates the plots of $(k_{obsd} - k_A)^{-1}$ vs. $[Cr^{2+}]/[S]$

for the reactions of $CrC(CH_3)_2OH^{2+}$ with various substrates S. It indeed

shows the linearity and a common intercept as expected. In the plot for

S being $V(H_2O)_6^{2+}$, the kinetic data determined at different $[H^+]$ and

different ionic strength fall on the same line, indicating that the

slope, $k_{Cr}/k_H k_V$, and the intercept, k_H^{-1}, are independent of $[H^+]$ and

the ionic strength. With the kinetic data summarized in Table I-5 and

the values of k_A under the corresponding conditions, shown in Table

I-4, and the value of k_H being 0.127 S^{-1}, the ratio of k_{Cr}/k_V can be

directly evaluated as 241 ± 6 by a nonlinear least-squares fit to

Equation I-35. Since k_{Cr} is 5.1×10^7 $M^{-1}s^{-1}$, as measured by the

pulse radiolysis techniques (32), k_V is $(2.10 \pm 0.05) \times 10^5$ $M^{-1}s^{-1}$.

The error given is that from the fit, without considering the error of

k_{Cr}. The latter is substantial ($\sim \pm 15\%$), and the same error is at-

tributed to the absolute value of k_V.

Primary deuterium isotope effect   Kinetic experiments for the

reaction of $\cdot C(CH_3)_2OH$ with V^{2+} were also carried out in 92% D_2O. The

rate constant for acidolysis of $CrC(CH_3)_2OH^{2+}$ was measured as 1.43×10^{-3} S^{-1}

at 25.0°C under the conditions shown in Table I-4. The value of k_H is

the same as that obtained in H_2O (7), being 0.129 S^{-1}, as proved by the

common intercept for the plot in Figure I-2. Table I-6 shows the

kinetic data, from which $k_{Cr}/k_V(D_2O)$ was determined to be 1380 ± 100,

and then $k_V(D_2O) = (3.70 \pm 0.27) \times 10^4$ $M^{-1}s^{-1}$. The isotope effect

expressed by the ratio $k_V(H_2O)/k_V(D_2O)$ being 5.7 ± 0.6, is very

substantial.

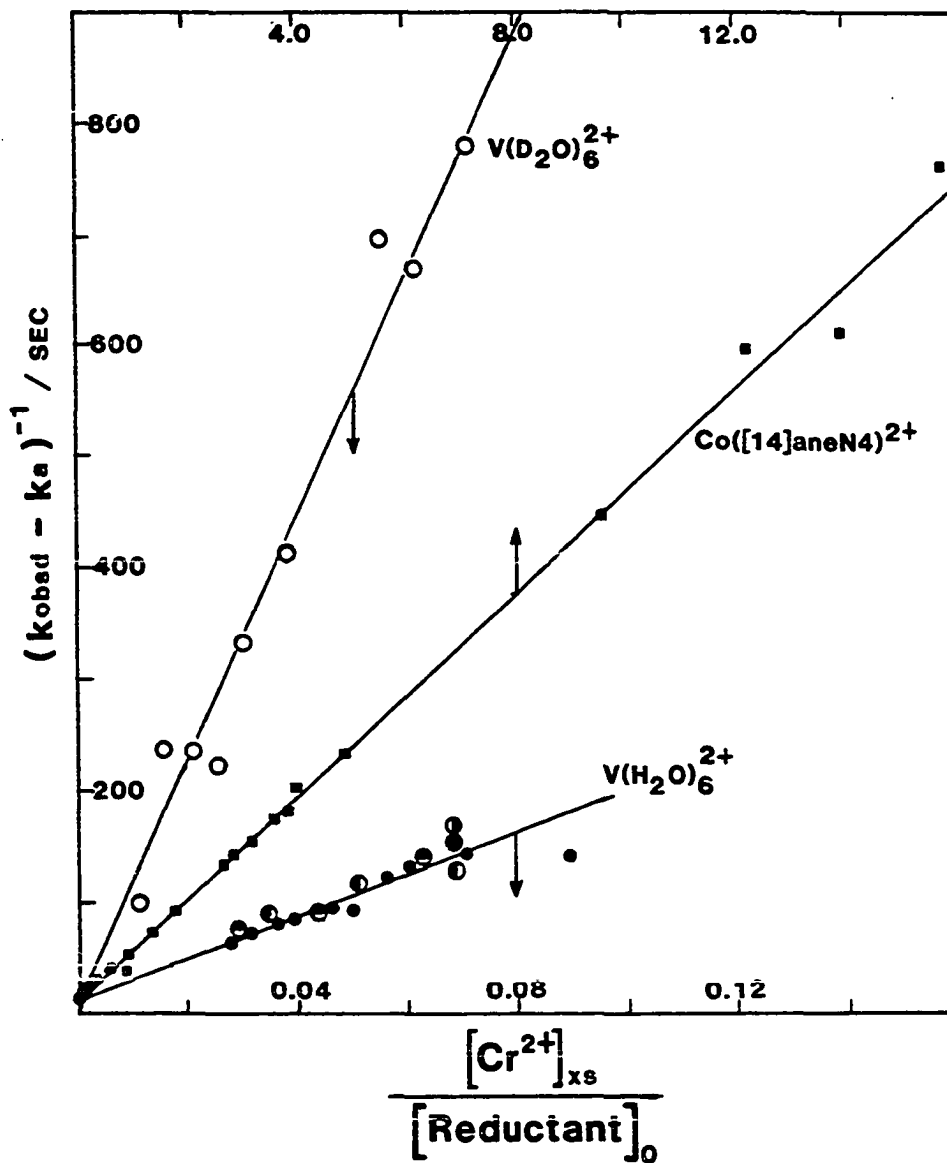Figure I-2. The first-order rate constants correlate with the concentra-
tions of the competitive reagents for the ·C(CH₃)₂OH
radical according to Equation I-32. Data are shown for
V(H₂O)₆²⁺ (●), Coᴵᴵ([14]aneN₄)²⁺ (■), and V(D₂O)₆²⁺ (○).
In the plot for V(H₂O)₆²⁺, different symbols represent
the runs carried out at [H⁺] = 0.2M μ = 1.5 (●), μ = 0.5
(●), μ = 1.0 (●) (given in Table I-5, I-6, and I-8).

Table I-5. Kinetic data for the oxidation of $V(H_2O)_6^{2+}$ by $\cdot C(CH_3)_2OH$ at 25.00 ± 0.05°C

μ	$[H^+]/M$	$10^4[H_2O_2]_0/M$	$10^3[Cr^{2+}]_0/M$	$10^2[V^{2+}]_0/M$	$10^2 k_{obsd}/S^{-1}$	$\dfrac{[Cr^{2+}]_{XS}^a}{[V^{2+}]}$	$(k_{obsd} - k_A^b)^{-1}/sec$
1.5	1.0	2.48	2.51	7.17	2.64	2.80×10^{-2}	61.3
1.5	0.2	3.47	4.18	11.2	1.86	3.11×10^{-2}	71.8
1.5	1.0	4.14	2.93	6.57	2.44	3.20×10^{-2}	70.4
0.5	0.2	3.40	2.50	5.12	1.61	3.55×10^{-2}	87.3
1.5	1.0	4.14	2.93	5.71	2.25	3.68×10^{-2}	80.6
1.5	1.0	4.14	2.93	5.25	2.18	4.00×10^{-2}	85.5
1.5	0.2	3.47	4.18	5.82	1.58	4.46×10^{-2}	89.9
1.5	1.0	4.14	2.93	4.53	2.11	4.63×10^{-2}	90.9
1.5	1.0	4.14	2.93	4.20	2.09	5.00×10^{-2}	92.6
0.5	0.2	3.40	3.33	5.12	1.35	5.18×10^{-2}	113
1.5	1.0	99.3[c]	2.00[d]	3.58	1.84	5.59×10^{-2}	122
1.5	1.0	2.48	2.51	8.33	1.82	5.61×10^{-2}	123
1.5	1.0	4.14	2.93	3.48	1.78	6.03×10^{-2}	130
1.5	0.2	3.47	4.18	5.58	1.20	6.24×10^{-2}	137
0.5	0.2	3.40	4.17	5.12	1.16	6.82×10^{-2}	147
1.0	0.2	3.40	4.17	5.12	1.08	6.82×10^{-2}	154
1.5	0.2	3.40	4.17	5.12	1.09	6.82×10^{-2}	158
1.5	1.0	4.14	2.93	2.96	1.73	7.09×10^{-2}	139
1.5	1.0	4.14	2.93	2.36	1.71	8.90×10^{-2}	143

$^a[Cr^{2+}]_{XS} = [Cr^{2+}]_0 - 2[H_2O_2]_0$.

$^b k_A = (3.3 \times 10^{-3} + 6.9 \times 10^{-3}[H^+])S^{-1}$ at $\mu = 1.5$; $(3.31 \times 10^{-3} + 4.91 \times 10^{-3}[H^+])S^{-1}$ at $\mu = 1.0$; $4.64 \times 10^{-3} S^{-1}$ at $[H^+] = 0.2M$, $\mu = 0.5$.

^{c}This run was done by injecting 0.25 mL of pre-made $CrC(CH_3)_2OH^{2+}$ into 5.75 mL of V^{2+} solution, this value being actually $[H_2O_2]_0$ used for making $CrC(CH_3)_2OH^{2+}$.

^{d}This value is actually $[Cr^{2+}]_{XS}$.

Table I-6. Kinetic data for the oxidation of deuterated V^{2+a} by $\cdot C(CH_3)_2OH$ at $25.00 \pm 0.05°C$, $[H^+] = 0.2M$, $\mu = 0.5$

$10^4[CrC(CH_3)_2OH^{2+}]^b/M$	$10^3[Cr^{2+}]^c_{XS}/M$	$10^2[V^{2+}]_0/M$	$10^3 k_{obsd}/s^{-1}$	$\dfrac{[Cr^{2+}]_{XS}}{[V^{2+}]_0}$	$(k_{obsd} - k_A^d)^{-1}/s$
0.91	0.826	7.12	11.6	1.16×10^{-2}	98.3
1.22	1.10	7.12	5.66	1.55×10^{-2}	236
1.22	1.49	7.12	5.69	2.10×10^{-2}	235
1.22	1.85	7.12	5.99	2.60×10^{-2}	219
1.22	2.18	7.12	4.48	3.07×10^{-2}	328
3.04	3.93	7.12	2.88	5.53×10^{-2}	690
3.04	4.42	7.12	2.93	6.21×10^{-2}	667
3.04	5.11	7.12	2.71	7.18×10^{-2}	781

[a]Reactions were done in 92% D_2O.

[b]70% of $[H_2O_2]_0$ used.

[c]$[Cr^{2+}]_{XS} = [Cr^{2+}]_0 - 2[H_2O_2]_0 + [CrC(CH_3)_2OH^{2+}]_{ave.}$, in which $[CrC(CH_3)_2OH^{2+}]_{ave.} = [H_2O_2]_0$ x 70% x 0.5.

[d]$k_A = 1.43 \times 10^{-3}s^{-1}$ (conditions are shown in Table I-4).

The analogous analysis for the reactions of $\cdot CH(CH_3)OC_2H_5$ with V^{2+} and $Co([14]aneN_4)^{2+}$ according to Equation I-36 also shows a linear relationship between $(k_{obsd} - k_A)^{-1}$ and $[Cr^{2+}]/[V^{2+}]$ or $[Co([14]aneN_4)^{2+}]$ and a common intercept of k_H^{-1} as depicted in Figure I-3. The kinetic data for V^{2+} reaction are given in Table I-7. With $k_A = (5 \times 10^{-7} + 3.1 \times 10^{-5}[H^+])s^{-1}$ (41), $k_H = 2.04 \times 10^{-3}s^{-1}$ (10), the value of k_{Cr}/k_V was calculated as 563 ± 34, and k_V as $(6.0 \pm 0.4) \times 10^4$ $M^{-1}s^{-1}$, since k_{Cr} is 3.4×10^7 $M^{-1}s^{-1}$ in this case (32).

The reactions of $(H_2O)_2Co^{II}([14]aneN_4)^{2+}$ with radicals

The linear plots of $(k_{obsd} - k_A)^{-1}$ vs. $[Cr^{2+}]/[Co([14]aneN_4)^{2+}]$ are shown in Figures I-2 and I-3 for the reactions of $\cdot C(CH_3)_2OH$ and $\cdot CH(CH_3)OC_2H_5$, respectively. The kinetic data are listed in Tables I-8 and I-9. A nonlinear least squares fit of these data to Equation I-35 gives the values of k_{Cr}/k_{Co} and k_{Co} for Reaction I-37 can be determined with the known value of corresponding k_{Cr}.

$$R\cdot + Co^{II}([14]aneN_4)^{2+} \xrightarrow{k_{Co}} R-Co^{III}([14]aneN_4)^{2+} \qquad (I-37)$$
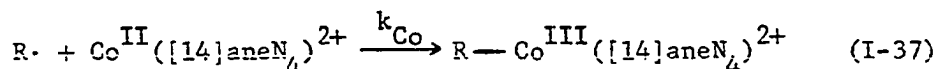
Therefore, for the reaction of $\cdot C(CH_3)_2OH$, k_{Cr}/k_{Co} is 5.82 ± 0.25, and k_{Co} is $(8.8 \pm 0.4) \times 10^6$ $M^{-1}s^{-1}$; for the reaction of $\cdot CH(CH_3)OC_2H_5$, $k_{Cr}/k_{Co} = 19.7 \pm 1.1$, and $k_{Co} = (1.7 \pm 0.1) \times 10^6$ $M^{-1}s^{-1}$.
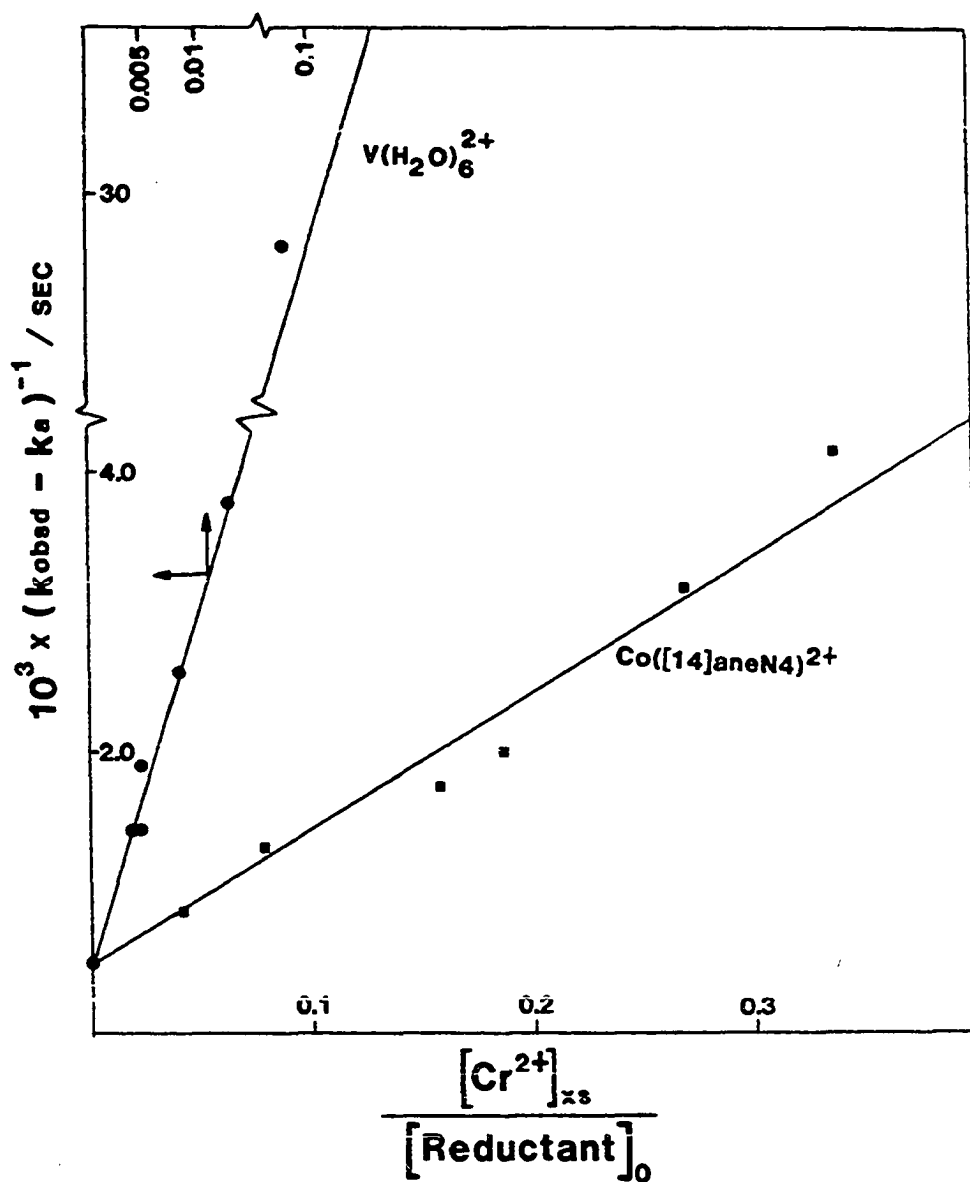
Figure I-3. The first-order rate constants correlate with the concentrations of the competitive reagents for the $\cdot CH(CH_3)OC_2H_5$ radical according to Equation I-32. Data are shown for $V(H_2O)_6^{2+}$ (●) and $Co^{II}([14]aneN_4)^{2+}$ (■) (given in Tables I-7 and I-9).

Table I-7. Kinetic data for the oxidation of V^{2+} by $\cdot CH(CH_3)OC_2H_5$ at $25.00 \pm 0.05°C$

μ/M	$[H^+]/M$	$10^4[CrCH(CH_3)OC_2H_5^{2+}]/M$	$10^3[Cr^{2+}]_{XS}^a/M$
1.55	0.967	1.0	0.837
1.55	0.967	1.0	0.837
1.51	0.750	1.0	2.51
1.50	0.90	1.0	2.51
0.50	0.19	2.6	8.37

$^a[Cr^{2+}]_{XS} = [Cr^{2+}]_o$

$^b k_A = (5 \times 10^{-7} + 3.1 \times 10^{-5}[H^+])S^{-1}$ (41)

$[V^{2+}]_o/M$	$10^4 k_{obsd}/s^{-1}$	$\dfrac{[Cr^{2+}]_{XS}}{[V^{2+}]_o}$	$10^3(k_{obsd} - k_A^b)^{-1}/s$
0.185	7.14	4.52×10^{-3}	1.90
0.185	5.55	4.52×10^{-3}	1.46
0.299	4.13	8.39×10^{-3}	2.57
0.201	2.85	1.25×10^{-2}	3.89
0.0949	0.415	8.82×10^{-2}	28.1

Table I-8. Kinetic data for the oxidation of $Co^{II}([14]aneN_4)^{2+}$ by $\cdot C(CH_3)_2OH$ at 25.00 ± 0.05°C, $[H^+] = 0.1M$, $\mu = 0.5$

$10^3[H_2O_2]_o$/M	$10^2[Cr^{2+}]_o$/M	$10^3[Co([14]aneN_4)^{2+}]$/M	$10^2 k_{obsd}$/s^{-1}	$\dfrac{[Cr^{2+}]_{XS}^a}{[Co([14]aneN_4)^{2+}]}$	$(k_{obsd} - k_A^b)^{-1}$
0.331	1.81	1.11	0.560	15.7	769
0.331	1.87	1.25	0.594	13.9	610
0.331	1.87	1.43	0.598	12.2	595
0.331	1.88	1.89	0.655	9.58	444
0.331	1.70	3.38	0.857	4.83	234
1.66	2.07	4.38	0.928	3.97	201
0.331	1.36	3.38	0.989	3.83	179
1.66	1.88	4.38	1.01	3.54	172
1.66	1.70	4.38	1.09	3.13	152
0.331	1.02	3.38	1.14	2.82	141
1.66	1.51	4.48	1.20	2.69	130
1.66	1.13	4.48	1.55	1.82	89.3
0.331	0.678	3.38	1.54	1.81	90.1
1.66	0.942	4.38	1.84	1.39	70.9
1.66	0.753	4.38	2.53	0.963	47.6
0.331	0.377	3.38	3.42	0.920	33.4
1.66	0.565	4.38	3.12	0.534	37.2
1.66	0.565	8.75	5.82	0.267	18.5
1.66	0.377	4.38	6.62	0.105	16.2

$^a[Cr^{2+}]_{XS} = [Cr^{2+}]_o - 2[H_2O_2]_o$.

$^b k_A = (4.30 \pm 0.3) \times 10^{-3}$ s^{-1} (reaction conditions are shown in Table I-4).

Table I-9. Kinetic data for the oxidation of $Co^{II}([14]aneN_4)^{2+}$ by $\cdot CH(CH_3)OC_2H_5$ at 25.00 ± 0.05^oC, $\mu = 0.5$

$[H^+]/M$	$10^4[CrCH(CH_3)OC_2H_5^{2+}]/M$	$10^3[Cr^{2+}]_{XS}^a/M$	$10^2[Co^{II}]_o/M$	$10^4 k_{obsd}/s^{-1}$	$\dfrac{[Cr^{2+}]_{XS}}{[Co^{II}]_o}$	$10^3(k_{obsd} - k_A^b)^{-1}$
0.100	3.11	1.88	4.71	11.8	0.0399	0.850
0.0340	2.2	2.51	3.27	7.55	0.0768	1.33
0.0430	5.3	5.02	3.17	5.73	0.158	1.75
0.0430	6.9	5.86	3.14	4.93	0.187	2.03
0.0430	5.3	8.37	3.11	3.17	0.269	3.17
0.0355	5.3	8.37	2.49	2.42	0.336	4.15

$^a[Cr^{2+}]_{XS} = [Cr^{2+}]_o$.

$^b k_A = (5 \times 10^{-7} + 3.1 \times 10^{-5}[H^+])s^{-1}$ (41).

INTERPRETATION AND DISCUSSION

Mechanisms of the Oxidation of Vanadium(II) Ion with Free Radicals

Competitive kinetics

The competitive kinetics prove that the indicated reactions occur according to the second-order kinetic equation,

$$- \frac{d[V^{2+}]}{dt} = k_V[V^{2+}][R\cdot] \tag{I-38}$$

and afford a means of evaluating the second-order rate constants k_V. However, these studies supply direct information about the reaction mechanism no further than Scheme I-2 (page 32), since the kinetics were studied only by monitoring the disappearance of the organochromium complexes with time.

The roles of radicals and vanadium(II) ion

The α-hydroxyalkyl radicals are reactive reducing agents toward a variety of chemical compounds. The radicals are oxidized to ketone or acyl compounds. For example, 2-hydroxy-2-propyl radical can be oxidized to acetone, as illustrated in Equation I-14.

$$\cdot C(CH_3)_2 OH = (CH_3)_2 CO + H^+ + e^- \tag{I-14}$$
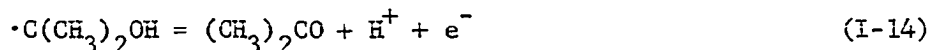
On the other hand, the α-hydroxyalkyl radical can also react with reducing substrates to "repair" the radicals by the way of hydrogen atom transfer. One typical case is the reduction of $\cdot C(CH_3)_2 OH$ by ascorbic acid, yielding 2-propanol with a rate constant $(1.2 \pm 0.1) \times 10^6$ $M^{-1}s^{-1}$ (49).

The reactions of α-alkoxyalkyl radicals are expected to resemble those of α-hydroxyalkyl radicals in the reducing aspect, although fewer

studies have been made. The <u>oxidation</u> of 1-ethoxyethyl radical yields <u>acetaldehyde</u> and <u>ethanol</u> according to the following equation (10):

$$CH_3CH_2O\overset{\cdot}{C}HCH_3 + H_2O = CH_3CHO + CH_3CH_2OH + H^+ + e^- \qquad (I-39)$$
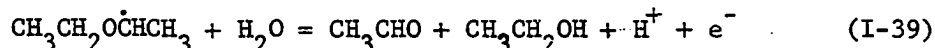
The single known case of the <u>reduction</u> of $\cdot CH(CH_3)OC_2H_5$ by Cr^{2+}, gives the Cr^{III}-$CH(CH_3)OC_2H_5$ complex, and ultimately produces Cr^{3+} and $\underline{(C_2H_5)_2O}$, only more slowly by decomposition of the organometallic complex.

The absence of acetone and acetaldehyde in the reactions of $V(H_2O)_6^{2+}$ with $\cdot C(CH_3)_2OH$ and $\cdot CH(CH_3)OC_2H_5$ proves that these radicals are not oxidized. This is not unreasonable in spite of the fact that $\cdot C(CH_3)_2OH$ and $\cdot CH(CH_3)OC_2H_5$ are commonly known as good reducing agents, since $V(H_2O)_6^{2+}$ is also a good reducing species ($E^o = -0.255V$).

In the reaction of $V(H_2O)_6^{2+}$ and $\cdot C(CH_3)_2OH$, 2-propanol was found as the only organic substance remaining in the reacted solution. Although a large amount of 2-propanol was employed to be a co-solvent, this result still implied that $\cdot C(CH_3)_2OH$ acted as an oxidizing agent, and was "repaired" by the abstraction of a hydrogen atom.

The significant content of d_1-2-propanol found in the deuterated system can be attributed to a mixture of $(CH_3)_2CDOH$, $(CH_3)(CH_2D)CHOH$, and $(CH_3)_2CHOD$. Among them, the solvent-exchanged product, $(CH_3)_2CHOD$, was not considered, since it did not appear in the blank solution either. The β-deuterated species is not important according to Equation I-21. Therefore, only $(CH_3)_2CDOH$ is the major product, suggesting the following redox reaction between $\cdot C(CH_3)_2OH$ and $V(D_2O)_6^{2+}$:

$$V(D_2O)_6^{2+} + \cdot C(CH_3)_2OH = (D_2O)_5VOD^{2+} + (CH_3)_2CDOH \qquad (I\text{-}40)$$
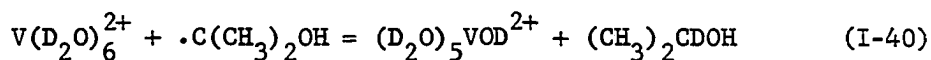
Evidence to confirm the occurrence of Equation I-40 is the discovery of $V(H_2O)_6^{3+}$ as a primary product. The reduction of $V(H_2O)_6^{3+}$ by Cr^{2+} following Equation I-40 was also proved. This result also explains the eventual recovery of V^{2+} and loss of Cr^{2+}, as found by chromatography.

In the reaction of $V(H_2O)_6^{2+}$ with $\cdot CH(CH_3)OC_2H_5$, the formation of diethyl ether in a yield of 90% of theoretical and as the only organic product is similarly attributed to the reduction of the radical by $V(H_2O)_6^{2+}$:

$$V(H_2O)_6^{2+} + \cdot CH(CH_3)OC_2H_5 = (H_2O)_5VOH^{2+} + (C_2H_5)_2O \qquad (I\text{-}41)$$
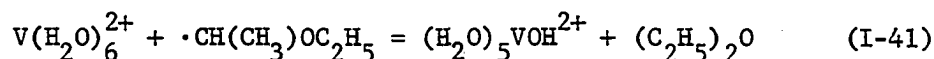
Reaction mechanisms

Outer-sphere electron transfer

An outer-sphere process for the reduction of radicals by $V(H_2O)_6^{2+}$ can be argued against for two reasons. First of all, the direct formation of the aliphatic anion from the radical as in Equation I-42 is energetically disfavored.

Scheme I-3

$$V(H_2O)_6^{2+} + \cdot C(CH_3)_2OH \longrightarrow V(H_2O)_6^{3+} + \overset{\ominus}{:}C(CH_3)_2OH \qquad (I\text{-}42)$$

$$\overset{\ominus}{:}C(CH_3)_2OH + H^+ \xrightarrow{\text{fast}} (CH_3)_2CHOH \qquad (I\text{-}43)$$
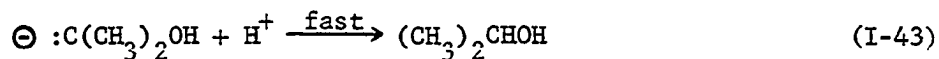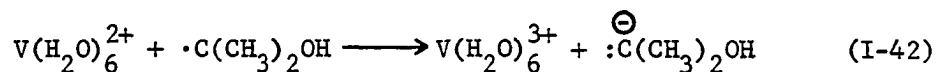
Secondly, a significant primary isotope effect with $k_H/k_D = 5.7$ was observed. The value of k_D was determined in a solution of 92% deuterium content. For convenience of discussion, the ratio may be

mathematically extrapolated to 100% of D_2O, being 6.2. In the reduction

of $Co(NH_3)_6^{3+}$ by $\cdot C(CH_3)_2OH$, the hydrogen exchange between the co-

ordinated ammonias and solvent water was negligibly slow. The rate

constants for $Co(ND_3)_6^{3+}$, therefore, could be individually measured

either in H_2O or in D_2O. A very small isotope effect with $k_H/k_D = 1.35$

in H_2O, or 1.68 in D_2O was found in strongly acidic medium, which sup-

ported the outer-sphere mechanism (7). In contrast, the rate constants

of the reaction of vanadium(II) were substantially lower in D_2O.

Since they are independent of pH and of the ionic strength, the isotope

effect must be attributed only to the reaction itself. It strongly

suggests that a hydrogen transfer to $\cdot C(CH_3)_2OH$ in forming 2-propanol

has to be important in the rate-limiting-step. The outer-sphere

mechanism does not explain this result at all.

Hydrogen atom abstraction   A plausible mechanism which rationalizes

all the experimental observations is one in which the $\cdot C(CH_3)_2OH$ radical

abstracts one hydrogen atom from a water molecule coordinated to V^{2+}.

Scheme I-4

$$V(H_2O)_6^{2+} + \cdot C(CH_3)_2OH \longrightarrow \left[(H_2O)_5V-O \overset{H}{\underset{H\cdots\cdots\cdot C(CH_3)_2OH}{\cdots}} \right]^{2+\ddagger} \longrightarrow$$

$$(CH_3)_2\underset{(D)}{CHOH} + (H_2O)_5VOH^{2+}$$

$$(I-44)$$
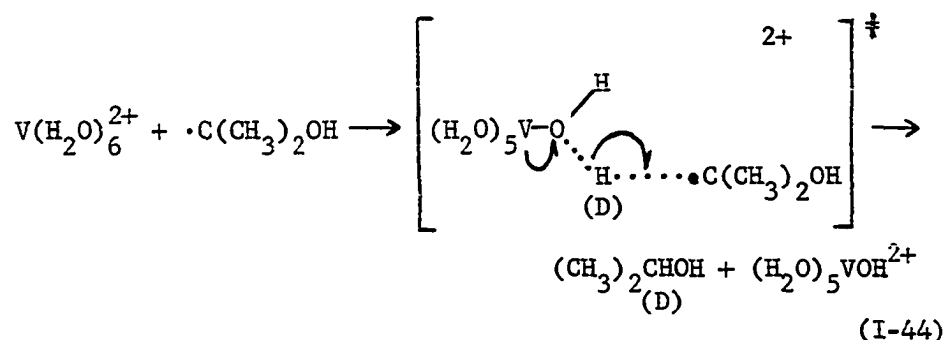
Generally speaking, this process is disfavored because it shows a

stronger O-H bond breaking concertedly with the formation of a weaker

C-H bond. Nevertheless, the strong reducing center of V^{2+} might afford a compensating driving force for the hydrogen atom transfer. A relatively low rate constant, 2.1×10^5 $M^{-1}s^{-1}$, of this reaction is not surprising.

In the deuterated system, a large primary isotope effect is naturally expected, because the transfer of a deuterium atom occurs in the rate-limiting-step. In addition, an α-deuterated 2-propanol, $(CH_3)_2CDOH$, ought to be and is the product. In the analogous reaction of $\cdot CH(CH_3)OC_2H_5$, $CH_3CHDOCH_2CH_3$ is the product as expected.

V-C bond formation followed by acidolysis   An associative pathway leading to an organovanadium(III) intermediate, which decomposes by acidolysis, is illustrated in Scheme I-5.

Scheme I-5

$$V(H_2O)_6^{2+} + \cdot C(CH_3)_2OH \underset{k_{-45}}{\overset{k_{45}}{\rightleftharpoons}} (H_2O)_6V-C(CH_3)_2OH^{2+} \qquad (I-45)$$

$$(H_2O)_6V-C(CH_3)_2OH^{2+} \xrightarrow{k_{46}} (H_2O)_5VOH^{2+} + (CH_3)_2CHOH \qquad (I-46)$$
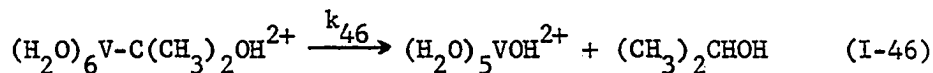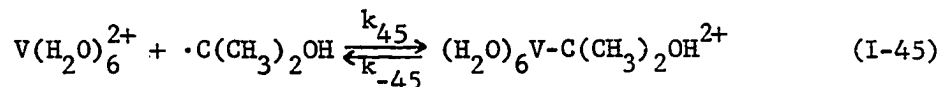
The seven-coordinate organovanadium(III) species is proposed because $V(H_2O)_6^{2+}$ is a d^3 kinetically inert ion which does not permit the substitution of $\cdot C(CH_3)_2OH$ for H_2O on this time scale. A similar case is the oxidation of $V(H_2O)_6^{2+}$ by the methyl radical. The intervention of a seven-coordinate organovanadium species was also postulated (23), but no evidence of this intermediate was obtained.

With the steady-state approximation for $[(H_2O)_6VC(CH_3)_2OH^{2+}]$, an expression for k_V, which can be referred to in Scheme I-2, is established.

$$k_V = \frac{k_{45} k_{46}}{k_{-45} + k_{46}} \tag{I-47}$$

If $k_{46} \gg k_{-45}$, Equation I-47 is simplified to $k_V = k_{45}$, which suggests

the formation of the V-C bond is rate-limiting. This case is unlikely,

because it does not explain the substantial isotope effect.

Reaction I-46 is actually the acidolysis of 2-hydroxy-2-propylvanadium-

(III), which can be written in the form of Equation I-48.

Scheme I-6

$$(H_2O)_6 VC(CH_3)_2OH^{2+} \longrightarrow \left[(H_2O)_5 V \overset{\overset{\displaystyle H}{O} \cdots H}{\underset{C(CH_3)_2OH}{\diagup}} \right]^{\ddagger} \longrightarrow (H_2O)_5 VOH^{2+}$$

$$+ (CH_3)_2CHOH$$

$$\tag{I-48}$$
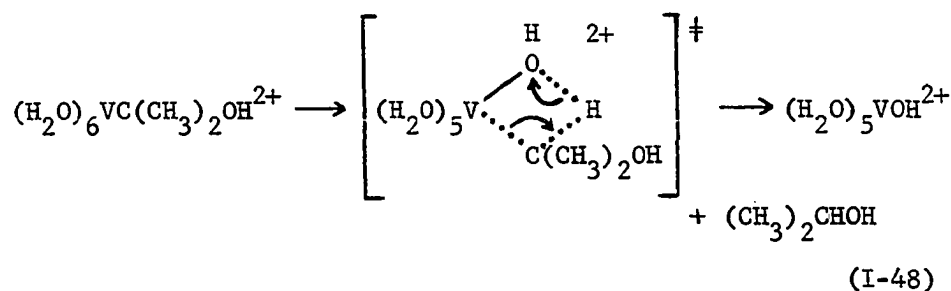
The proton transfer in the transition state is expected to contribute

a large isotope effect in the deuterated system. It will come true if

$k_{46} \ll k_{-45}$, then

$$k_V \cong (\frac{k_{45}}{k_{-45}})k_{46}, \tag{I-49}$$

indicating that the acidolysis of Scheme I-6 is the rate-limiting step.

The intermolecular pathway of acidolysis is not considered, because

k_V is known to be acid independent in the experimental region ($[H^+]$ =

0.2M - 1.0M). The intramolecular route is feasible and prevails because

the seven-coordinated intermediate is too crowded to be stable.

Preequilibrium process   The mechanism shown in Scheme I-7,

in which a rapid equilibrium between $V(H_2O)_6^{2+}$ and the 2-hydroxy-2-propyl

group-bound vanadium precedes the acidolysis, is mathematically in-

distinguishable from that in Scheme I-5.

Scheme I-7

$$V(H_2O)_6^{2+} + \cdot C(CH_3)_2OH \xrightleftharpoons{K_{50}} (H_2O)_6VC(CH_3)_2OH^{2+} \qquad (I-50)$$

$$(H_2O)_6VC(CH_3)_2OH^{2+} \xrightarrow{k_{51}} (H_2O)_5VOH^{2+} + (CH_3)_2CHOH \qquad (I-51)$$
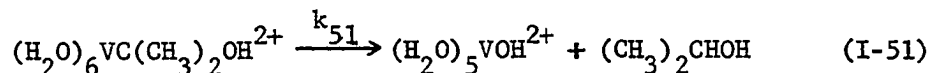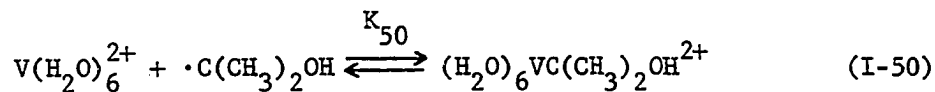
The form of k_V is derived as Equation I-52

$$k_V = \frac{k_{51}K_{50}}{1 + K_{50}[V^{2+}]} \qquad (I-52)$$

When $K_{50}[V^{2+}] \gg 1$, $k_V = k_{51}/[V^{2+}]$. This is not true within the experimental region ($[V^{2+}] \cong 2 \times 10^{-2}M - 1.1 \times 10^{-1}M$) because the experimental data show no further $[V^{2+}]$-dependence in k_V. If $K_{50}[V^{2+}] \ll 1$, the upper limit of K_{50} is $10^{-1}M^{-1}$; and $k_{51} > 2 \times 10^6 s^{-1}$ since $k_V = k_{51}K_{50}$. These values imply that the seven-coordinated organovanadium species is extremely unstable.

Mechanisms of Reactions of $Co^{II}([14]aneN_4)^{2+}$ with Radicals

The possibility of the reduction of $\cdot C(CH_3)_2OH$ and $\cdot CH(CH_3)OC_2H_5$ by $Co^{II}([14]aneN_4)^{2+}$ complex is eliminated, because acetone and acetaldehyde are found to be the products instead of 2-propanol and diethyl ether, respectively. Therefore, only the mechanisms leading to the oxidation of the radicals are considered. Both inner-sphere and outer-sphere pathways will be discussed.

Inner-sphere mechanism

The pathway of the Co-C bond formation   According to the results

of the radiolytic studies, these reactions can be immediately attributed

to the formation of the organocobalt(III) intermediates.

Scheme I-8

$$(H_2O)_2Co^{II}([14]aneN_4)^{2+} + \cdot C(CH_3)_2OH \longrightarrow \underset{\underset{H_2O}{|}}{\overset{\overset{HOC(CH_3)_2}{|}}{Co}}{}^{III}([14]aneN_4)^{2+} + H_2O$$

$$(I-53)$$

$$(H_2O)_2Co^{II}([14]aneN_4)^{2+} + \cdot CH(CH_3)OC_2H_5 \longrightarrow \underset{\underset{H_2O}{|}}{\overset{\overset{OC_2H_5}{\overset{|}{\underset{|}{H-C-CH_3}}}}{Co}}{}^{III}([14]aneN_4)^{2+}$$

$$(I-54)$$
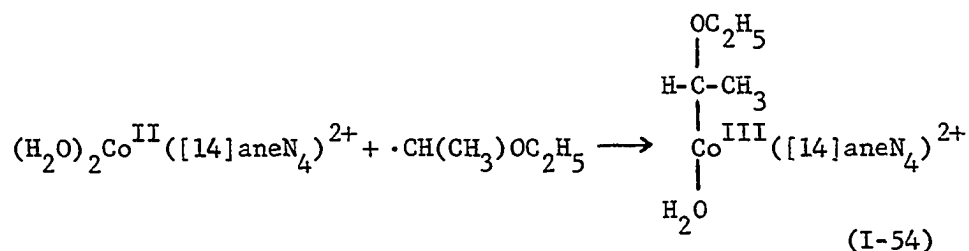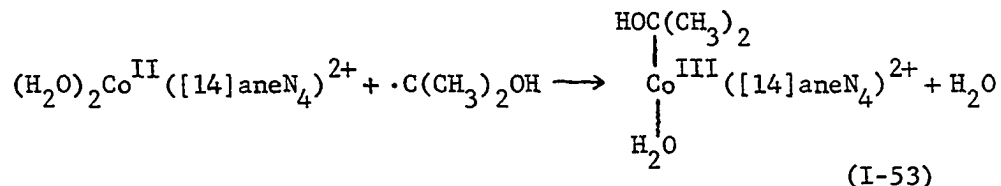
The bimolecular rate constants, k_{Co} being 8.8×10^6 $M^{-1}s^{-1}$ for Equation

I-53, and 1.7×10^6 $M^{-1}s^{-1}$ for Equation I-54, are consistent with those

expected (27). They show the same trend as those for the formation of

the organochromium complexes, $k_{Cr} = 5.1 \times 10^7$ $M^{-1}s^{-1}$ for $CrC(CH_3)_2OH^{2+}$

and $k_{Cr} = 3.4 \times 10^7$ $M^{-1}s^{-1}$ for $CrCH(CH_3)OC_2H_5^{2+}$. The less prominent

difference in the chromium system may be invoked by the better lability

of the nonmacrocyclic $Cr(H_2O)_6^{2+}$ leveling out the electronic effect of

the radicals (13, 27). Of course, this is not necessarily the only

factor.

The formation of $PhCH_2Co([14]aneN_4)OH_2^{2+}$ complex in the model

benzyl system also supports that the organocobalt(III) species is a

reasonable primary product of the free radical and $Co^{II}([14]aneN_4)^{2+}$.

It also proves that the coexistence of organochromium and

$Co^{II}([14]aneN_4)^{2+}$ indeed constitute a suitable system to carry out this kind of reaction. Conventional spectrophotometry did not provide detectable evidence for $([14]aneN_4)CoC(CH_3)_2OH^{2+}$ and $([14]aneN_4)Co-CH(CH_3)OC_2H_5^{2+}$. This may be because both of these species have very short lifetimes and had been decomposing during the course of the reactions which were rate-limited by the homolysis of the organochromium complexes. This is not surprising since $Co^{III}L-CH_2OH(L = Me_6[14]dieneN_4$ through this section) decomposes with $k = 0.1$ S^{-1}, and for $Co^{III}L-CH(CH_3)OH$, $k = 1 \times 10^2$ S^{-1} at pH 7 and $\sim 2 \times 10^3$ S^{-1} at pH 1. The electron-donating group on the radical would enhance its reducing ability and thus would destabilize the Co-C bond (27).

The decomposition of the Co-C bond   The $Co^{III}L-CH_2OH$ decomposes by the way of a two-equivalent electron transfer to give formaldehyde and Co^IL complex

$$Co^{III}L-CH_2OH \longrightarrow Co^IL + HCHO \qquad (I-55)$$
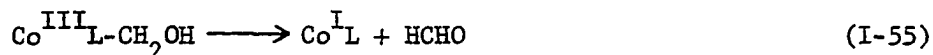
The formation of Co(I) species in the reaction of $Co^{II}(1,3,8,10$-tetra-eneN$_4)^{2+}$ with $\cdot C(CH_3)_2OH$ was directly monitored by pulse radiolysis at pH 1 and 6.5 (29). It is reasonable to conceive that both the organocobalt(III) intermediates also heterolytically cleave their Co-C bonds as depicted in Scheme I-9, to yield the organic products of the oxidized radicals.

Scheme I-9

$$HO-C(CH_3)_2$$
$$| \qquad\qquad 2+$$
$$Co^{III}([14]aneN_4) \longrightarrow (CH_3)_2CO + HCo^{III}([14]aneN_4)^{2+}$$
$$|$$
$$H_2O \qquad\qquad\qquad\qquad\qquad\qquad\qquad\qquad (I\text{-}56)$$

$$OC_2H_5$$
$$|$$
$$H-C-CH_3$$
$$| \qquad\qquad\qquad\qquad H_2O$$
$$Co^{III}([14]aneN_4)^{2+} \xrightarrow{\quad} CH_3CHO + C_2H_5OH + HCo^{III}([14]aneN_4)^{2+}$$
$$|$$
$$H_2O \qquad\qquad\qquad\qquad\qquad\qquad\qquad\qquad (I\text{-}57)$$
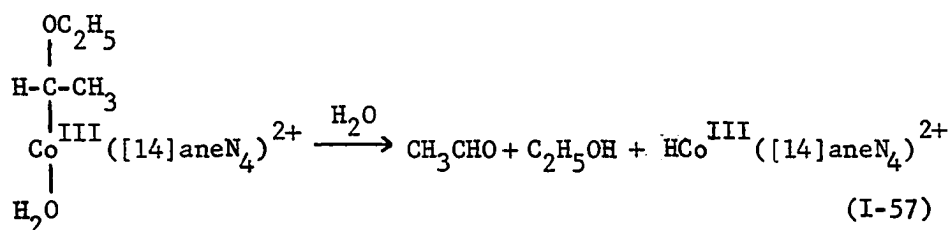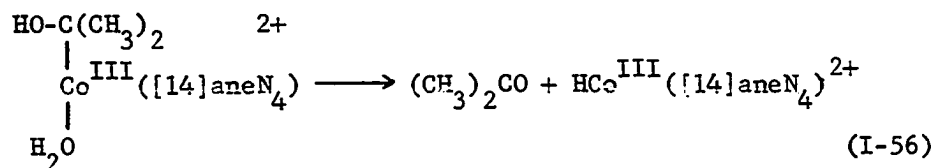
The Co(I) species is actually the conjugate base of the hydridocobalt(III) complex. At pH < 1, it ought all to be in the latter form. Further chemistry of the hydridocobalt(III) complex will be discussed in the following section.

A general scheme of this reaction is worth more consideration. Scheme I-10 represents this sequence. The form of the apparent rate constant, k_{Co}, is shown in Equation I-60.

Scheme I-10

$$R\cdot + (Co^{II}) \underset{k_{-58}}{\overset{k_{58}}{\rightleftarrows}} R(Co^{III}) \qquad\qquad\qquad (I\text{-}58)$$

$$R(Co^{III}) \xrightarrow{k_{59}} Products \qquad\qquad\qquad (I\text{-}59)$$
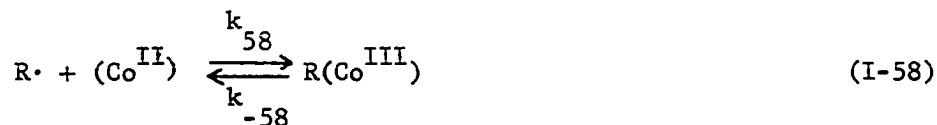
$$k_{Co} = \frac{k_{58}k_{59}}{k_{-58} + k_{59}} \qquad\qquad\qquad (I\text{-}60)$$

If $k_{59} \gg k_{-58}$, then $k_{Co} = k_{58}$. This is the very case cited before.

If $k_{59} \ll k_{-58}$, $k_{Co} \cong \dfrac{k_{58}k_{59}}{k_{-58}}$. For the purpose of comparison, the

values of k_{59} for the complexes with the $Me_6[14]dieneN_4$ ligand are used. It is noted that k_{59} for $Co^{III}L-CH(CH_3)OH$ is 10^4 times greater than that of $Co^{III}L-CH_2OH$ at pH 1. With this trend, the value of k_{59} for $Co^{III}L-C(CH_3)_2OH$ would be 10^8 s^{-1}, and $k_{-58} > 10^8$ s^{-1}, an unusually high rate for the homolytic cleavage of the Co-C bond. It suggests that the decomposition of the organocobalt intermediates is unlikely to be rate-limiting.

Reactions of hydridocobalt complex   Hydrido complexes of cobalt(III) are conjugate acids of the corresponding Co(I) complexes. These two species, however, show very different reactivity (50, 51). The hydride complexes of cobalt have been found to be unstable, slowly decomposing to form Co(II) complexes and evolve molecular hydrogen (52).

$$2(\overset{\overset{\displaystyle H}{\displaystyle |}}{Co}^{III}) = 2(Co^{II}) + H_2 \qquad (I-61)$$

Related studies for Reaction I-61 are the decomposition of vitamin B_{12S} (53), $HCo(CN)_5^{3-}$ (54), and $HCo(dmgH)_2P(n-Bu)_3$ (55). In the last one, a bimolecular pathway shown in Equation I-62, and a hydride transfer process forming Co(III), as in Equation I-63 were proposed.

Scheme I-11

$$2HCo(dmgH)_2P(n-Bu)_3 \longrightarrow [(Co)H \cdots H(Co)]^{\ddagger} \longrightarrow$$
$$H_2 + 2Co^{II}(dmgH)_2P(n-Bu)_3 \qquad (I-62)$$

$$HCo(dmgH)_2P(n-Bu)_3 + H_3O^+ \longrightarrow H_2OCo^{III}(dmgH)_2P(n-Bu)_3^+ + H_2$$
$$(I-63)$$
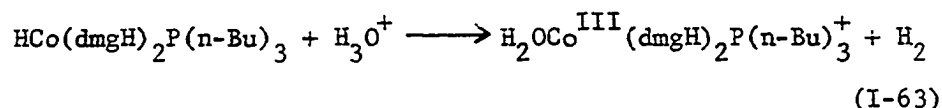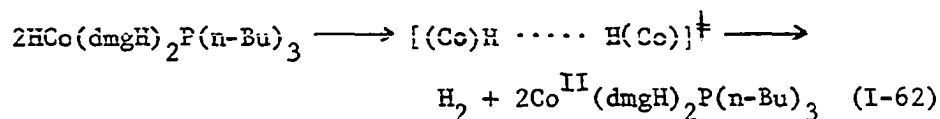
Both of these routes may be used to explain the decomposition of $HCo([14]aneN_4)^{2+}$. The former one might be more important since it reacted with a rate constant 4×10^4 fold greater than the other route for the $Co(dmgH)_2$ system. In the reaction between $CrC(CH_3)_2OH^{2+}$ and $Co([14]aneN_4)^{2+}$, the cobalt(II) complex was found to be completely recovered at the end of the reaction. The amount of Cr^{2+} left over was also found to be the same as that of initial $CrC(CH_3)_2OH^{2+}$ used (47). These results also support that the coupling pathway is dominant, because it produces the Co(II) complex directly. But, the primary product of the hydride transfer route would be $Co^{III}([14]aneN_4)^{3+}$, which would need to be reduced to $Co^{II}([14]aneN_4)^{2+}$ by Cr^{2+}.

Outer-sphere electron transfer

The direct outer-sphere reduction of $Co^{II}([14]aneN_4)^{2+}$ by the free radical cannot be arbitrarily precluded.

Scheme I-12

$$Co^{II}([14]aneN_4)^{2+} + \cdot C(CH_3)_2OH \longrightarrow Co^I([14]aneN_4)^+$$

$$+ \; H^+ + (CH_3)_2CO \tag{I-64}$$

$$Co^{II}([14]aneN_4)^{2+} + \cdot CH(CH_3)OC_2H_5 \xrightarrow{H_2O} Co^I([14]aneN_4)^+$$

$$+ \; H^+ + CH_3CHO + C_2H_5OH \tag{I-65}$$
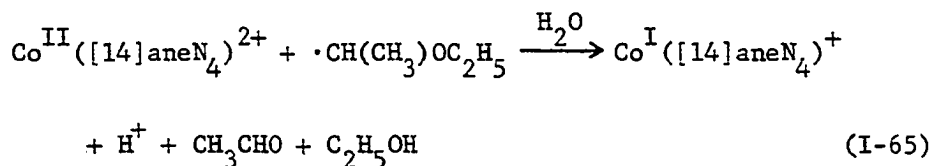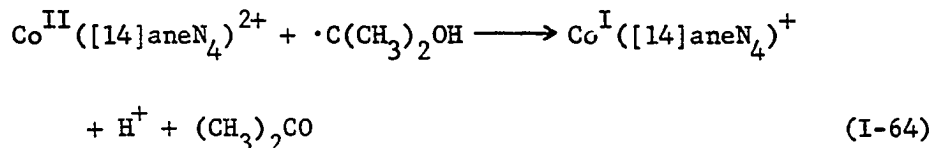
The analogous chemistry of Equation I-64 was found for the $Co^{II}(1,3,8,10\text{-tetraeneN}_4)^{2+}$ complex with a rate constant $5.5 \times 10^9 \; s^{-1}$. Nevertheless, $Co^{II}([14]aneN_4)^{2+}$ is a much stronger reducing agent than

$Co^{II}(1,3,8,10\text{-}tetraeneN_4)^{2+}$, thus, the direct reduction of $Co^{II}([14]aneN_4)^{2+}$ is not necessarily as feasible as $Co^{II}(1,3,8,10\text{-}tetraeneN_4)^{2+}$.

CONCLUSIONS

Among the mechanisms cited before for the reactions of $V(H_2O)_6^{2+}$ with radicals, Schemes I-4, I-5, and I-7 are all in agreement with the experimental observations. The last two schemes are mathematically indistinguishable. Therefore, only the two routes which are very different in a chemical sense are considered. The first one is that the carbon-centered radical directly abstracts a hydrogen atom from a water molecule coordinated to vanadium(II) ion. In this case, the hydroxovanadium(III) ion is the immediate product which rapidly equilibrates with H_3O^+ to yield $V(H_2O)_6^{3+}$ (pKa ~ 3-4). In addition, the radical is "repaired." The second mechanism invokes the formation of a seven-coordinate organovanadium(III) intermediate, which undergoes rate-limiting intramolecular acidolysis to give the corresponding products. No detectable evidence for the organovanadium species is available. At this time, further distinction between the alternative mechanisms cannot be made.

In summary, the reactions between $Co^{II}([14]aneN_4)^{2+}$ and the radicals can be illustrated according to the following sequence:

$$Co^{II}([14]aneN_4)^{2+} \underset{\cdot CH(CH_3)OC_2H_5}{\overset{\cdot C(CH_3)_2OH}{\Bigg<}}$$

$$\xrightarrow{\cdot C(CH_3)_2OH} ([14]aneN_4)Co^{III}C(CH_3)_2OH^{2+} \quad (I\text{-}66a)$$

$$\xrightarrow{\cdot CH(CH_3)OC_2H_5} ([14]aneN_4)Co^{III}CH(CH_3)OC_2H_5^{2+} \quad (I\text{-}66b)$$

$$([14]aneN_4)Co^{III}C(CH_3)_2OH^{2+} \longrightarrow HCo^{III}([14]aneN_4)^{2+} + (CH_3)_2CO \quad (I\text{-}67a)$$

$$([14]aneN_4)Co^{III}CH(CH_3)OC_2H_5^{2+} \xrightarrow{H_2O} HCo^{III}([14]aneN_4)^{2+} + CH_3CHO$$

$$+ C_2H_5OH \quad (I\text{-}67b)$$

$$2HCo^{III}([14]aneN_4)^{2+} \longrightarrow 2Co^{II}([14]aneN_4)^{2+} + H_2 \quad (I\text{-}68)$$
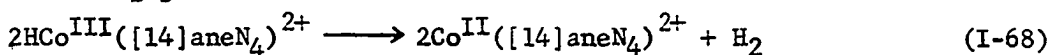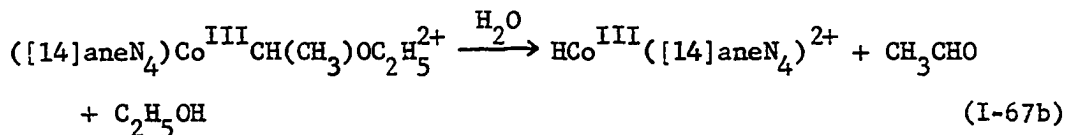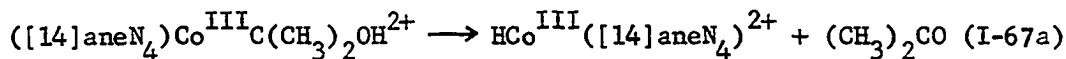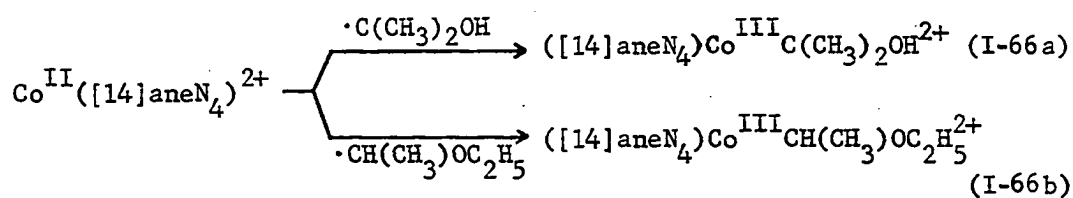
This sequence is essentially analogous to the previously studied reactions of $Co^{II}([14]dieneN_4)^{2+}$ and B_{12r} with the same radicals.

PART II.   REACTIONS OF (ALKYLPEROXY)COBALOXIMES

IN ACIDIC AQUEOUS SOLUTIONS

INTRODUCTION

Literature Background

The reactions involving molecular oxygen and transition metal compounds have continued to receive a great deal of attention, not only because of their catalytic usage in industry (2, 56), but also because of their versatile roles in the biological realm (57). One of the areas in which extensive work has concentrated is the metal catalyzed autoxidation of organic compounds (2). It is known that in almost every case, these reactions occur by radical routes in which peroxo or hydroperoxo complexes are intermediates (2, 58). The direct investigation of peroxo complexes, therefore, attracts special interest.

Many metal peroxides, $M{\overset{O}{\underset{O}{|}}}$ or M-O-O, have been synthesized through oxidative addition reactions of O_2 and the complexes of the following metals: Ti, V, Nb, Cr, Mo, W, U, Co, Rh, Ir and Pt (59). The metal-coordinated dioxygen was found to be generally more reactive than molecular oxygen.

Dinuclear peroxo transition metal complexes have also been reported for these metals: Mn, Fe, Co, Rh and Mo (60). The μ-peroxo dicobalt compounds have been extensively studied. A number of them decompose to give the corresponding mononuclear cobalt(III) complexes and hydrogen peroxide in acidic solutions. One of these cases is the complete hydrolysis of the μ-peroxodecacyanodicobalt ion. Haim and Wilmarth found that the $[(NC)_5Co^{III}-O-O-Co^{III}(CN)_5]^{6-}$ ion requires two equivalents of acid per mole to decompose, in a reaction forming two moles of $(H_2O)Co(CN)_5^{2-}$ ion and one mole of H_2O_2 (61).

$$[(NC)_5Co^{III}\text{-}O\text{-}O\text{-}Co^{III}(CN)_5]^{6-} + 2H^+ + 2H_2O \longrightarrow H_2O_2$$

$$+ 2(H_2O)Co(CN)_5^{2-} \qquad (II\text{-}1)$$
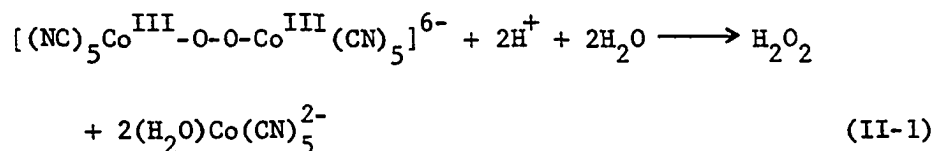
Winfield and his coworkers confirmed this result and proved that the hydrolysis proceeded via the hydroperoxo complex, $HOOCo^{III}(CN)_5^{3-}$ (62):

$$[(NC)_5Co^{III}\text{-}O\text{-}O\text{-}Co^{III}(CN)_5]^{6-} + H^+ \rightleftharpoons$$

$$[(NC)_5Co^{III}\text{-}O\text{-}\overset{H}{\underset{|}{O}}\text{-}Co^{III}(CN)_5]^{5-} \qquad (II\text{-}2)$$

$$[(NC)_5Co^{III}\text{-}O\text{-}\overset{H}{\underset{|}{O}}\text{-}Co^{III}(CN)_5]^{5-} + H_2O \longrightarrow$$

$$HOOCo(CN)_5^{3-} + (H_2O)Co(CN)_5^{2-} \qquad (II\text{-}3)$$

$$HOOCo^{III}(CN)_5^{3-} + H_3O^+ \longrightarrow (H_2O)Co^{III}(CN)_5^{2-} + H_2O_2 \qquad (II\text{-}4)$$
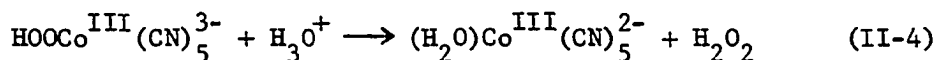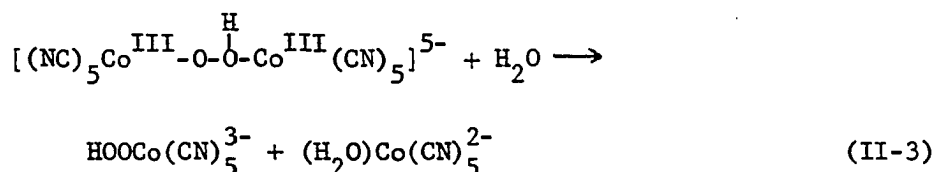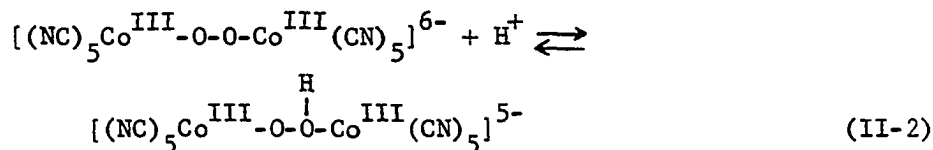
The hydroperoxo cobalt ion was hydrolyzed comparatively slowly, and could be isolated and analyzed as the potassium salt. It may also be synthesized by direct addition of O_2 to $HCo^{III}(CN)_5^{3-}$. Both methods yield the $HOOCo^{III}(CN)_5^{3-}$ ion, which has an absorption maximum at 272 nm.

Another interesting case involving a Co-OOH species is the oxidation of 2-propanol in a solution of Co(salen). The reaction is greatly accelerated, and oxygen uptake takes place in a reversible manner, when triphenylphosphine is added. Kinetic investigations of both the alcohol oxidation reaction and the prereaction equilibrium suggest the formation of a labile complex of $[ROH\cdots\overset{\cdot}{O}_2Co(salen)PPh_3]$. The rate-determining step of the reaction is postulated to involve an outer-sphere hydrogen migration from the alcohol to the dioxygen ligand to

give the hydroperoxo complex, Equation II-5. Further steps in the

reaction were not delineated (63).

$$+ \quad CR_1R_2OH \tag{II-5}$$
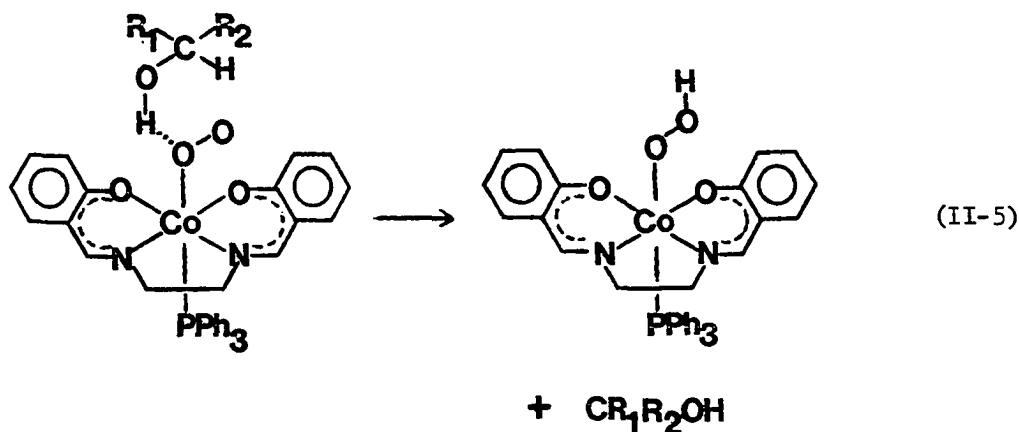
Other metal-coordinated hydroperoxides, such as $Fe^{III}-OOH$, are

commonly invoked to explain the metal ion assisted decomposition of

hydrogen peroxide, or as intermediates in the autoxidation of ferro-

hemoglobin (64).

The organoperoxy metallic compounds, MOOR, of many main group

metals drew increasing attention during the decade of 1960 (65). These

compounds were prepared by the reaction of organometallic compounds

with oxygen or peroxides. For transition metal complexes, however,

very few compounds were known.
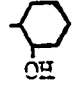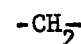
A series of stable organoperoxy cobalt complexes was prepared by

Giannotti, Gaudemer, and their coworkers during the early 1970s. Alkyl-

or aralkylperoxycobaloximes, $R-O-O-Co(dmgH)_2L$ (wherein $R = -CH_3$,

$-C_2H_5$, $-n-C_3H_7$, $-CH(CH_3)_2$, $-CH(CH_3)(C_2H_5)$, $-CH_2CH(CH_3)_2$, $-n-C_5H_{11}$,

$-CH_2CH=CR_2$, $-CH_2C_6H_5$, $-C_6H_{11}$(cyclohexyl), etc.; $L = -OH_2$, N- pyridine,

N- pyrazine, N- piperidine, and their derivatives) may be either photo-

chemically or thermally synthesized by the reaction of molecular

oxygen with alkyl- or aralkylcobaloximes (66). Their structures are shown in Figure II-1.

$$RCo(dmgH)_2L \xrightarrow[\substack{CHCl_3,\ CH_2Cl_2,\ (CH_3)_2CO, \\ C_6H_6,\ aq.\ CH_3OH,\ etc.}]{h\nu(vis)\ or\ \Delta/O_2} ROOCo(dmgH)_2L \qquad (II-6)$$
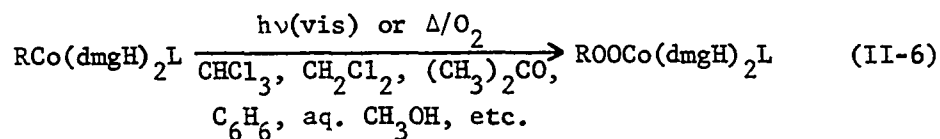
R = alkyl, aralkyl

These peroxo compounds were isolated in the form of reddish-brown to black crystals, the color varying with the alkyl group. They were well-characterized by ^1H and ^{13}C NMR, UV-visible, and IR spectroscopies and elemental analysis. The data indicated that two oxygen atoms were inserted between the alkyl carbon atom and the cobalt atom in the compound. The X-ray structures of ethylphenylperoxy- and cumylperoxy-(pyridine)cobaloximes confirmed this conclusion and showed that the O-Co bond was approximately perpendicular to the pyridine plane and projectively bisected one of the dimethylglyoxime groups (67).

Giannotti et al. have studied the thermal and the photochemical decomposition of $ROOCo(dmgH)_2Py$, (R = [phenyl], [cyclohexyl], $-CH_2$[phenyl with OH], and [naphthyl]) (68). They were irradiated at the wavelength 254 nm or thermalyzed by refluxing in either methanol or benzene. The decomposition of the peroxo group leads to the formation of the corresponding carbonyls (ketones or aldehydes) or alcohols. It was suggested by Giannotti that alkylperoxycobaloxime, like dialkyl peroxides, homolytically cleave to R-O· and M-O· radicals under the conditions used.

In 1976, Bied-Charreton and Gaudemer reported the decomposition of $R-O-O-Co(dmgH)_2Py$, (R = $-CH_2CH_3$, $-CH_2C_6H_5$, $-CH(CH_3)(C_2H_5)$,
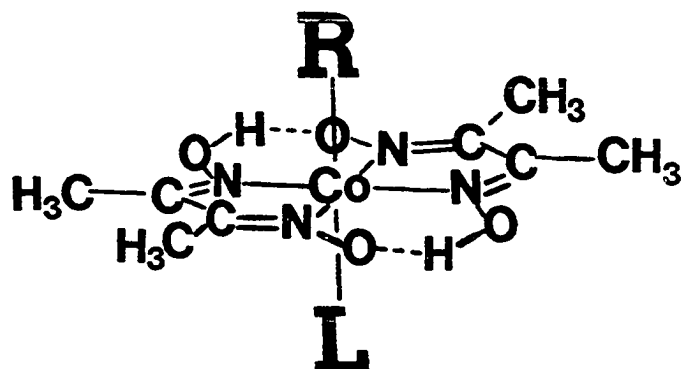
Figure II-1a.   The structure of an organocobaloxime
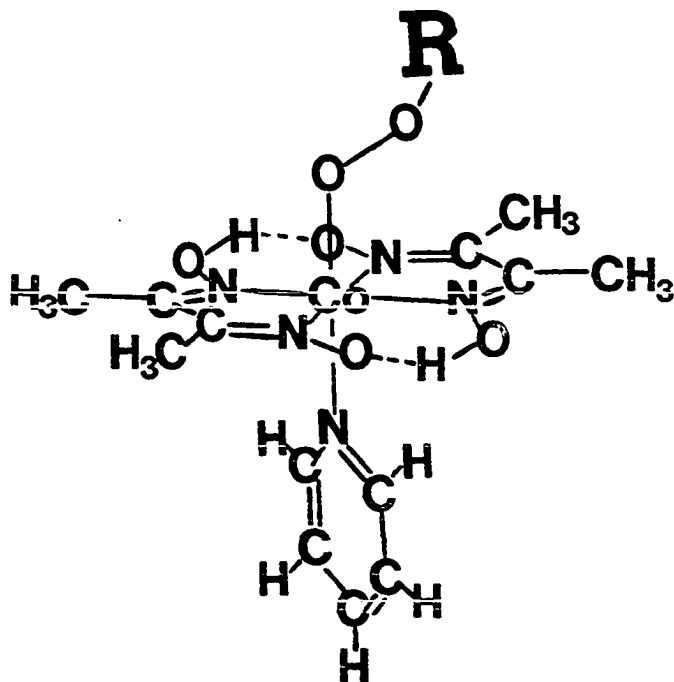
Figure II-1b.   The structure of an organoperoxy(pyridine)cobaloxime

$-CH(C_6H_{13})(CH_3)$, $-CH(C_6H_5)(CH_3)$, $-CH(P-C_6H_5CH_3)(CH_3)$, $-C(CH_3)_2(CH=CH_2)$,

$-C(CH_3)(C_2H_5)(C\equiv CH))$ in acidic nonaqueous solutions (69). The peroxides

were treated with 4% trifluoroacetic acid or 1% perchloric acid in

deuterated chloroform. The relative yields of the organic products

were identified as alkyl hydroperoxides, ketones, aldehydes, and/or

alcohols by ^{1}H NMR. A consecutive mechanism was proposed as Equation

II-7,

$$R_3-\underset{\underset{R_2}{|}}{\overset{\overset{R_1}{|}}{C}}-O-O-Co(dmg)_2Py \xrightarrow{H^+} R_3-\underset{\underset{R_2}{|}}{\overset{\overset{R_1}{|}}{C}}-O-O-H \qquad \begin{array}{l} \nearrow R_1R_2C=O + H_2O \quad (R_3=H) \\ \\ \searrow R_2R_3C=O + R_1OH \quad (R_1 \ne H) \end{array} \qquad (II\text{-}7)$$
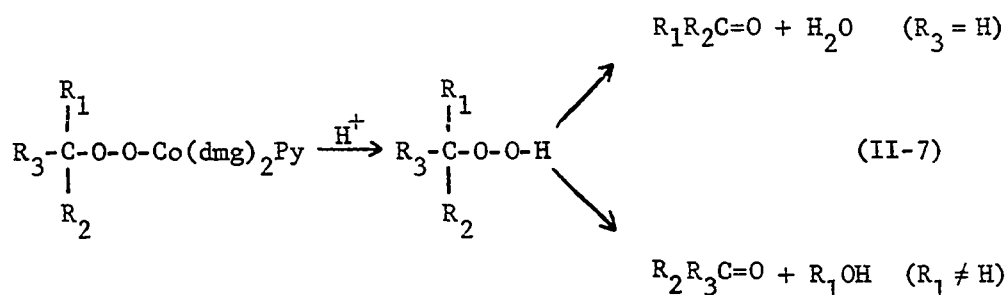
in which the decomposition of alkylperoxycobaloxime first gave the

corresponding alkyl hydroperoxide, ROOH, which was either stable or

further decomposed to give carbonyls or hydroxyl compounds. The reaction

rate was only qualitatively described to be dependent on the nature of

the alkyl groups and the nature of acids. Quantitative kinetic studies,

however, were not done.

Ryan and Espenson recently reported the reaction of isopropyl-

chromium(III) ion with molecular oxygen (70). A rate law with only a

3/2-power dependence on $[CrCH(CH_3)_2^{2+}]$ and no dependence on $[O_2]$ and

$[H^+]$ within the studied region was obtained. The organic products

consist of acetone primarily and smaller amounts of 2-propanol. No

2-propyl hydroperoxide was detected. A chain mechanism containing a

postulated isopropylperoxychromium(III) cation was presented as below:

Initiation: $CrCH(CH_3)_2^{2+} \xrightarrow{\ 1\ } Cr^{2+} + \cdot CH(CH_3)_2$ (II-8)

Propagation: $O_2 + \cdot CH(CH_3)_2 \xrightarrow{\ 2\ } \cdot OOCH(CH_3)_2$ (II-9)

$CrCH(CH_3)_2^{2+} + \cdot OOCH(CH_3)_2 \xrightarrow{\ 3\ } CrOOCH(CH_3)_2^{2+}$

$+ \cdot CH(CH_3)_2$ (II-10)

Termination: $2 \cdot OOCH(CH_3)_2 \xrightarrow{\ 4\ } (CH_3)_2 C{=}O + (CH_3)_2 CHOH + O_2$

(II-11)
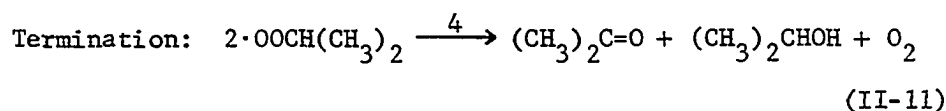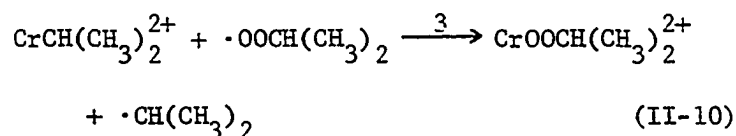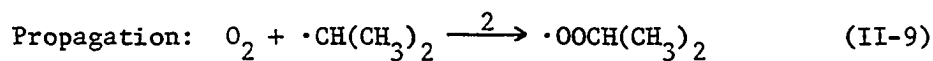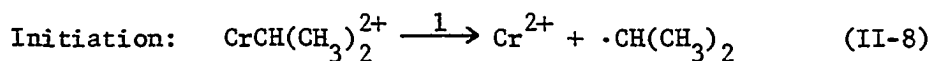
With the steady state approximation for the chain-carrying intermediates
and the assumption of a long chain length, the rate law is derived as
Equation II-12

$$- \frac{d[CrCH(CH_3)_2^{2+}]}{dt} = k_3 \left(\frac{k_1}{2k_4}\right)^{1/2} [CrCH(CH_3)_2^{2+}]^{3/2} \qquad (II\text{-}12)$$

The mechanism shows the isopropylperoxychromium(III) cation as the
immediate product of Equation II-10. It is assumed to react rapidly
with H_3O^+ to yield chromium(III) ion and acetone by the reaction

$$(H_2O)_5 CrOOCH(CH_3)_2^{2+} + H^+ \longrightarrow (CH_3)_2 C{=}O + Cr(H_2O)_6^{3+} \qquad (II\text{-}13)$$
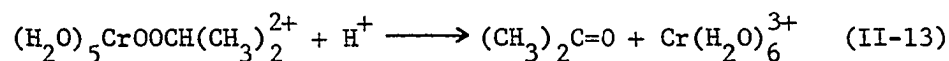
Since the isopropylperoxychromium ion has not been identified yet
among the products, the unavailability of this species for direct
study and observation left the mechanism of its decomposition in acidic
medium as an unsolved problem.

Statement of the Research Problem

To explore kinetics and mechanism of the acid-induced decomposition of the organoperoxy metallic complexes, the stable alkylperoxycobaloximes have been chosen as appropriate species. Among the questions to be answered are how this decomposition reaction actually occurs, and how the alkyl group and the axial ligand influence it. Since the proposed scheme of Equation II-7 has not been verified yet, one would ask whether the alkylperoxycobaloxime was truly decomposed consecutively, such that the ketone is produced by the decomposition of the hydroperoxide, or whether two products are formed in concurrent reactions.

In this project, the reactions of organoperoxycobaloximes with aqueous perchloric acid were studied. The compounds examined are (1) $ROOCo(dmgH)_2(Pyridine)$ complexes with R = 2-propyl, 2-butyl, cyclopentyl, benzyl and d_7-2-propyl and (2) $(CH_3)_2CHOOCo(dmgH)_2L$ complexes with L = pyridine, piperidine, water and ammonia.

^1H NMR has been used throughout to characterize and quantify peroxide reactants and organic and inorganic products. In addition, iodometric titrations were used to analyze the alkyl hydroperoxide, and GLC techniques to identify ketones and to study the kinetics of their formation.

The major kinetic studies were done spectrophotometrically at $25.0 \pm 0.1^\circ C$. The temperature dependence was evaluated only for the 2-butyl-peroxy(pyridine)cobaloxime. The kinetics of the decomposition of $(CD_3)_2CDOOCo(dmgH)_2Py$ was also studied, as was the product yield, the amount of $(CD_3)CDOCH$ being determined by iodometric titration. The latter

experiment was designed to measure whether a significant isotope effect would be found for the ketone formation.

Variation of the axial ligand in the series of 2-propylperoxycobaloxime also permits an evaluation of its effect on the base strength of the oxime oxygens in this series of compounds.

EXPERIMENTAL

Materials

Cobalt compounds

Organocobaloxime, $RCo(dmgH)_2L$ A nucleophilic process gives the
best synthetic method for organocobalt complexes, where the parentheses
represent

$$(Co^{I})^{-} + RX \longrightarrow R\text{-}(Co^{III}) + X^{-} \qquad (II\text{-}14)$$
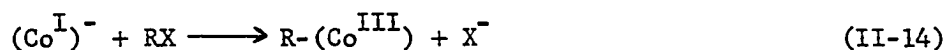
a four-coordinated macrocyclic ring of ligand(s), e.g.: two dimethyl-
glyoximes in this case.

Two preparative procedures have been used in this work. The
first method used to synthesize 2-propyl, d_7-2-propyl, 2-butyl(pyridine)-
cobaloxime, 2-propyl(aquo)cobaloxime and 2-propyl(piperidine)cobaloxime
was carried out by an adaption of the general procedure developed by
Schrauzer (71), in which, $NaBH_4$ was the reducing agent.

Another published procedure followed was the OH^{-} promoted dispro-
portionation of the cobalt(II) complex in the presence of the desired
halide (72)

$$2Co^{II}(dmgH)_2L \xrightarrow{OH^{-}} Co^{I}(dmgH)_2L^{-} + HOCo^{III}(dmgH)_2L \qquad (II\text{-}15)$$

$$Co^{I}(dmgH)_2L^{-} + RX \longrightarrow RCo(dmgH)_2L + X^{-} \qquad (II\text{-}16)$$
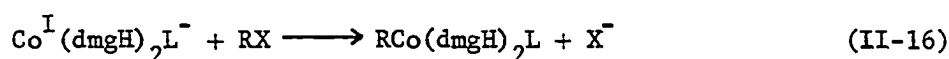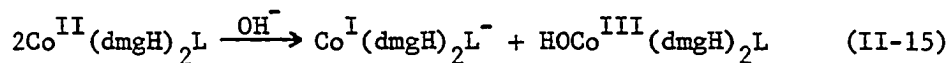
Cyclopentyl(pyridine)cobaloxime and cyclopentyl(aquo)cobaloxime were
prepared by this method.

Alkylperoxycobaloxime, R-O-O-Co(dmgH)$_2$L

R = -CH(CH$_3$)$_2$, -CD(CD$_3$)$_2$, -CH(CH$_3$)(C$_2$H$_5$), and -C$_5$H$_9$(cyclopentyl).

L = pyridine, piperidine, water, and ammonia.

Alkylperoxycobaloximes were prepared by a photoinduced oxygen-insertion method developed by Giannotti and Gaudemer. Details are as follows:

An amount of 100-150 mg of the given alkylcobaloxime with the desired axial ligand was dissolved in 200 mL of solvent (CHCl$_3$, CH$_2$Cl$_2$, aqueous methanol, or acetone). The solution was placed in a Pyrex flask fitted with a gas dispersion tube to promote the dispersal of oxygen. The irradiation was carried out with the temperature maintained between 5-10°C, or at -10°C for the aquo compounds, a vigorous stream of oxygen being maintained throughout. The light, produced by a Sorensen 150 watt XLS1 Xenon lamp, was filtered by a UV filter or a solution of CuSO$_4$ (73). The initially orange solution turned brown during the course of the reaction, which was monitored by TLC until the yellow spot of the starting complex disappeared completely. The solution was evaporated to form a brown solid, which was purified by thin layer chromatography on a silica gel column. A mixture of chloroform-ethyl acetate-methanol with volume ratio of 2:2:1 was used as the eluent. The first reddish-brown band was collected. When CH$_2$Cl$_2$ was used as the solvent of the reaction, the first orange band was CHCl$_2$Co(dmgH)$_2$Py, and the reddish-brown band would contain the peroxo product along with a little ClCo(dmgH)$_2$Py (74). The solvent of the desired fraction was evaporated by mildly blowing air over it. The compound was recrystallized

from methanol.

The final product was in the form of blackish-brown to greenish-brown crystals, varying with the alkyl group, in an overall yield of 50-60%. The preparation of 2-propylperoxy(ammine)cobaloxime started with 2-propyl(aquo)cobaloxime, to which was added an excess of concentrated ammonia, followed by the irradiation.

Diaquocobaloxime perchlorate, $[(H_2O)_2Co(dmgH)_2]ClO_4$ Solid diaquocobaloxime perchlorate provided by G. W. Kirker was made by stirring $H[Cl_2Co(dmgH)_2]$ (75) with $AgClO_4$ in aqueous solution overnight, then crystallized with $LiClO_4$ (76).

A solution containing $[(H_2O)_2Co(dmgH)_2]^+$ ion was also prepared by adding acidic Hg^{2+} into aqueous $CH_3Co(dmgH)_2OH_2$. The resulting solution actually consisted of $(H_2O)_2Co(dmg_2H_3)^{2+}$ ion, CH_3Hg^+, and excess Hg^{2+} ion (77).

(Aquo)(pyridine)cobaloxime perchlorate, $[(H_2O)Co(dmgH)_2Py]ClO_4$ (78) $[(H_2O)Co(dmgH)_2Py]ClO_4$ was prepared by dissolving 119 mg of $[(H_2O)_2Co(dmgH)_2]ClO_4$ in 1 mL H_2O at 5-10°C, to which was then added 0.02 mL of reagent grade pyridine in 1 mL of methanol. Upon mixing these two solutions, a yellow slurry was attained. It was recrystallized from methanol.

Organic compounds

Cyclopentyl hydroperoxide   The starting material, cyclopentyl methane sulfonate was prepared by Mosher's method (79). It was oxidized by H_2O_2 under alkaline conditions (80):

$$\square\text{-OH} + \text{CH}_3\text{SO}_2\text{Cl} \xrightarrow{\text{Pyridine}} \square\text{-O}\overset{\overset{\text{O}}{\|}}{\underset{\underset{\text{O}}{\|}}{\text{S}}}\text{CH}_3 \xrightarrow[\text{KOH}]{\text{H}_2\text{O}_2} \square\text{-OOH} \qquad \text{(II-17)}$$
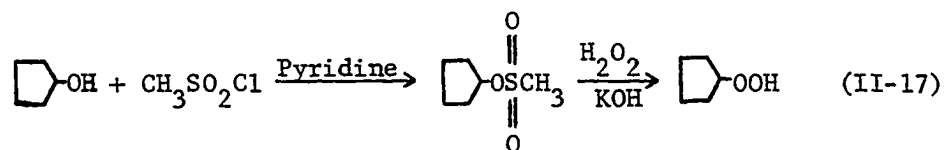
Miscellaneous reagents

The LiClO$_4$ solution was prepared by neutralizing Li$_2$CO$_3$ with HClO$_4$, followed by evaporation of the solvent to yield LiClO$_4$ crystals. After recrystallization, a concentrated stock solution was prepared and standardized by titration of the acid which was displaced from a cation exchange column by a quantitative aliquot of the LiClO$_4$ solution.

Other commercially available reagents, such as: HClO$_4$, CoCl$_2\cdot$6H$_2$O, dimethylglyoxime, alkyl halides, cyclopentanol, methane sulfonylchloride, etc. were used without further purification.

Methods

Characterization of the synthesized compounds

Elemental analyses for C, H and N were done by the Ames Laboratory analytical service group. Cobalt was determined as Co(NCS)$_4^{2-}$ spectrophotometrically ($\varepsilon_{623\ nm} = 1842\ \text{M}^{-1}\text{cm}^{-1}$) after fuming the sample in perchloric acid. Their data are listed in Table II-1.

The cobalt compounds were also characterized by electronic absorption and ^{1}H NMR spectroscopies; the latter affords the most characteristic features useful for the identifications.

The UV-visible spectra were recorded using a Cary 219 spectrophotometer. The analogous species exhibit similar absorptions. Spectra of 2-propylcobaloximes and 2-propylperoxycobaloximes are shown in Figures II-2 and II-3,

Table II-1. Data of elemental analysis of some cobalt complexes

Compound	Formular weight	% found (calcd.)			
		C	H	N	Co
c-C_5H_9Co(dmgH)$_2$py	437	49.05(49.43)	6.40(6.50)	15.39(16.01)	13.50(13.47)
c-C_5H_9OOCo(dmgH)$_2$py	469	45.70(46.06)	5.93(6.01)	14.70(14.92)	—
iso-C_3H_7OOCo(dmgH)$_2$py	443	42.69(43.34)	5.78(5.90)	15.66(15.80)	—
[H_2OCo(dmg$_2H_3$)py](ClO$_4$)$_2$	586	27.00(26.6)	4.15(3.75)	12.34(11.9)	11.87(10.1)
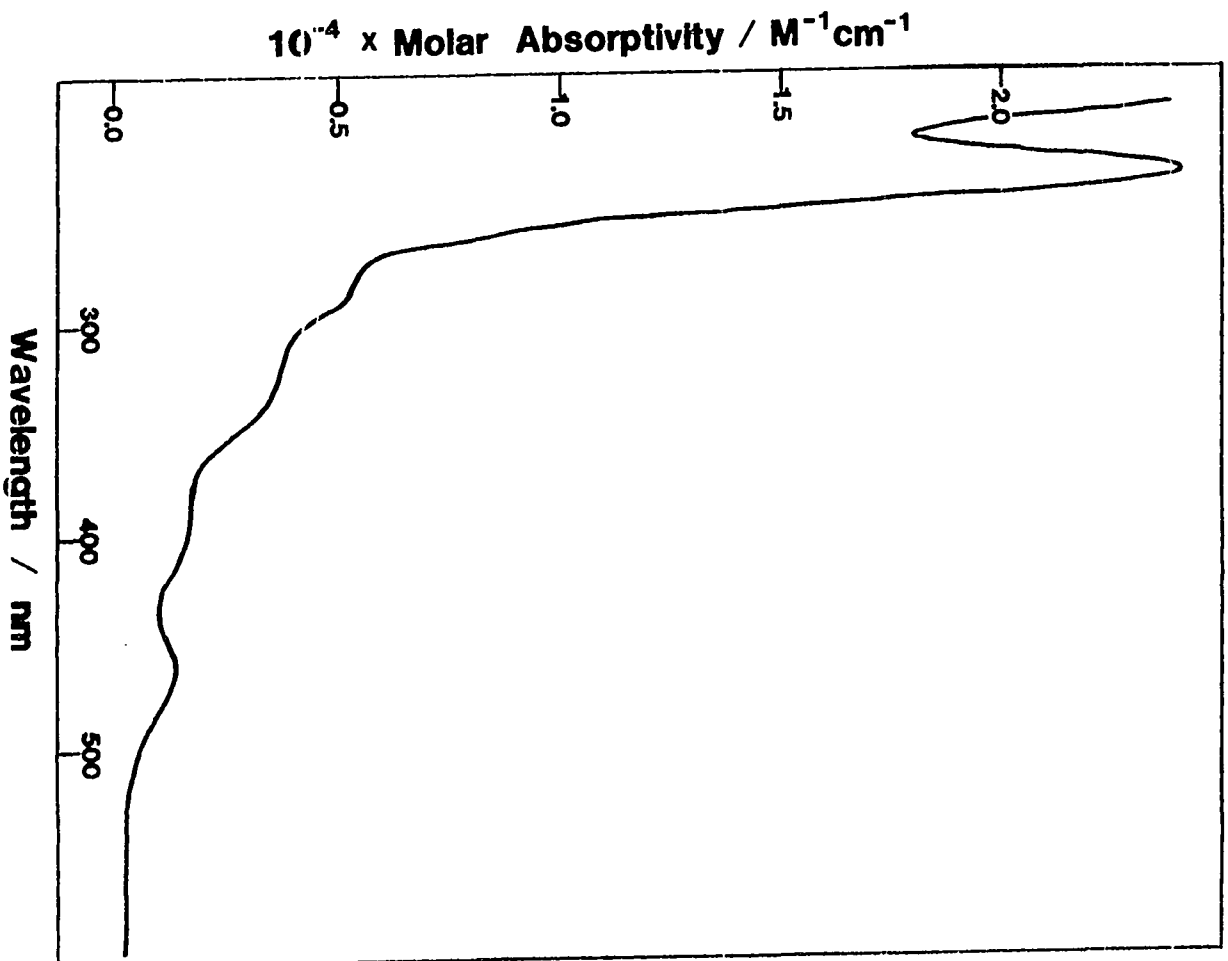
Figure II-2. The UV-visible spectrum of $(CH_3)_2CHCo(dmgH)_2Py$ in H_2O, pH 7

73
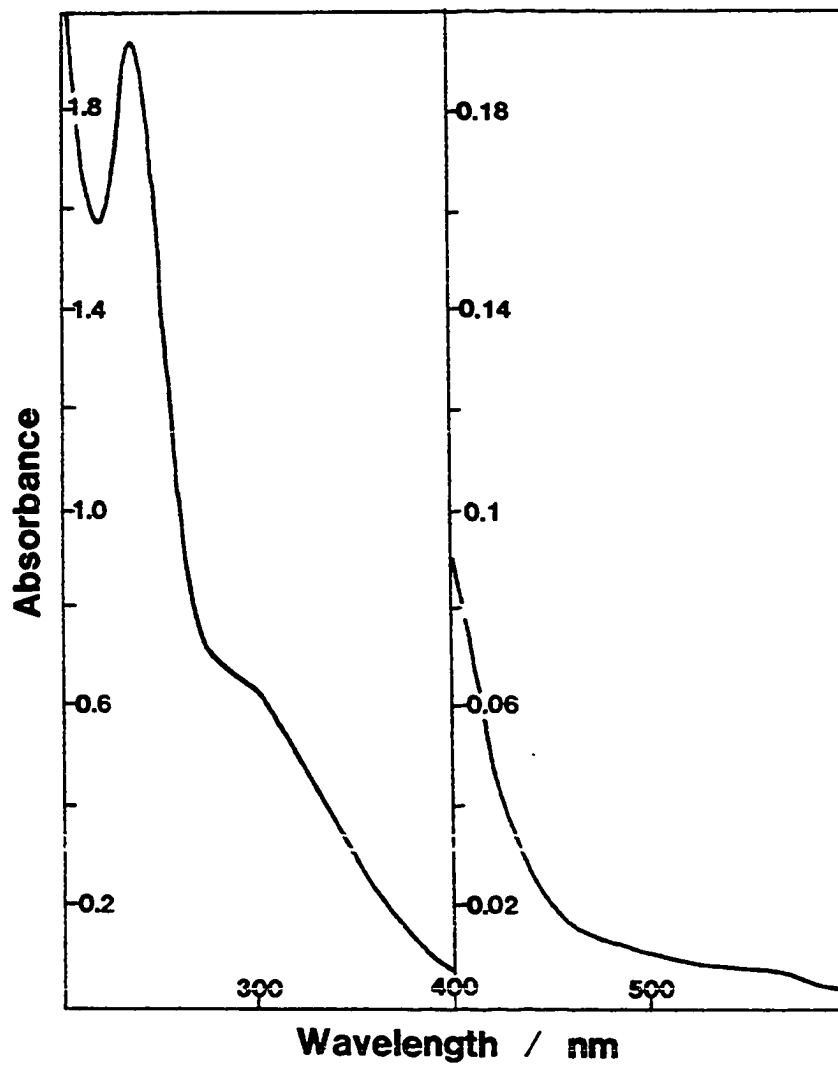
Figure II-3. The UV-visible spectrum of 8.0 x 10^{-5}M $(CH_3)_2CHOOCo(dmgH)_2Py$. The absorption range is 2.0 in the region of λ 200-400 nm and 400-600 nm, 1 cm path length

and a complete data summary is shown in Table II-2. The NMR spectra

were taken at room temperature on a 60 MHz of Perkins-Hitachi R-20B

high resolution model or a Varian HA-100 spectrometer. Figures II-4

to II-6 show these spectra of the cobalt compounds.

The ^{1}H NMR spectra of cyclopentyl methane sulfonate and cyclopentyl

hydroperoxide are shown in Figures II-7 and II-8. The later compound

was also characterized with a high resolution AE1-902 mass spectrometer.

Its molecular weight was evaluated as 102.06805 (calculated 102.06808).

The spectrum is shown in Figure II-9. Table II-3 gives the complete

^{1}H NMR data.

Product identification

In addition to the NMR studies of the products, as will be il-

lustrated later, gas chromatography and an iodometric titration method

were used to do either qualitative or quantitative analyses for the

organic products.

A gas chromatograph instrument, Hewlett-Packard Model 5700A, was

used to analyze the products from 2-propylperoxy(pyridine)cobaloxime

after decomposition by acid in aqueous solution, and a Tracor 560 instru-

ment was used for cyclopentylperoxy(pyridine)cobaloxime. In both

cases, a 10% FFAP column was used with a column temperature of 100°C.

The major product in each case was identified by examining the overlap

of the most prominent peak from the sample solution in comparison

with the peak obtained for the authentic compound.

A method of iodometric titration originally used for hydrogen

peroxide was satisfactorily used to determine the amount of alkyl

Table II-2. Data for UV-visible absorption of the cobalt complexes

Compound	Solvent	
(a) Organocobaloximes[a]		
iso-$C_3H_7Co(dmgH)_2$-Py	H_2O	462(-)
iso-$C_3D_7Co(dmgH)_2$-Py	MeOH/H_2O	462(-)
iso-$C_3H_7Co(dmgH)_2$-OH_2	H_2O	462(1300)
iso-$C_3H_7Co(dmgH)_2$-Pip	H_2O	462(1300)
sec-$C_4H_9Co(dmgH)_2$-Py	H_2O	462(-)
c-$C_5H_9Co(dmgH)_2$-Py	H_2O	460(-)
c-$C_5H_9Co(dmgH)_2$-OH_2	MeOH/H_2O	460(-)
(b) Alkylperoxycobaloximes		
iso-$C_3H_7OOCo(dmgH)_2$-Py	H_2O	298sh(8100)
iso-$C_3D_7OOCo(dmgH)_2$-Py	H_2O	294sh(6000)
iso-$C_3H_7OOCo(dmgH)_2$-OH_2	H_2O	292sh(7500)
iso-$C_3H_7OOCo(dmgH)_2$-pip	H_2O	288sh(9000)
iso-$C_3H_7OOCo(dmgH)_2$-NH_3	H_2O	288sh(5100)
c-$C_5H_9OOCo(dmgH)_2$-Py	H_2O	280sh(-)
(c) Inorganic $Co^{(III)}$-Cobaloximes		
[$(H_2O)_2Co(dmgH)_2$][ClO_4][b]	H_2O	340(2000)
($H_2O)Co(dmgH)_2$Py](ClO_4)	H_2O	340sh(-)

[a]Organocobaloximes "instantaneously" lose axial base in aqueous solution; the species being studied is thus $RCo(dmgH)_2OH_2$.

[b]From R. A. Heckmann, Ph.D. dissertation, Iowa State University; see Ref. (37).

λ_{max}/nm (ϵ/dm^{3}mol^{-1}cm^{-1})			
386sh(-)	320sh(-)	280sh(-)	230(-)
388sh (-)	320sh(-)	288sh(-)	230(-)
386sh(1600)	320sh(4200)	280sh(6200)	230(24000)
382sh(1700)	316sh(3800)	280sh(5400)	230(24000)
384sh(-)	320sh(-)	280sh(-)	230(-)
380sh(-)	316sh(-)	278sh(-)	230(-)
380sh(-)	320sh(-)	280sh(-)	Not determined
242(24000)	—	—	—
244(18000)	—	—	—
244(23000)	—	—	—
244(22000)	—	—	—
244(15000)	—	—	—
244(-)	—	—	—
240(21000)	—	—	—
242(24000)	—	—	—
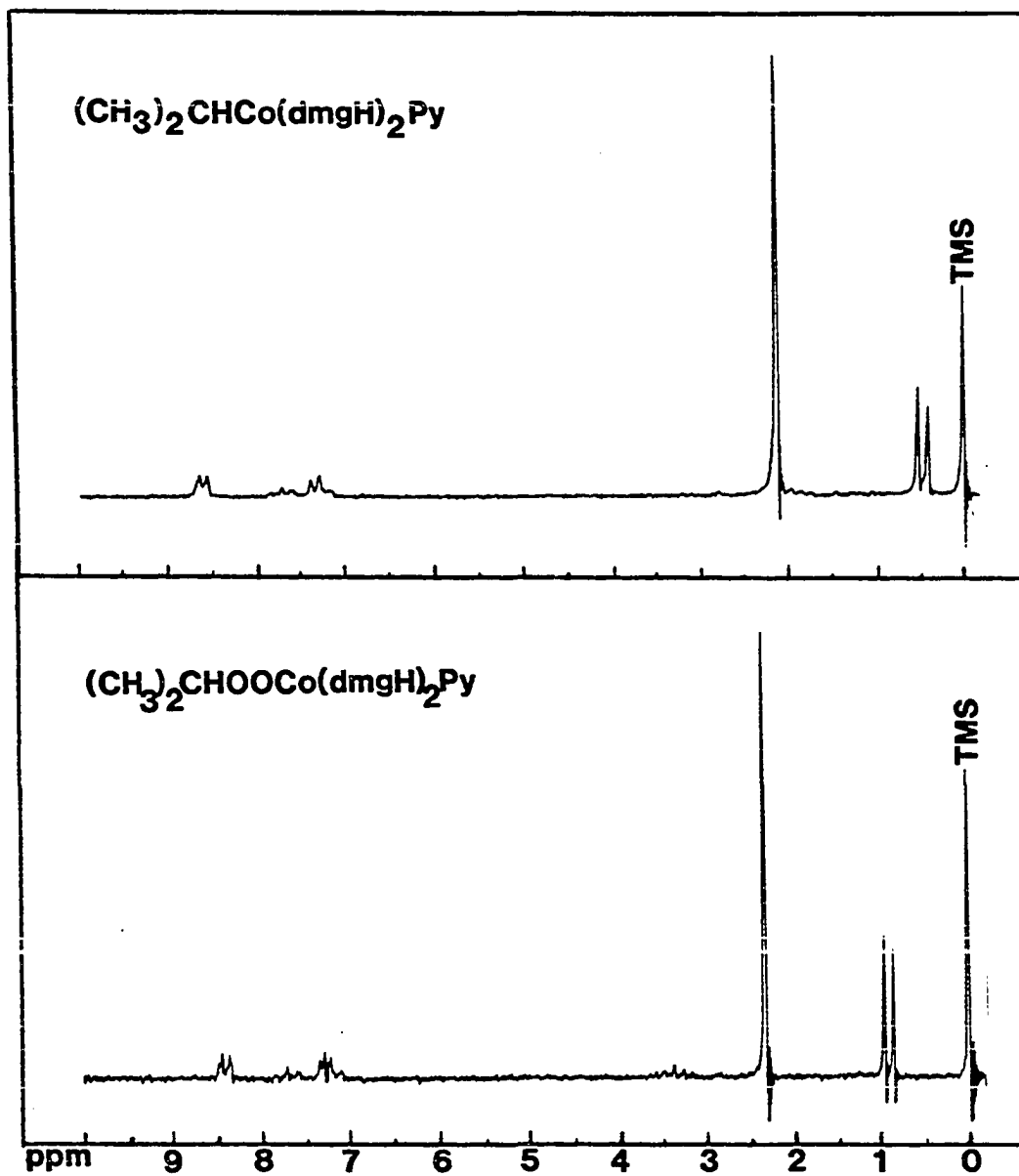
Figure II-4. The ¹H NMR spectra of 2-propyl- and 2-propylperoxy(pyridine)-cobaloximes in CDCl₃
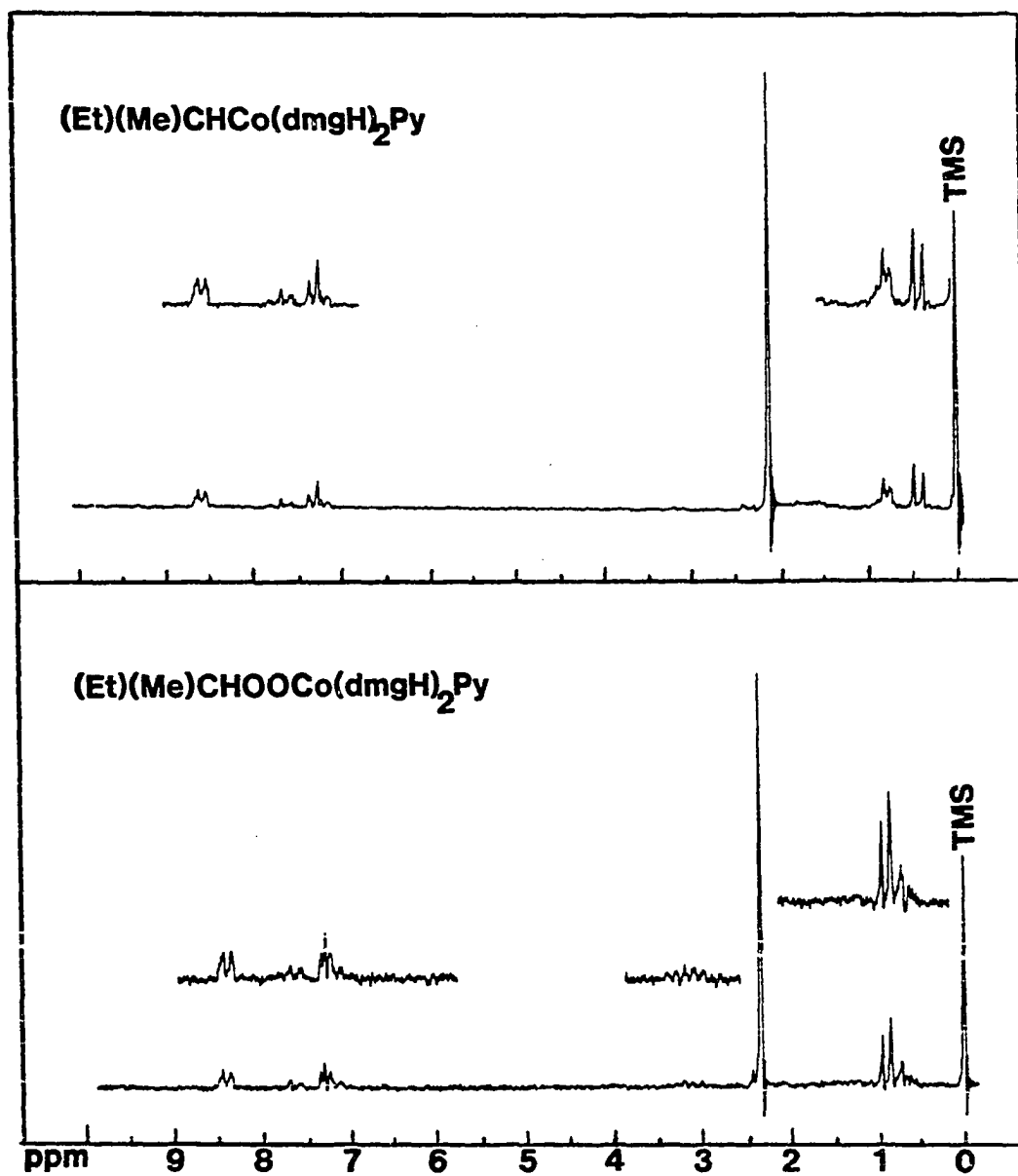
Figure II-5. The ^{1}H NMR spectra of 2-butyl- and 2-butylperoxy(pyridine)-cobaloximes in CDCl$_3$
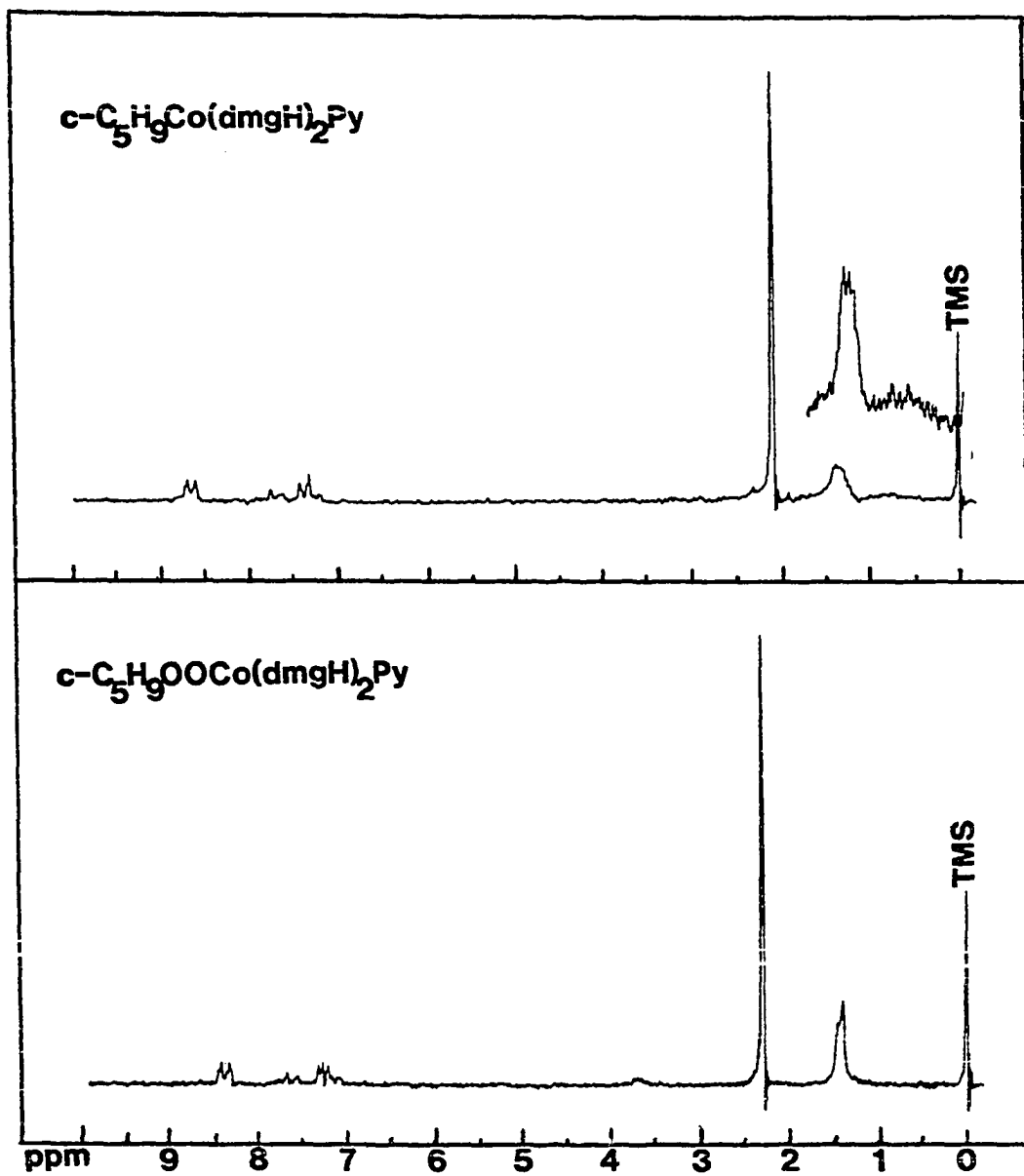
Figure II-6. The ^{1}H NMR spectra of cyclopentyl- and cyclopentylperoxy-(pyridine)cobaloximes in CDCl$_3$
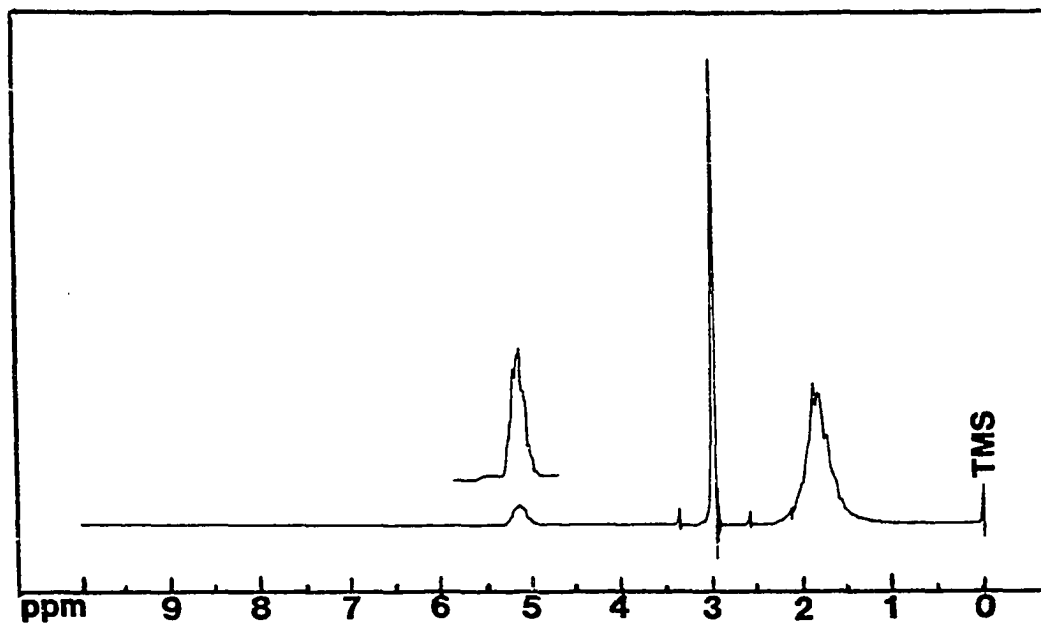
Figure II-7. The ^{1}H NMR spectrum of cyclopentyl methanesulfonate, neat sample

Figure II-8. The ^{1}H NMR spectrum of cyclopentyl hydroperoxide, neat sample
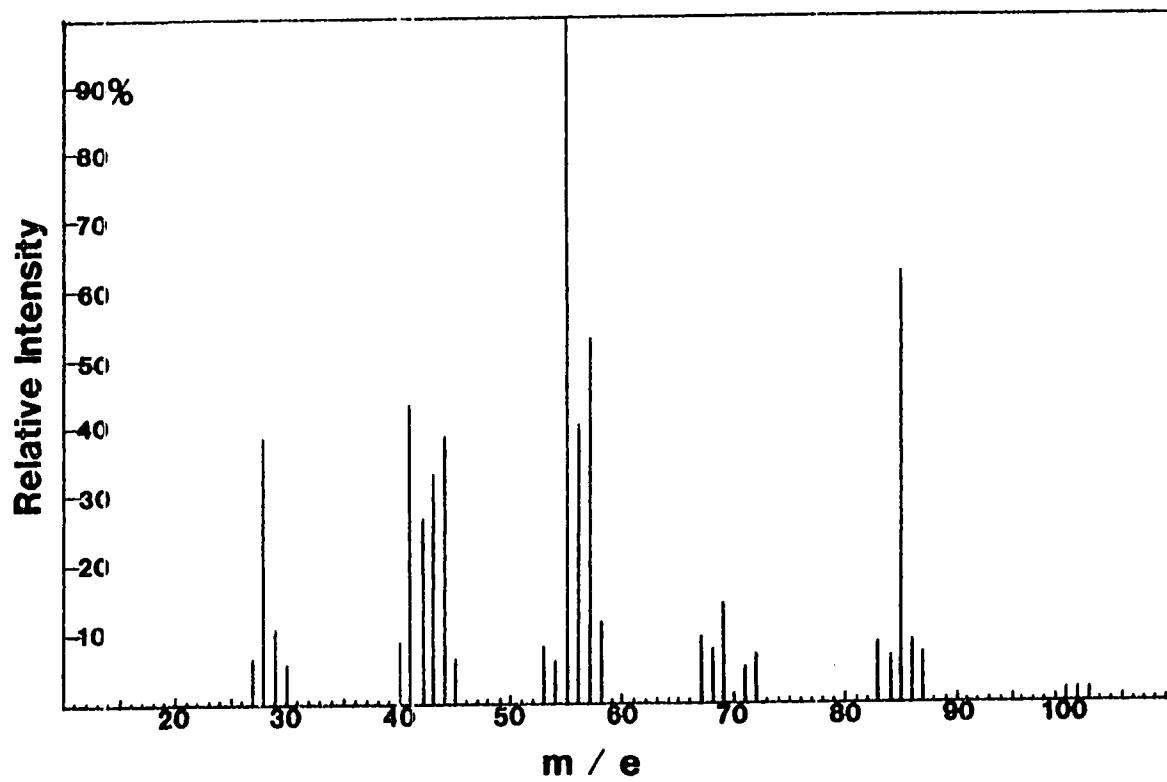
Figure II-9. The mass spectrum of cyclopentyl hydroperoxide, anal. mass: 102.06805, clcd. mass: 102.06808

Table II-3. ^{1}H NMR data of synthesized compounds

	Compound	Solvent
Part A.	**Organocobaloximes**	
	iso-$C_3H_7Co(dmgH)_2$-Py	$CDCl_3$
	iso-$C_3D_7Co(dmgH)_2$-Py	$CDCl_3$
	iso-$C_3H_7Co(dmgH)_2$-OH_2	CD_3OD
	iso-$C_3H_7Co(dmgH)_2$-Pip	$CDCl_3$
	iso-$C_3H_7Co(dmgH)_2$-NH_3	D_2O
	(Et)(Me)$CHCo(dmgH)_2$-Py	$CDCl_3$
	c-$C_5H_9Co(dmgH)_2$-Py	$CDCl_3$
	c-$C_5H_9Co(dmgH)_2$-OH_2	CD_3OD
Part B.	**Alkylperoxycobaloximes**	
	iso-$C_3H_7OOCo(dmgH)_2$-Py	$CDCl_3$
	iso-$C_3D_7OOCo(dmgH)_2$-Py	$CDCl_3$
	iso-$C_3H_7OOCo(dmgH)_2$-OH_2	D_2O
	iso-$C_3H_7OOCo(dmgH)_2$-Pip	D_2O
		$CDCl_3$

Chemical shift/ppm vs. TMS						
Alkyl group				CH$_3$-DMGH	Base ligand		

0.46(d) -CH(CH$_3$)$_2$	2.13(m) -CH(CH$_3$)$_2$			2.13(s)	8.48(m) Hα-Py	7.28(m) Hβ-Py	7.69(m) Hγ-Py
—	—			2.12(s)	8.59(m) Hα-Py	7.25(m) Hβ-Py	7.68(m) Hγ-Py
0.20(d) -CH(CH$_3$)$_2$	2.23(m) -CH(CH$_3$)$_2$			2.23(s)	—		
0.37(d) -CH(CH$_3$)$_2$	2.28(m) -CH(CH$_3$)$_2$			2.28(s)	1.56(m,6H)	2.77(m,4H)	
0.41(d) -CH(CH$_3$)$_2$	2.21(m) -CH(CH$_3$)$_2$			2.21(s)	—		
0.43(d) -CH$_3$(Me)	0.83(t) -CH$_3$(Et)	1.2(m) -CH$_2$(Et)	1.63(m) -CH	2.13(s)	8.58(m) Hα-Py	7.28(m) Hβ-Py	7.58(m) Hγ-Py
1.40(m) (CH$_2$)$_4$	2.11(m) -CH			2.11(s)	8.67(m) Hα-Py	7.35(m) Hβ-Py	7.77(m) Hγ-Py
1.33(m) (CH$_2$)$_4$	2.23(m) -CH			2.23(s)	—		
0.91(d) -CH(CH$_3$)$_2$	3.40(m) -CH(CH$_3$)$_2$			2.30(s)	8.37(m) Hα-Py	7.26(m) Hβ-Py	7.67(m) Hγ-Py
—	—			2.30(s)	8.37(m) Hα-Py	7.22(m) Hβ-Py	7.64(m) Hγ-Py
0.79(d) -CH(CH$_3$)$_2$	3.15(m) -CH(CH$_3$)$_2$			2.53(s)	—		
0.81(d)	3.23(m)			2.45(s)	1.35(m,6H)	2.67(m,4H)	
0.84(d) -CH(CH$_3$)$_2$	3.21(m) -CH(CH$_3$)$_2$			2.42(s)	1.45(m,6H)	1.73(m,4H)	

Table II-3. Continued

Compound	Solvent
iso-C_3H_7OOCo(dmgH)$_2$-NH_3	D_2O
	CD_3OD
(Et)(Me)CHOOCo(dmgH)$_2$-Py	$CDCl_3$
c-C_5H_9OOCo(dmgH)$_2$-Py	$CDCl_3$
Part C. Organic compounds	
Cyclopentyl methane sulfonate	Neat $CDCl_3$
Cyclopentyl hydroperoxide	Neat $CDCl_3$ D_2O

Chemical shift/ppm vs. TMS				CH$_3$-DMGH	Base ligand		
Alkyl group							
0.85(d)	3.35(m)			2.43(s)	—		
0.81(d)	—			2.37(s)	—		
-CH(C<u>H</u>$_3$)$_2$	-C<u>H</u>(CH$_3$)$_2$						
0.91(d)	0.74(t)	1.15(m)	3.13(m)	2.30(s)	8.37(m)	7.20(m)	7.66(m)
CH$_3$(Me)	CH$_3$(Et)	CH$_2$(Et)	-CH		Hα-Py	Hβ-Py	Hγ-Py
1.42(m)	3.68(m)			2.28(s)	8.38(m)	7.26(m)	7.68(m)
(CH$_2$)$_4$	-CH				Hα-Py	Hβ-Py	Hγ-Py
1.80(m)	3.00(s)	5.15(m)					
1.68(m)	3.00(s)	5.15(m)					
(CH$_2$)$_4$	-CH$_3$	-CH					
1.68(m)	4.63(m)	8.40(s)					
1.68(m)	4.63(m)	5.88(s)					
1.68(m)	4.63(m)	—					
-(CH$_2$)$_4$	-CH	-OOH					

hydroperoxide (81). The sample solution was prepared in a total volume of 25.0 mL and contained 1M of $HClO_4$ and alkylperoxycobaloxime of the order of millimolar concentration. This solution was deaerated with N_2 for more than two hours which was long enough to let the reaction go over 99% completion without air oxidation of iodide. This solution was divided into several portions. Into each portion, a large excess ($\sim$ 1 g) of NaI was added, followed by 5 drops of saturated starch indicator. The dark purple solution was titrated with 3.007 x 10^{-3}M $Na_2S_2O_3$ solution to light yellow. The relative stoichiometric relationship for produced ROOH and $S_2O_3^{2-}$ is 1:2 according to the equations below.

$$ROOH + 2I^- + 2H^+ \longrightarrow I_2 + H_2O + ROH \qquad \text{(II-18)}$$

$$I_2 + 2S_2O_3^{2-} \longrightarrow S_4O_6^{2-} + 2I^- \qquad \text{(II-19)}$$
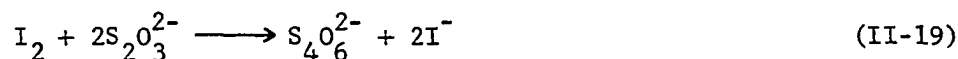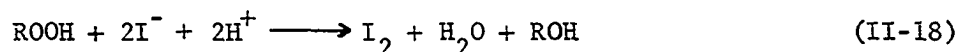
Kinetics

Spectrophotometry   Two methods were used to study the kinetics. The first one was the conventional spectrophotometric method which was carried on all peroxo cobaloximes. The concentration of perchloric acid in the runs was varied from 0.001M to 0.1M. It was present in large excess over alkylperoxycobaloxime to achieve pseudo-first-order conditions. Lithium perchlorate was used to adjust the ionic strength to 1.00M. All solutions were well thermostated at 25.0 $\pm$ 0.1°C, then mixed in a 1 cm quartz cell. After shaking the mixture for several seconds, the reactions were monitored using Cary 219 spectrophotometer by measuring the absorbance decrease of alkylperoxycobaloximes at about

300 nm versus time.

The pseudo-first-order rate constants, k_{obsd}, were determined by evaluating the slopes of the plots of $\ln(D_t - D_\infty)$ against time according to Equation II-20

$$\ln(D_t - D_\infty) = \ln(D_o - D_\infty) - k_{obsd}t \tag{II-20}$$

where D_o, D_t and D_∞ are the respective absorbance readings at the initial time, time t and at the completion of the reaction. One example for the reaction of $(CH_3)_2CHOOCo(dmgH)_2Py$ is shown in Figure II-10. The values of k_{obsd} were mostly calculated by a nonlinear least-squares program, but occasionally by a graphical method.

In some kinetic runs, a two-stage reaction was observed. The plots of $\ln(D_t - D_\infty)$ vs. time in such cases consisted of two added straight line segments according to Equation II-21

$$D_t - D_\infty = \alpha e^{-k_I t} + \beta e^{-k_{II} t} \tag{II-21}$$

If $k_I > k_{II}$, k_{II} may be determined simply by measuring the slope of the long-term linear portion of the plot. The k_I value will be calculated by constructing a new parameter, Δ,

$$\Delta = D_t - D_\infty - \beta e^{-k_{II} t} = \alpha e^{-k_I t} \tag{II-22}$$

where $\beta e^{-k_{II} t}$ for each t was obtained by estimating the value at time t on the extrapolating line of the slow portion, and a plot of $\ln\Delta$ against time affords k_I. A typical case of this biphasic reaction is illustrated in Figure II-11; the corresponding data are given in Table II-4.
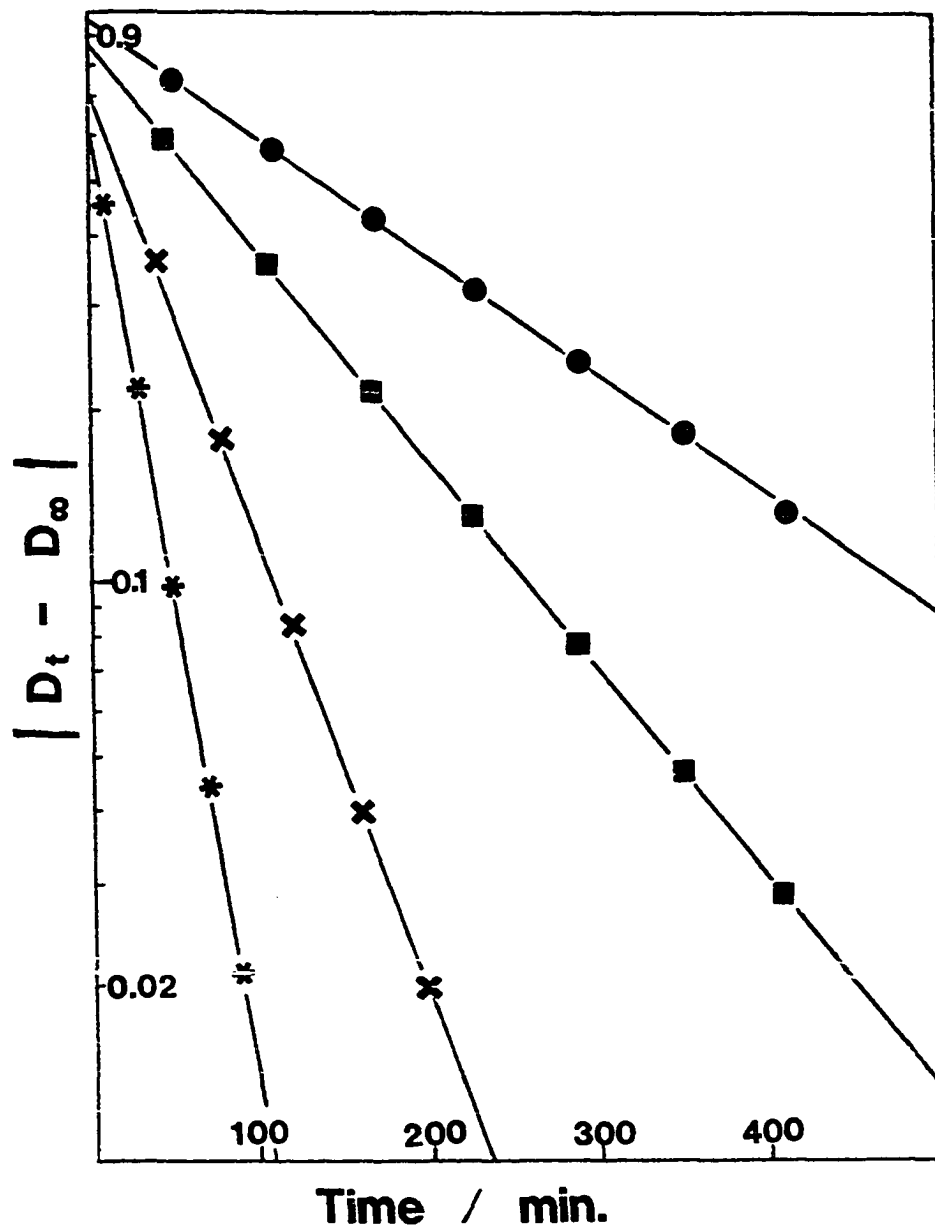
Figure II-10. The pseudo-first-order plots of the decomposition of
(CH$_3$)$_2$CHOOCo(dmgH)$_2$Py at 25.0°C, μ = 1.0M [H$^+$] =
0.0099M (●); 0.03M (■); 0.07M (✗); and 0.6M (✳)
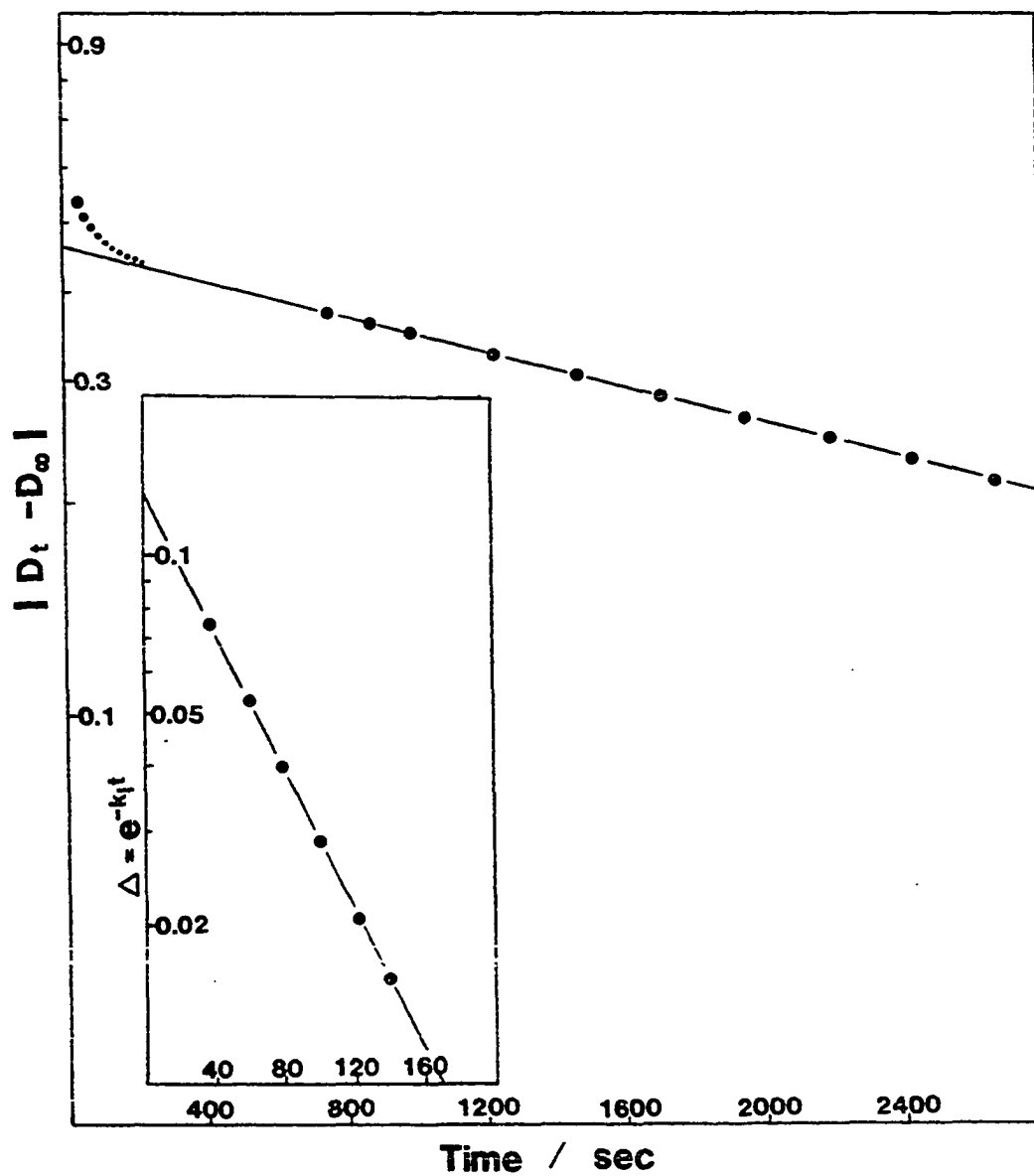
Figure II-11. The pseudo-first-order plots for the biphasic kinetic data of Table II-4, the reaction of 9.0×10^{-5}M $(CH_3)_2CHOOCo(dmgH)_2Py$ with 0.07M $HClO_4$ at 25.0°C, μ = 1.0M

Table II-4. The data for a typical biphasic kinetic experiment[a] on
the decomposition of a mixture of $(CH_3)_2CHOOCo(dmgH)_2Py$
and $(CH_3)_2CHOOCo(dmgH)_2OH_2$ by perchloric acid

t/s	D_t	χ[b]	Δ[c]	t/s	D_t
40	0.474	0.228	0.0375	750	0.397
60	0.462	0.226	0.0270	870	0.391
80	0.454	0.225	0.0200	990	0.385
100	0.447	0.224	0.0140	1230	0.373
120	0.443	0.223	0.0105	1470	0.363
140	0.439	—	—	1710	0.352
160	0.436	—	—	1950	0.344
180	0.433	—	—	2190	0.335
200	0.431	—	—	2430	0.326
220	0.429	—	—	2670	0.319
				∞	0.209

[a]Conditions of this reaction are $[(CH_3)_2CHOOCo(dmgH)_2Py]_0 =$
$9.0 \times 10^{-5}M$, $[H^+] = 0.07049M$, $\mu = 1.0$, $\lambda = 320$ nm, $T = 25.0°C$,
optical path 1 cm.

[b]$\chi = \beta e^{-k_{II}t}$.

[c]$\Delta = D_t - D_\infty - \chi = \alpha e^{-k_I t}$.

Gas chromatography   In addition to the spectrophotometric method,
the reaction was also monitored by measuring the formation rate of
the ketone by gas chromatography. These studies were only done for
2-propylperoxy(pyridine)cobaloxime and cyclopentylperoxy(pyridine)-
cobaloxime.

The reaction solutions consisted of alkylperoxycobaloxime in

millimolar concentration, and 0.2M $HClO_4$ for the 2-propyl or 0.1M $HClO_4$ for the cyclopentyl complex. The ionic strength was fixed at 1.0M. Temperature was not controlled in the course of the reaction, but reasonably estimated as $23 \pm 2^{o}C$. The peaks corresponding to the products were identified by comparison with reagent grade acetone and cyclopentanone, and their peak heights were measured against time. Since the sensitivity of the instrument varied occasionally, certain organic reagents were added as internal reference. In the reaction of the 2-propyl system, 2-propanol was used as the standard, and acetone was used for the cyclopentyl system. The ratios of the peak heights of ketone to the peak heights of the standard were plotted vs. time, allowing the apparent rate constants of the formation of ketone to be determined and compared with that obtained spectrophotometrically.

RESULTS

Product Analysis

^{1}H NMR analysis

The organic products of the decomposition of secondary-alkylperoxy-cobaloximes $R_1R_2CHOOCo(dmgH)_2L$, by aqueous perchloric acid have been identified as a mixture of secondary-alkyl hydroperoxide, R_1R_2CHOOH, and ketone, $R_1R_2C=O$. The ^{1}H NMR analyses of the products were done for $(CH_3)_2CHOOCo(dmgH)_2L$ with L = pyridine, piperidine, and water, $(CH_3)(C_2H_5)CHOOCo(dmgH)_2Py$ and $c-C_5H_9OOCo(dmgH)_2Py$.

According to Ried-Charreton and Gaudemer's study, 2-butylperoxy-(pyridine)cobaloxime was exclusively decomposed to 2-butyl hydroperoxide by 4% CF_3COOH in $CDCl_3$ (69). Reaction (3) repeated this experiment, and the data exhibited in Table II-5 confirmed this result. In Entry (8), the cyclopentyl complex was reacted with CF_3COOH under the same condition. The product was confirmed to be cyclopentyl hydroperoxide, because its NMR spectrum was in good agreement with that of the authentic sample. Their data are listed in Entries (10) and (11). The reaction product of 2-propylperoxy(pyridine)cobaloxime with CF_3COOH shown in Entry (1) was reasonably recognized as 2-propyl hydroperoxide.

The NMR data for the alkyl hydroperoxides and for the authentic ketones as the standards, the organic products of the Reactions 2, 5, 6, 7, and 9 in Table II-5 are identified and summarized in Table II-6. Their yields were afforded by integration of the areas of the corresponding resonances. A typical spectrum of reaction 5, illustrated in Figure II-12, gives positive evidence for the formation of 2-butanone

Table II-5. The ^{1}H NMR data of the organic products of the decomposition of $R_1R_2CHOOCo(dmgH)_2L$ by perchloric acid
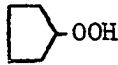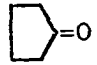
Reaction	Solvent	Chemical shift/ppm (δ)	
		R_1R_2CHOOH	$R_1R_2C{=}O$
(1) $(CH_3)_2CHOOCo(dmgH)_2Py$ + CF_3COOH	$CDCl_3$	1.27(d) 4.34(m) -CH_3 -CH	
(2) $(CH_3)_2CHOOCo(dmgH)_2Py$ + $HClO_4$	D_2O	1.18(d) 4.23(m) -CH_3 -CH	2.22(s) -CH_3
(3) $(C_2H_5)(CH_3)CHOOCo$- $(dmgH)_2Py$ + CF_3COOH	$CDCl_3$	0.93(t) 1.25(d) 1.58(m) 4.15(m) CH_3(Et) CH_3(Me) CH_2(Et) -CH	
(4) $(C_2H_5)(CH_3)CHOOCo$- $(dmgH)_2Py$ + $HClO_4$	$CDCl_3$	0.93(t) 1.23(d) 1.55(m) 4.02(m) CH_3(Et) CH_3(Me) CH_2(Et) -CH	2.12(s) 1.04(t) CH_3(Me) CH_3(Et)
(5) $(C_2H_5)(CH_3)CHOOCo$- $(dmgH)_2Py$ + $HClO_4$	D_2O	0.88(t) 1.18(d) 1.53(m) 4.01(m) CH_3(Et) CH_3(Me) CH_2(Et) -CH	2.19(s) 1.00(t) 2.57(m) CH_3(Me) CH_3(Et) CH_2(Et)
(6) $(CH_3)_2CHOOCo(dmgH)_2Pip$ + $HClO_4$	D_2O	1.19(d) 4.23(m) -CH_3 -CH	2.25(s) -CH_3
(7) $(CH_3)_2CHOOCo(dmgH)_2H_2O$ + $HClO_4$	D_2O	1.19(d) 4.23(m) -CH_3 -CH	

94

Table II-5. Continued

Reaction	Solvent	Chemical shift/ppm (δ)	
		R_1R_2CHOOH	$R_1R_2C=O$
(8) c-C_5H_9OOCo(dmgH)$_2$Py + CF_3COOH	CDCl$_3$	1.70(m) 4.66(m) -(CH$_2$)$_4$ -CH	
(9) c-C_5H_9OOCo(dmgH)$_2$Py +HClO$_4$	CDCl$_3$[a]	1.72(m) 4.58(m) -(CH$_2$)$_4$ -CH	1.99(m) 2.14(m) -CH$_2$ -CH$_2$
(10) C_5H_9OOH	CDCl$_3$	1.70(m) 4.63(m) 6.63(m) -(CH$_2$)$_4$ -CH -OOH	
(11) C_5H_9OOH + HClO$_4$	D$_2$O	1.72(m) 4.60(m) -(CH$_2$)$_4$ -CH	
(12) C_5H_9OOH + HClO$_4$ + HClO$_4$	D$_2$O	1.70(m) 4.60(m) -(CH$_2$)$_4$ -CH	1.99(m) 2.26(m) -CH$_2$ -CH$_2$
(13) (CH$_3$)$_2$CO	D$_2$O		2.22(s) -CH$_3$
(14) (C$_2$H$_5$)(CH$_3$)CO	D$_2$O		2.20(s) 1.00(t) 2.58(q) CH$_3$(Me) CH$_3$(Et) CH$_2$(Et)

[a]Using CDCl$_3$ as the solvent instead of D$_2$O is because of the low solubility of c-C_5H_9OOCo(dmgH)$_2$Py in D$_2$O.

Table II-6. Organic products of the decomposition of secondary-
alkylperoxycobaloximes by perchloric acid

Reaction	Solvent	Organic product (% yield)	
$(CH_3)_2CHOOCo(dmgH)_2Py$ + $HClO_4$	D_2O	H_3C—CHOOH (65%) H_3C	H_3C—C=O (35%) H_3C
$(CH_3)_2CHOOCo(dmgH)_2Pip$ +$HClO_4$	D_2O	H_3C—CHOOH (71%) H_3C	H_3C—C=O (29%) H_3C
$(CH_3)_2CHOOCo(dmgH)_2OH_2$ +$HClO_4$	D_2O	H_3C—CHOOH (100%) H_3C	
$(C_2H_5)(CH_3)CHOOCo(dmgH)_2Py$ +$HClO_4$	D_2O	H_5C_2—CHOOH (65%) H_3C	H_5C_2—C=O (35%) H_3C
$c-C_5H_9OOCo(dmgH)_2Py$ +$HClO_4$	$CDCl_3$	⬠—OOH	⬠=O

and 2-butyl hydroperoxide. All peaks owing to ketone are enhanced,
showing that it is feasible to recognize this product by adding authentic
2-butanone to the reacted solution. It was found that all these acidified
solutions containing hydroperoxide and ketone remained stable for more
than 24 hours during which they showed exactly the same NMR spectra.
That indicated that alkyl hydroperoxides were stable toward decomposition
to ketone in acidic aqueous solution. In other words, alkyl hydro-
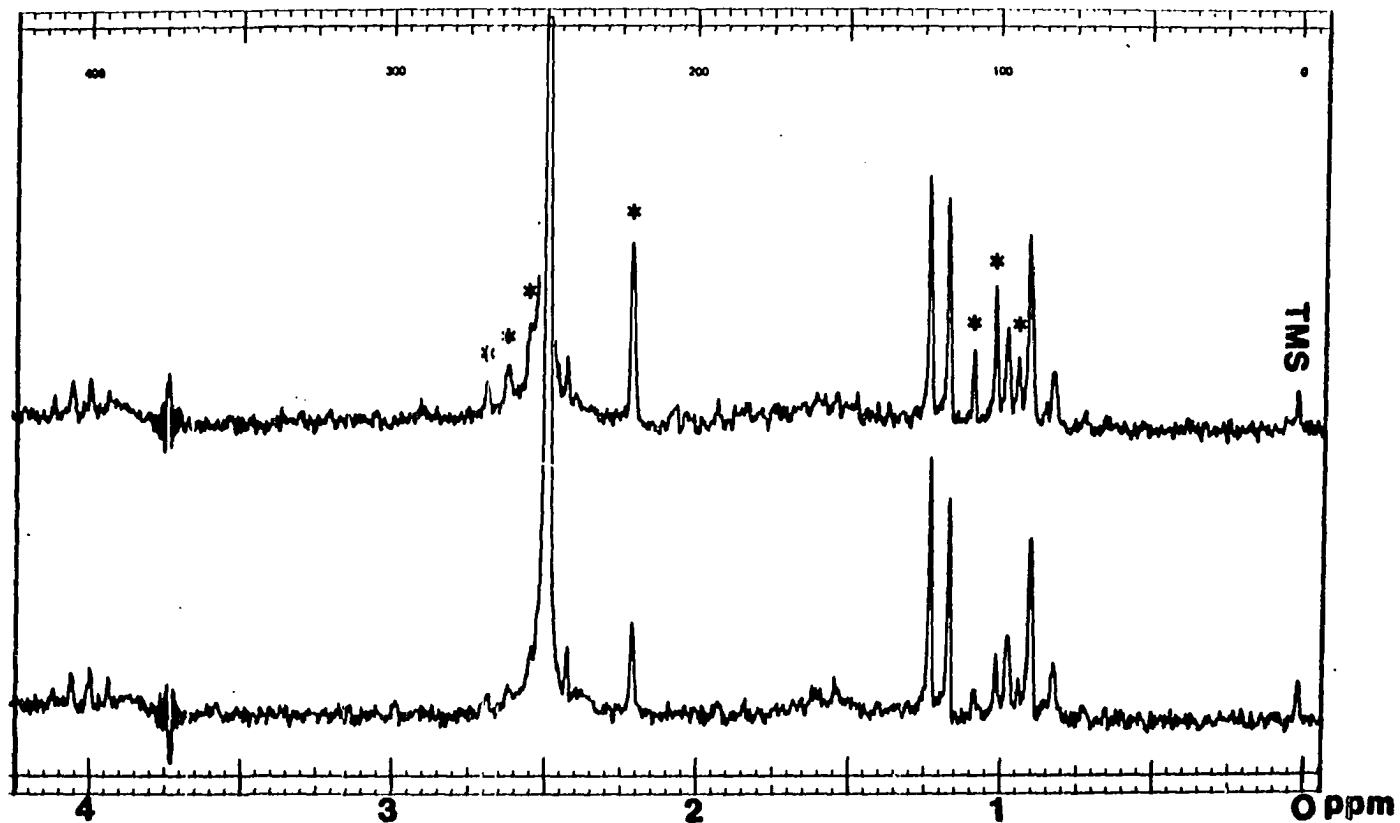
Figure II-12. The ^{1}H NMR spectrum of a mixture of 2-butanone, 2-butyl hydroperoxide, and
H$_2$OCo(dmgH)$_2$Py$^+$ ion, produced from the decomposition of 2-butylperoxy(pyridine)-
cobaloxime by conc. HClO$_4$ in D$_2$O. The data are analyzed in Table II-5, Entry (5).
Adding trace of 2-butanone into the solution, all ketone peaks (labeled with *)
are enhanced

peroxide and ketone were formed in parallel during the decomposition of the alkylperoxo cobalt complex, and not formed subsequently.

The inorganic cobalt products of the reactions investigated were identified as cobalt(III) complexes in which the original axial ligand coordinated to the cobaloxime was retained. That is, the reactions formed $(H_2O)Co^{III}(dmgH)_2L^+$, recognized by NMR studies, and not $(H_2O)_2Co^{III}(dmgH)_2^+$. Table II-7 gives these data; the pyridine resonances are not good evidence for identification, since they are not well-distinguished from free pyridinium ion, but the sharp singlet of the $(dmgH)_2$-methyl groups is very useful for distinction.

A yellow precipitate named as product X in Table II-7, collected from a reacted solution of saturated 2-propylperoxy(pyridine)cobaloxime and excess of perchloric acid, was recrystallized from methanol. Its NMR spectrum has a sharp singlet at 2.5 ppm (δ) due to the $(dmgH)_2$-methyl groups, which matches satisfactorily with that of $H_2OCo(dmgH)_2Py^+$ ion, and is distinguishable from $(H_2O)_2Co(dmgH)_2^+$ ion. Also from the elemental analysis, product X is believed to be protonated aquo-(pyridine)cobaloxime salt, $[(H_2O)Co(dmg_2H_3)Py](ClO_4)_2$ Anal: calcd. for $C_{13}H_{22}N_5Cl_2O_{13}Co$: C, 27.00; H, 4.15; N, 12.34; Co, 11.87, found: C, 26.6; H, 3.75; N, 11.9; Co, 10.1.

The NMR spectrum of the cobalt product of the decomposed $(CH_3)_2CHOOCo(dmgH)_2OH_2$ agrees with that of $(H_2O)_2Co(dmgH)_2^+$, having the resonance of the $(dmgH)_2$-methyl groups at 2.7 ppm (δ). The piperidine species gives the corresponding singlet at 2.6 ppm (δ) under the same conditions, which is apparently distinct from either

Table II-7. The ^{1}H NMR data of the cobalt(III) products and other known cobalt species

Compound or condition	Solvent	Chemical shift/ppm (δ)			
		CH_3(DMG)	Axial ligand		

Part A: $(H_2O)_2Co(dmgH)_2^+$ ion

(1) $[(H_2O)_2Co(dmgH)_2]ClO_4$	CD_3OD	2.71(s)			
(2) $[(H_2O)_2Co(dmgH)_2]ClO_4$ $+$ $HClO_4$	D_2O	2.70(s)			
(3) $CH_3Co(dmgH)_2H_2O$ $+$ $Hg^{2+}/HClO_4$	H_2O	2.69(s)			

Part B: $(H_2O)Co(dmgH)_2Py^+$ ion

			Hα-Py	Hβ-Py	Hγ-Py
(4) $[(H_2O)Co(dmgH)_2Py]ClO_4$	$(CD_3)_2CO$	2.51(s)	7.95(m)	7.3(m)	7.8(m)
(5) $[(H_2O)_2CO(dmgH)_2]ClO_4$ $+$ $HClO_4$ $+$ Py(Xs)	D_2O	2.51(s)	$-^a$		
(6) $CH_3Co(dmgH)_2H_2O$ $+$ $Hg^{2+}/HClO_4$ $+$ Py(Xs)	H_2O	2.52(s)	$-^a$		

Part C: Real System:

(7) $ROOCo(dmgH)_2Py + HClO_4$ R $=$ 2-propyl, 2-butyl or cyclopentyl	D_2O	2.49(s)	7.93(m)	7.3(m)	7.75(m)
(8) Product X^b	CD_3OD	2.52(s)	8.0(m)	7.3(m)	7.8(m)
	$(CD_3)_2CO$	2.50(s)	7.95(m)	7.3(m)	7.8(m)
(9) Product X $+$ $HClO_4$	D_2O	2.48(s)	7.95(m)	7.3(m)	7.8(m)

^{a}Signals covered by the strong resonances of free pyridine.

^{b}Product X is the crystal sample which was obtained from the reaction of saturated aqueous $(CH_3)_2CHOOCo(dmgH)_2Py$ and excess of $HClO_4$, then crystallized from methanol.

Table II-7. Continued

Compound or condition	Solvent	CH$_3$(DMG)	Axial ligand		
		Chemical shift/ppm (δ)			
(10) [H$_2$OCo(dmgH)$_2$Py]ClO$_4$ + Product X	(CD$_3$)$_2$OD	2.51(s)	7.95(m)	7.3(m)	7.8(m)
(11) [(H$_2$O)$_2$Co(dmgH)$_2$]ClO$_4$ + Product X + HClO$_4$	D$_2$O	2.48(s) 2.70(s)	7.95(m)	7.3(m)	7.8(m)
(12) (CH$_3$)$_2$CHOOCo(dmgH)$_2$Pip + HClO$_4$	D$_2$O	2.60(s)	1.37(m,6H)	2.40(m,4H)	
(13) (CH$_3$)$_2$CHOOCo(dmgH)$_2$OH$_2$ + HClO$_4$	D$_2$O	2.70(s)			

(H$_2$O)Co(dmgH)$_2$Py$^+$ or (H$_2$O)$_2$Co(dmgH)$_2^+$ ion. It is thought to be

(H$_2$O)Co(dmgH)$_2$Pip$^+$.

Iodometric titration

The amount of alkyl hydroperoxides from the reactions of 2-propyl

complex and its deuterated analogue was determined by iodometric titra-

tion. A test for a standard H$_2$O$_2$ solution shows good accuracy and

reproducibility in Table II-8.

Table II-8. Titrations of standard H$_2$O$_2$ solution

Volume of 0.1M H$_2$O$_2$/mL	Volume of 0.003007M Na$_2$S$_2$O$_3$/mL	Calculated [H$_2$O$_2$]/M
1.0	6.52	0.09802
1.5	9.80	0.09823
2.0	13.10	0.09848

The imitative solutions containing known amounts of hydrogen peroxide, pyridine, acetone, diaquocobaloxime ion, perchloric acid or the combination of these species showed no influence on the titration. The data are shown in Table II-9.

Tables II-10 and II-11 give the data of the titrations for the real systems, in which the percentage yields of hydroperoxide are listed in the last column. The average yield of $(CH_3)_2CHOOH$ produced by the acid decomposition of $(CH_3)_2CHOOCo(dmgH)_2Py$ is 58%, which is consistent, within experimental error, with the 65% yield determined by the NMR measurements and is believed to be more precise than the latter. For the deuterated system, the average yield of $(CD_3)_2CDOOH$ is 92%.

Kinetics

Spectrophotometry

The kinetics were studied in aqueous solution. Since some pyridine complexes were not very soluble in water, vigorous and long-term stirring was necessary at times to dissolve the solid cobalt compounds prior to initiation of the reaction by addition of $HClO_4$. A spectrophotometric method was used for the kinetic measurements. First of all, the spectral scans of the reaction were done to decide the best wavelength for kinetic monitoring and the proper concentration of the peroxy complexes to give a good absorbance change. A typical set of scans is shown in Figure II-13. After mixing the reactants, an instant drop at the 300 nm shoulder and an instant rise at the 244 nm absorption maximum may be seen on the spectra. This can be attributed to the rapid protonation equilibrium at one of the oxime oxygen atoms,

Table II-9. Titrations of H_2O_2 in imitative solutions

	Solution I	Solution II	Solution III
Amount of H_2O_2 deliberately added (mmol)	0.09824	0.09824	0.09824
Volume of pyridine (mL)	—	—	0.14(1.7 mmol)
Volume of acetone (mL)	—	—	0.15(1.8 mmol)
Weight of $[(H_2O)_2Co(dmgH)_2]ClO_4$ (mg)	—	65(0.15 mmol)	83(0.20 mmol)
Volume of 1M $HClO_4$ (mL)	10	10	10
Volume of 0.03007M $Na_2S_2O_3$ (mL)	6.48	6.55	6.40
Calculated amount of H_2O_2 (mmol)	0.0974	0.0985	0.0962

Table II-10. Titrations of isopropyl hydroperoxide

Amount of $(CH_3)_2CHOOCo(dmgH)_2Py$ in reacted solution mmol	Volume of reacted solution mL	Volume of 0.003007M $Na_2S_2O_3$ mL	Amount of $(CH_3)_2CHOOH$ mmol	% relative yield of $(CH_3)_2CHOOH$
3.34×10^{-2}	10.0	11.85	1.78×10^{-2}	53
3.34×10^{-2}	10.0	12.45	1.87×10^{-2}	56
3.34×10^{-2}	10.0	14.00	2.10×10^{-2}	63
1.68×10^{-2}	5.0	6.40	9.62×10^{-3}	57
1.75×10^{-2}	5.2	8.20	1.23×10^{-2}	56
3.36×10^{-2}	10.0	12.60	1.89×10^{-2}	70
2.21×10^{-2}	6.0	8.10	1.22×10^{-2}	55
3.16×10^{-2}	8.6	12.20	1.83×10^{-2}	58
3.68×10^{-2}	10.0	13.40	2.01×10^{-2}	55

$$ROOCo(dmgH)_2L + H^+ \rightleftharpoons ROOCo(dmg_2H_3)L^+ \qquad (II-23)$$

which is shifted to the right upon addition of H^+. Following this, the
spectrum steadily changed and showed an isosbestic point at $\lambda 265$ nm
during the cleavage reactions with H^+, indicating that the protonated
species decomposed to a single cobalt product. Since all alkylperoxy-
cobaloximes have similar electronic spectra, the decay of the shoulder
at $\lambda 300$ nm was chosen to measure the kinetic runs.

The reaction studied under a large excess of $[H^+]$, followed
pseudo-first-order kinetics. The linearity of the standard plots of
$\ln(D_t - D_\infty)$ vs. time of most runs lasted for five half-lives confirming

Table II-11. Titrations of d_7-isopropyl hydroperoxide

Amount of $(CD_3)_2CDOOCo(dmgH)_2Py$ in reacted solution mmol	Volume of reacted solution mL	Volume of 0.003007M $Na_2S_2O_3$ mL	Amount of $(CD_3)_2CDOOH$ mmol	% relative yield of $(CD_3)_2CDOOH$
2.53×10^{-2}	7.0	15.30	2.30×10^{-2}	91
2.67×10^{-2}	7.4	16.15	2.43×10^{-2}	91
3.61×10^{-2}	10.0	22.75	3.42×10^{-2}	95
2.04×10^{-2}	5.0	15.10	2.27×10^{-2}	112
3.91×10^{-2}	9.6	24.05	3.62×10^{-2}	93
4.07×10^{-2}	10.0	23.35	3.51×10^{-2}	86
1.56×10^{-2}	5.2	88.60	1.29×10^{-2}	83
3.00×10^{-2}	10.0	17.30	2.60×10^{-2}	87
3.00×10^{-2}	10.0	19.50	2.93×10^{-2}	98

the first-order dependence on $[ROOCo(dmgH)_2L]$. The kinetic data for all the organoperoxycobaloximes are listed in Tables II-12 to II-18.

In some of these runs for the 2-propyl complexes, biphasic kinetics were observed. The rate constants for the slow portion are in agreement with other runs containing the same acid concentrations, but the first stage of the reaction gave an apparent rate constant, k^f_{obsd}, approximately 500 times greater, and an appreciable absorbance change, generally 20-30% of the total. Table II-19 gives these data which showed that values of k'_{obsd} and k^f_{obsd} are satisfactorily consistent with values of k_{obsd} for $(CH_3)_2CHOOCo(dmgH)_2Py$ and $(CH_3)_2CHOOCo(dmgH)_2OH_2$ in Tables II-12 and II-18, respectively, within the experimental error.
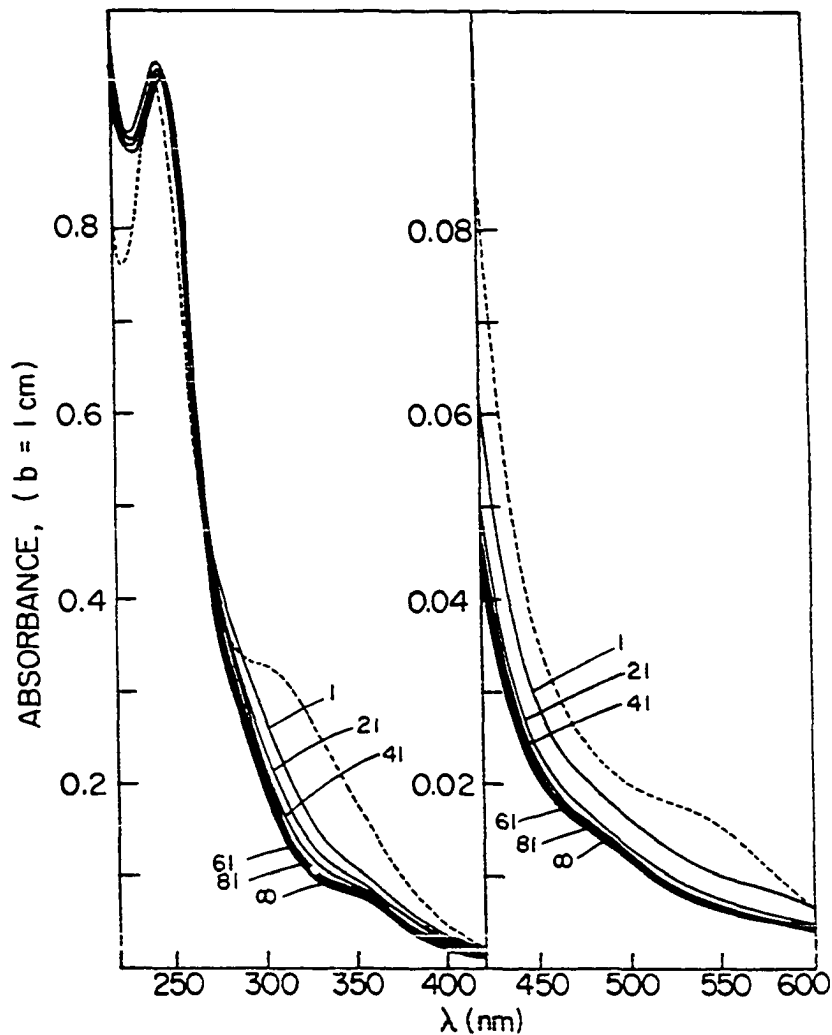
Figure II-13. UV-visible spectral scans during reactions of
$(CH_3)_2CHOOCo(dmgH)_2Py$ with $HClO_4$. Conditions: $[H^+]$ =
0.500M, μ = 1.0M, T = 25.0°C, $t_{1/2}$ = 18 min. (k_{obsd} =
6.42 x $10^{-4}s^{-1}$, $10^4[Complex]_o$ = 1.5M (right), 0.40M
(left)). The number shown for each spectrum is the
time (min.) at which the scan was begun. The dotted
line shows the spectrum of an unacidified solution of
the same complex at μ = 1.0M, the difference between it
and the first spectrum recorded in 0.500M H^+ solution
arising from the rapidly established protonation
equilibrium of Equation II-23.

Table II-12. Kinetic data for $(CH_3)_2CHOOCo(dmgH)_2Py + HClO_4$, at 25.0 ± 0.1°C, $\mu = 1.0M$

$10^4[Complex]_o/M$	$[H^+]/M$	$10^4 k_{obs}/s^{-1}$
—	0.00987	0.556 ± 0.003
—	—	0.563 ± 0.003
—	—	0.603 ± 0.004
4.98	0.0151	0.7869 ± 0.0005
4.95	0.0201	0.984 ± 0.004
4.95	0.0201	1.021 ± 0.004
4.90	0.0302	1.416 ± 0.03
4.90	0.0302	1.415 ± 0.003
—	0.0404	1.79 ± 0.05
—	0.0404	1.99 ± 0.09
1.54	0.0404	1.91 ± 0.05
3.84	0.0503	2.39 ± 0.05
3.84	0.0503	2.37 ± 0.05
1.92	0.0503	2.30 ± 0.01
2.88	0.0602	2.41[a]
2.88	0.0602	2.35
1.74	0.0700	3.16 ± 0.07
1.74	0.0700	3.08 ± 0.08
1.54	0.0700	3.06 ± 0.04
1.00	0.0799	3.22 ± 0.05
1.54	0.0799	3.10 ± 0.01
2.88	0.0898	3.08
2.88	0.0898	3.08
1.00	0.0898	3.10
1.00	0.0898	3.34 ± 0.06
1.54	0.0996	3.75 ± 0.02
1.92	0.0996	3.50 ± 0.009
1.92	0.1331	3.87 ± 0.01
1.92	0.1331	4.06 ± 0.01
3.84	0.2003	4.99 ± 0.04
3.84	0.2003	5.01 ± 0.05
1.54	0.2996	5.48 ± 0.01
2.03	0.6042	6.511 ± 0.009
2.03	0.6042	6.516 ± 0.011
2.03	0.6042	6.47 ± 0.01
2.10	0.9399	6.84 ± 0.02
2.10	0.9399	6.46 ± 0.01
2.10	0.9399	7.66 ± 0.05

[a]Data without standard deviation were analyzed by graphical method.

Table II-13. Kinetic data for $2\text{-}C_4H_9OOCo(dmgH)_2Py + HClO_4$ at $\mu = 1.0M$

$10^4[\text{Complex}]_o/M$	$[H^+]/M$	$T/^\circ C$	$10^4 k_{obs}/s^{-1}$
2.0	0.0101	25.0	0.688 ± 0.007
2.0	0.0101	25.0	0.655 ± 0.006
2.0	0.0151	25.0	1.001 ± 0.004
2.0	0.0151	25.0	0.752 ± 0.006
2.0	0.0201	25.0	1.294 ± 0.003
2.0	0.0302	25.0	1.848 ± 0.004
3.5	0.0404	25.3	2.188 ± 0.018
3.5	0.0404	25.3	2.186 ± 0.019
3.5	0.0799	25.4	3.362 ± 0.006
3.5	0.0799	25.4	3.328 ± 0.006
4.6	0.0996	25.7	4.156 ± 0.008
4.6	0.0996	25.7	4.164 ± 0.010
5.5	0.1499	25.7	4.674 ± 0.015
5.5	0.1499	25.7	4.737 ± 0.014
4.6	0.2003	25.7	5.156 ± 0.021
4.6	0.2003	25.7	5.414 ± 0.020
5.5	0.2996	25.5	6.142 ± 0.025
1.2	0.6042	25.0	7.57 ± 0.05
1.2	0.6042	25.0	7.66 ± 0.04
1.2	0.6042	25.0	7.61 ± 0.04
2.2	0.9399	25.0	8.17 ± 0.01
1.2	0.9399	25.0	8.11 ± 0.02
1.2	0.9399	25.0	8.09 ± 0.01
3.2	0.0404	15.8	0.5178 ± 0.0050
3.2	0.0799	15.8	0.7840 ± 0.0004
3.0	0.1331	15.8	1.105 ± 0.002
3.1	0.1470	15.8	1.053 ± 0.004
2.3	0.2996	15.8	1.047 ± 0.085
3.6	—	15.8	1.488 ± 0.002
3.0	0.0395	31.4	6.718 ± 0.009
3.0	0.0395	31.4	6.684 ± 0.014
3.0	0.0395	31.4	6.828 ± 0.016
3.0	0.0789	31.4	9.939 ± 0.013
3.0	0.0789	31.4	9.997 ± 0.028
3.0	0.1611	31.4	14.46 ± 0.69
3.0	0.1611	31.4	14.83 ± 0.22
3.0	0.3190	31.4	18.72 ± 0.03
3.0	0.3190	31.4	17.38 ± 0.08
3.0	0.3190	31.4	17.61 ± 0.04
3.7	0.0404	38.7	21.20 ± 0.22
3.7	0.0799	38.7	31.53 ± 0.26
3.4	0.1499	38.6	44.71 ± 0.30
3.1	0.2996	38.6	50.97 ± 0.47

Table II-13. Continued

$10^4 [\text{Complex}]_o /M$	$[H^+]/M$	$T/^oC$	$10^4 k_{obs}/s^{-1}$
3.7	0.01973	44.3	35.15 ± 0.32
3.7	0.01973	44.3	35.09 ± 0.35
3.7	0.01973	44.3	36.70 ± 0.52
1.9	0.03946	44.3	66.5 ± 3.0
1.9	0.03946	44.3	59.4 ± 1.2
3.7	0.05919	44.3	82.7 ± 1.2
3.7	0.05919	44.3	77.44 ± 0.61
2.5	0.07892	44.3	82.4 ± 1.1
2.5	0.07892	44.3	90.4 ± 1.4
2.5	0.07892	44.4	89.51 ± 0.80

Table II-14. Kinetic data for $c\text{-}C_5H_9OOCo(dmgH)_2Py + HClO_4$, at $\mu = 1.0M$

$10^4 [\text{Complex}]_o /M$	$[H^+]/M$	$T/^oC$	$10^4 k_{obs}/s^{-1}$
—	0.010	25.0	0.718 ± 0.004
—	0.010	25.0	0.738 ± 0.003
—	0.020	25.0	1.377 ± 0.007
—	0.020	25.0	1.380 ± 0.003
—	0.040	25.0	2.619 ± 0.004
—	0.040	25.0	2.578 ± 0.006
—	0.070	25.0	3.640 ± 0.007
5.0	0.1002	25.9	5.07 ± 0.07
5.0	0.1002	25.9	5.11 ± 0.06
3.0	0.2996	25.5	8.20 ± 0.038
3.0	0.500	25.0	9.10 ± 0.04
3.0	0.500	25.0	9.05 ± 0.06
1.0	0.799	25.9	9.86 ± 0.10

Table II-15.   Kinetic data for $(CD_3)_2CDOOCo(dmgH)_2Py + HClO_4$, at
25.0 $\pm$ 0.1°C, μ = 1.0M

$10^4[\text{Complex}]_o/\text{M}$	$[\text{H}^+]/\text{M}$	$10^4 k_{obsd}/s^{-1}$
3.0	0.0404	1.316 $\pm$ 0.004
		1.205 $\pm$ 0.002
3.0	0.0799	1.898 $\pm$ 0.018
		1.922 $\pm$ 0.008
3.0	0.0996	2.059 $\pm$ 0.010
		2.145 $\pm$ 0.008
1.0	0.1007	2.14[a]
1.95	0.197	2.931 $\pm$ 0.006
		3.029 $\pm$ 0.007
0.89	0.2014	2.93
3.0	0.2996	3.436 $\pm$ 0.008
		3.522 $\pm$ 0.008
0.78	0.3021	3.11

[a]Data without standard deviation were analyzed by a graphical method.

It suggests that the substitution of the axial pyridine by water occurs in the peroxy complex although not as rapidly as for alkyl(pyridine) cobaloximes. Equilibrium between the pyridine compound and the aquo compound in the alkylperoxycobaloximes is achieved gradually, and significant concentrations of both species build up, if the solutions are kept long enough. They react with acid simultaneously, but the aquo compound shows a much higher rate.

Table II-16. Kinetic data for $(CH_3)_2CHOOCo(dmgH)_2pip + HClO_4$, at
25.00 $\pm$ 0.02°C, μ = 1.0M

$10^4[Complex]_o/M$	$[HClO_4]/M$	$10^4 k_{obsd}/s^{-1}$
1.11	0.00988	2.40
		2.35
1.05	0.01515	3.15
		3.55
1.01	0.01976	3.96
		3.68
0.91	0.03030	4.78
		4.80
0.81	0.04018	5.70
		5.80
1.16	0.1976	8.70
		8.81
1.10	0.5006	10.1
		9.89
1.01	1.001	10.6
		10.6

The pseudo-first-order rate constant approaches a limiting maximum
when $[H^+]$ is high as in Figure II-14. In the plot of k_{obsd}^{-1} vs.
$[H^+]^{-1}$, a linear relationship was acquired for all alkylperoxycobaloximes.
The data for $(CH_3)_2CHOOCo(dmgH)_2Py$ and $(CD_3)_2CDOOCo(dmgH)_2Py$ shown in
Figure II-15 are typical. A mathematical form of this plot can be ex-

Table II-17. Kinetic data for $(CH_3)_2CHOOCo(dmgH)_2NH_3$[a] + $HClO_4$, at
25.00 ± 0.1°C, μ = 1.0M

$[H^+]$	$10^4 k_{obs}/s^{-1}$
0.00988	0.77
0.01515	0.986
0.01976	1.15
0.03030	1.38
0.1001	2.16
0.1976	2.38
1.001	2.45

[a] $[(CH_3)_2CHOOCo(dmgH)_2NH_3]_o \sim 10^{-4}M$.

pressed as Equation II-24, where a and b represent the slope and the
intercept on ordinate of the plot, respectively.

$$\frac{1}{k_{obsd}} = a\left(\frac{1}{[H^+]}\right) + b \qquad (II-24)$$

A computer fit of the values of k_{obsd} at each $[H^+]$ for $(CH_3)_2CHOOCo(dmgH)_2Py$
is given in Table II-20. The agreement between the calculated and the
experimental values also proves this relationship.

A comparable equation may also be derived from an equilibrium
leading mechanism. Since the equilibration by protonation on one of
the oxygen atoms of the oxime group has been well-known in alkyl-
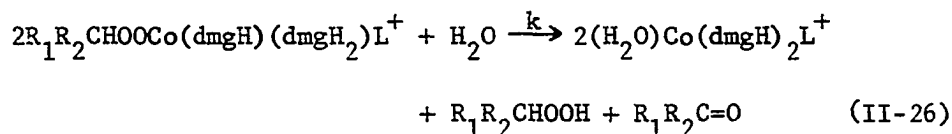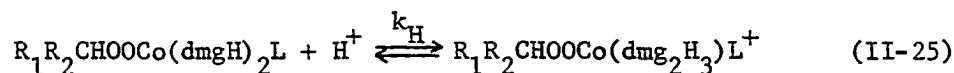cobaloximes, a basic mechanistic scheme may be designated as follows:

Table II-18. Kinetic data for $(CH_3)_2CHOOCo(dmgH)_2OH_2 + HClO_4$, at $25.00 \pm 0.05^{\circ}C$, $\mu = 1.0M$

$10^4[Complex]_o/M$	$[H^+]/M$	$10^2 k_{obs}/s^{-1}$
1.77	0.01007	0.245
1.77	0.01007	0.244
1.77	0.01007	0.244
1.77	0.01343	0.361
1.77	0.01343	0.345
1.75	0.02014	0.507
1.75	0.02014	0.520
1.73	0.03021	0.740
1.73	0.03021	0.760
1.69	0.05035	1.22
1.69	0.05035	1.22
1.67	0.07049	1.70
1.67	0.07049	1.71
1.63	0.09063	2.10
1.63	0.09063	2.10
1.61	0.1007	2.40
1.61	0.1007	2.46
1.43	0.2014	4.50
1.43	0.2014	4.50
1.26	0.3021	6.00
1.26	0.3021	6.10
1.26	0.3021	6.00
1.26	0.3021	5.90
1.07	0.4028	7.40
1.07	0.4028	7.50
1.07	0.4028	7.60
1.07	0.4028	7.70
0.901	0.5035	8.45
0.901	0.5035	8.90
0.55	0.7049	10.1
0.55	0.7049	10.1

Table II-19. Kinetic data of the reaction of $(CH_3)_2CHOOCo(dmgH)_2Py$ with $HClO_4$ in biphasic case, at $25.0^\circ C$, $\mu = 1.0M$

$10^4[Complex]_o/M$	$[H^+]/M$	$10^2 k^f_{obsd}/s^{-1}$	$10^4 k'_{obsd}/s^{-1}$
2	0.01	0.1	0.46
0.84	0.06042	1.7	2.4
0.91	0.06042	1.2	2.6
0.90	0.07049	1.6	2.8
2.7	0.07	1.4	2.8
0.89	0.0795	1.75	2.9
0.88	0.09063	2.2	3.1
0.81	0.1007	1.8	3.8

Scheme II-1

$$R_1R_2CHOOCo(dmgH)_2L + H^+ \xrightarrow{k_H} R_1R_2CHOOCo(dmg_2H_3)L^+ \qquad (II-25)$$

$$2R_1R_2CHOOCo(dmgH)(dmgH_2)L^+ + H_2O \xrightarrow{k} 2(H_2O)Co(dmgH)_2L^+$$

$$+ R_1R_2CHOOH + R_1R_2C=O \qquad (II-26)$$

Using the steady state approximation for $[R_1R_2CHOOCo(dmg_2H_3)L^+]$, the rate law may be written as Equation II-27

$$- \frac{d[ROOCo(dmgH)_2L]}{dt} = (\frac{kK_H[H^+]}{1 + K_H[H^+]})[ROOCo(dmgH)_2L]_T \qquad (II-27)$$

The pseudo-first-order rate constant thus has the form

$$k_{obsd} = \frac{kK_H[H^+]}{1 + K_H[H^+]} \qquad (II-28)$$
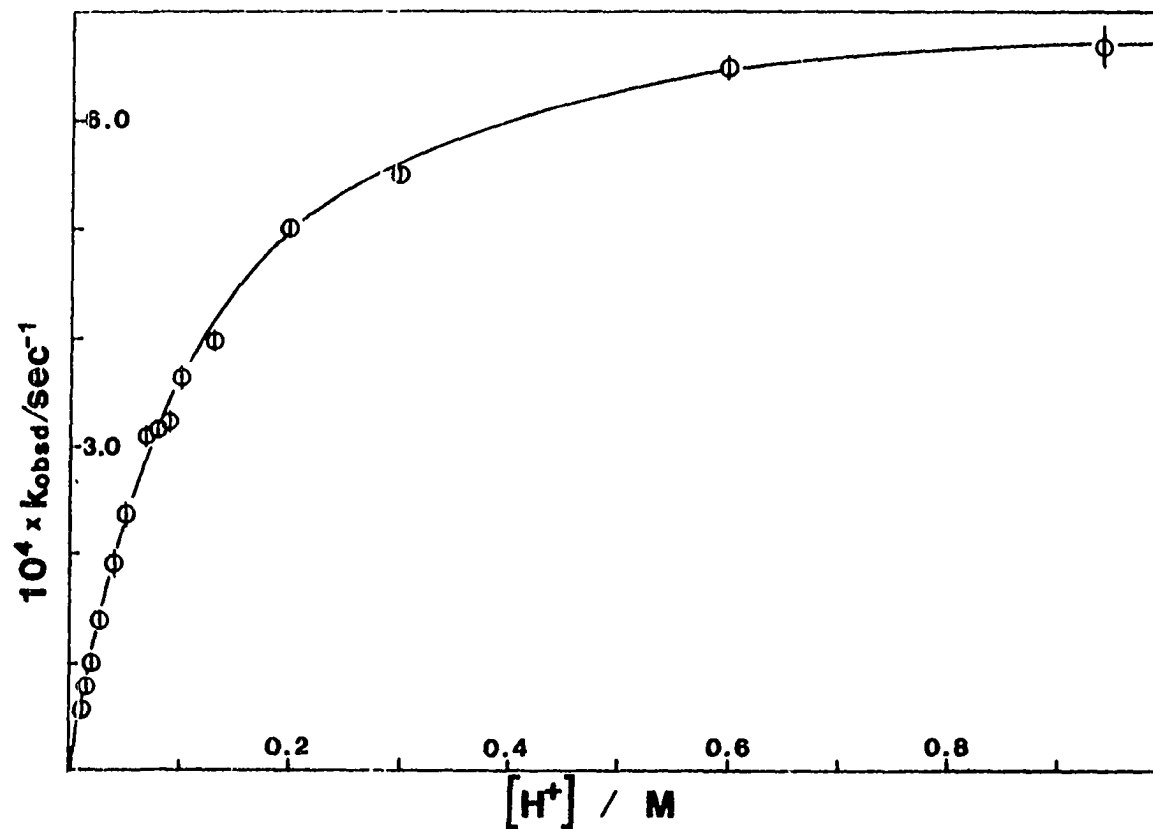
Figure II-14. Kinetic data for the reaction of $(CH_3)_2CHOOCo(dmgH)_2Py$ with $HClO_4$ at 25.0°C, μ = 1.0M, in a plot of k_{obsd} vs. $[H^+]$, illustrating Equation II-28

Figure II-15. Kinetic data for the reaction of isopropylperoxy-
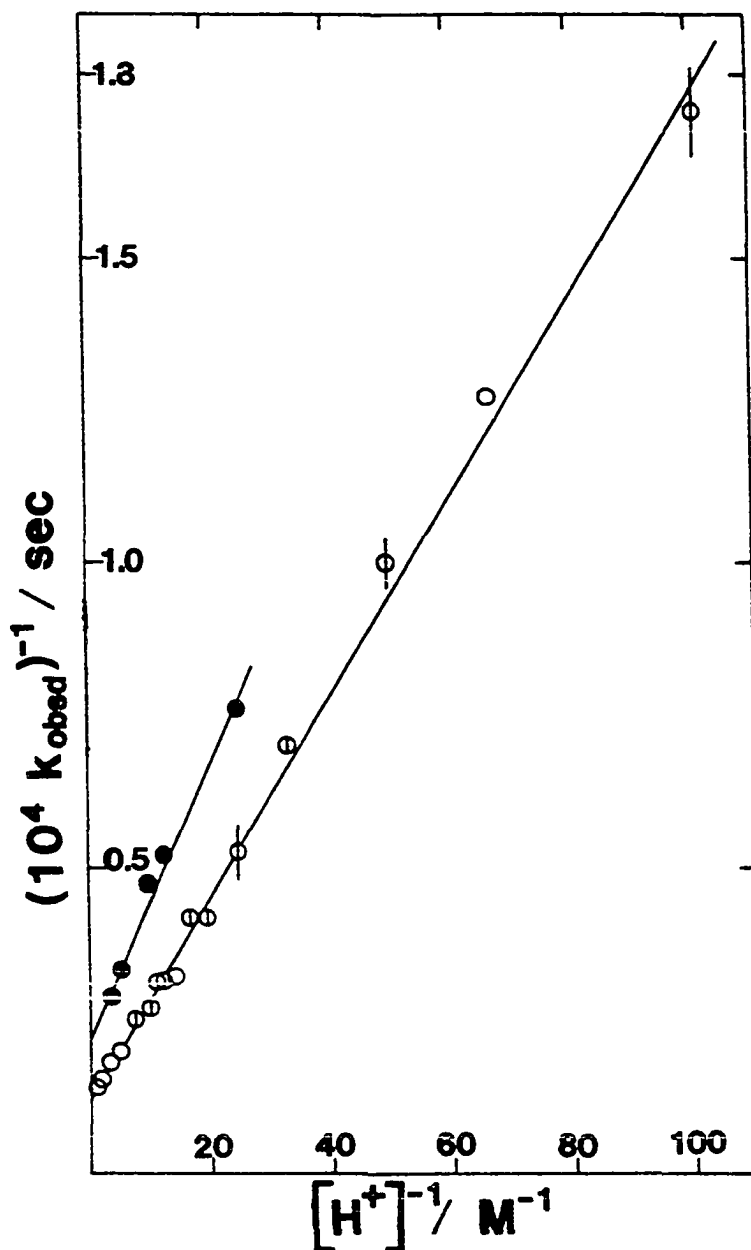(pyridine)cobaloxime with aqueous perchloric acid.
The plot depicts the linear variation of k_{obsd}^{-1} with
$[H^+]^{-1}$ according to Equation II-24. The points repre-
sent the experimental values and their standard devia-
tions, and the line corresponds to fit the data to
Equation II-24 using a nonlinear least-squares computa-
tion: $i-C_3H_7$ (O); $i-C_3D_7$ (●).

Table II-20. Observed[a] and calculated[b] pseudo-first-order rate constants for the overall disappearance os isopropyl-peroxy(pyridine)cobaloxime at various hydrogen ion concentrations

$[H^+]/M$	$10^4 k_{obs}^a /s^{-1}$	$10^4 k_{calc}^b /s^{-1}$
0.00987	0.574(25)	0.561
0.0151	0.787	0.827
0.0201	1.00(3)	1.06
0.0302	1.42(2)	1.50
0.0404	1.90(10)	1.89
0.0503	2.35(5)	2.22
0.0602	2.38(4)	2.52
0.0700	3.10(5)	2.79
0.0799	3.16(8)	3.03
0.0898	3.15(13)	3.25
0.100	3.62(18)	3.46
0.133	3.97(13)	4.03
0.200	5.00(1)	4.84
0.300	5.48	5.57
0.604	6.50(3)	6.58
0.940	6.99(61)	7.02

[a]Experimental conditions (1.0-3.8) x 10^{-4}M [(CH$_3$)$_2$CHOOCo(dmgH)$_2$Py]. 25.0 ± 0.1°C, ionic strength 1.00M (lithium perchlorate); the level of uncertainty in the last digit of k_{obs}, represented by the standard deviation between duplicate or triplicate runs, is shown in parentheses.

[b]Calculated according to Equation II-29 using the values of k = 8.00 x 10^{-4} s^{-1} and K_H = 7.63 M^{-1}.

Relating Equation II-28 to Equation II-24, a and b in the latter may

be replaced by $1/kK_H$ and $1/k$, i.e.,

$$\frac{1}{k_{obsd}} = (\frac{1}{kK_H}) \frac{1}{[H^+]} + \frac{1}{k} \tag{II-29}$$

Because the relatively small k values give a wide range of the inter-

cepts, for plotting purpose, Equation II-29 will rather be rearranged

by multiplying $[H^+]$ on both sides, and expressed as in Equation II-30

with also substitution k and K_H for a and b.

$$\frac{[H^+]}{k_{obsd}} = (\frac{1}{k})[H^+] + \frac{1}{kK_H} \tag{II-30}$$

Plotting $[H^+]/k_{obsd}$ against $[H^+]$, k may be evaluated by the inverse of

the slope and K_H by slope/intercept. Figure II-16 shows a series of

these linear plots for the decomposition of $ROOCo(dmgH)_2Py$ with various

alkyl groups. Accurate values of K_H and k may also be determined by

a nonlinear least-squares program. These data and those of benzyl

system are shown in Table II-21. It is noted that both parameters show

a narrow range of values, rather insensitive to the variation of alkyl

groups.

The reaction for 2-butyl complex was studied as a function of

temperature. The values of K_H and k are also summarized in Table II-21,

indicating that k is strongly temperature dependent, whereas K_H ap-

pears nearly invariant with temperature within experimental error.

The thermodynamic activation parameters for k can be evaluated em-

ploying Eyring's equation.

$$\ln (\frac{k}{T}) = - \frac{\Delta H^{\ddagger}}{RT} + \frac{\Delta S^{\ddagger}}{R} + \ln \frac{R}{Nh} \tag{II-31}$$

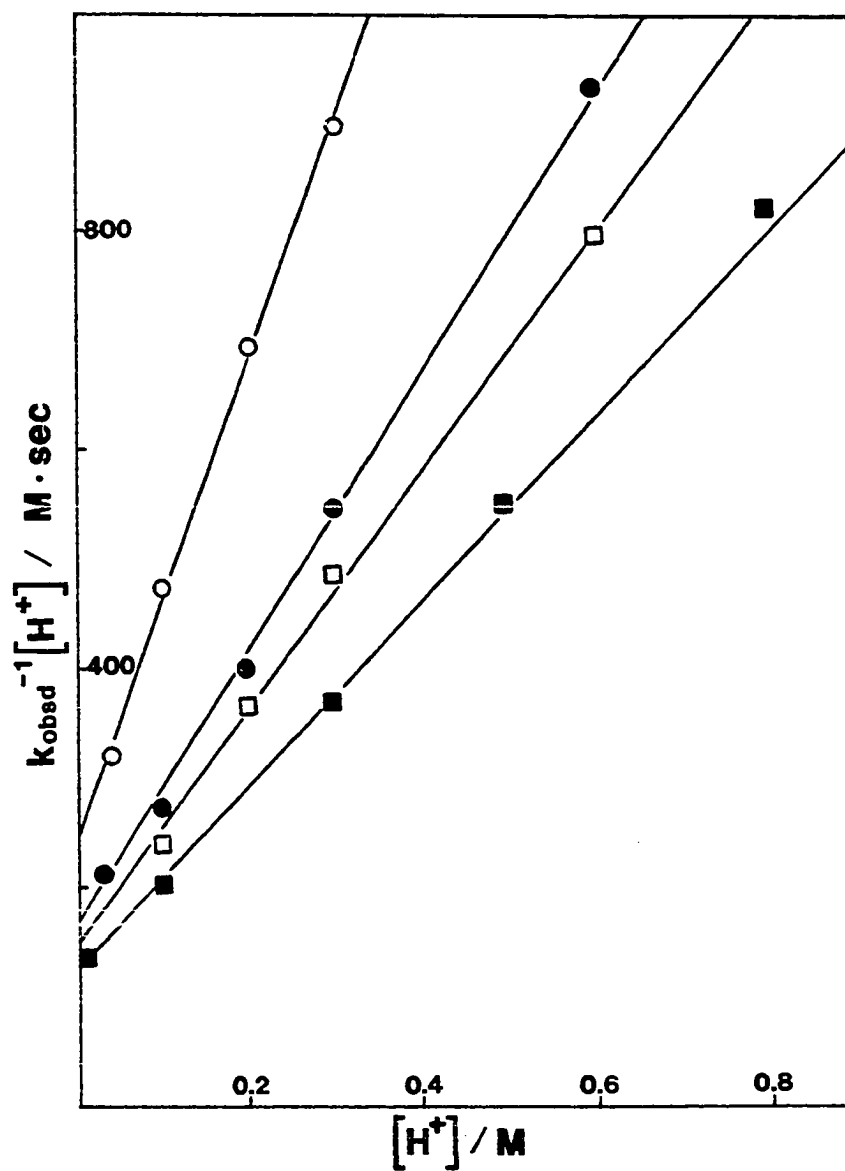Figure II-16. The kinetic plots illustrating Equation II-30 for the
reactions of ROOCo(dmgH)$_2$Py with HClO$_4$ at 25°C, μ = 1.0M.
R = (CD$_3$)$_2$CD- (O); (CH$_3$)$_2$CH- (●); (C$_2$H$_5$)(CH$_3$)CH- (□);
c-C$_5$H$_9$- (■)

Table II-21. Kinetic parameters[a] for the overall disappearance of
alkylperoxy(pyridine)cobaloximes, $ROOCo(dmgH)_2Py$

R(T/°C)	$10^4 k/s^{-1}$	K_H/M^{-1}
2-Propyl (25.0 $\pm$ 0.1)	8.00 $\pm$ 0.20	7.63 $\pm$ 0.29
Cyclopentyl (25.4 $\pm$ 0.4)	12.0 $\pm$ 0.3	6.60 $\pm$ 0.23
2-Butyl (15.8 $\pm$ 0.1)	2.04 $\pm$ 0.15	8.1 $\pm$ 0.10
(25.4 $\pm$ 0.4)	9.3 $\pm$ 0.3	7.35 $\pm$ 1.0
(31.4 $\pm$ 0.2)	23.5 $\pm$ 0.1	9.9 $\pm$ 0.9
(38.6 $\pm$ 0.2)	65.2 $\pm$ 0.5	11.9 $\pm$ 0.1
(44.3 $\pm$ 0.3)	178 $\pm$ 22	13.1 $\pm$ 3.0
d^7-2-Propyl (25.0 $\pm$ 0.05)	4.7 $\pm$ 0.2	8.6 $\pm$ 0.8
Benzyl (22 $\pm$ 3)	$\sim$ 14	$\sim$ 2

[a]The parameters are those of Equation II-29; conditions: aqueous
solution, 1.00M ionic strength.

A plot of $\ln(\frac{k}{T})$ vs. $\frac{1}{T}$ shows linear relationship in Figure II-17. A
nonlinear least-square data fit gives the values of $\Delta H^{\ddagger} = 118.4 \pm 5.9$
kJ mol^{-1} and $\Delta S^{\ddagger} = 93.3 \pm 19.2$ J mol^{-1} K^{-1}.

The variation of plots of Equation II-30 for the reactions of
$(CH_3)_2CHOOCo(dmgH)_2L$ with different axial base is illustrated in
Figure II-18. Their kinetic parameters calculated by computer are
listed in Table II-22. The K_H values slightly increase for the complexes
with stronger axial bases, such as piperidine and ammonia. The rate
constants of the decomposition step are not much different for most of
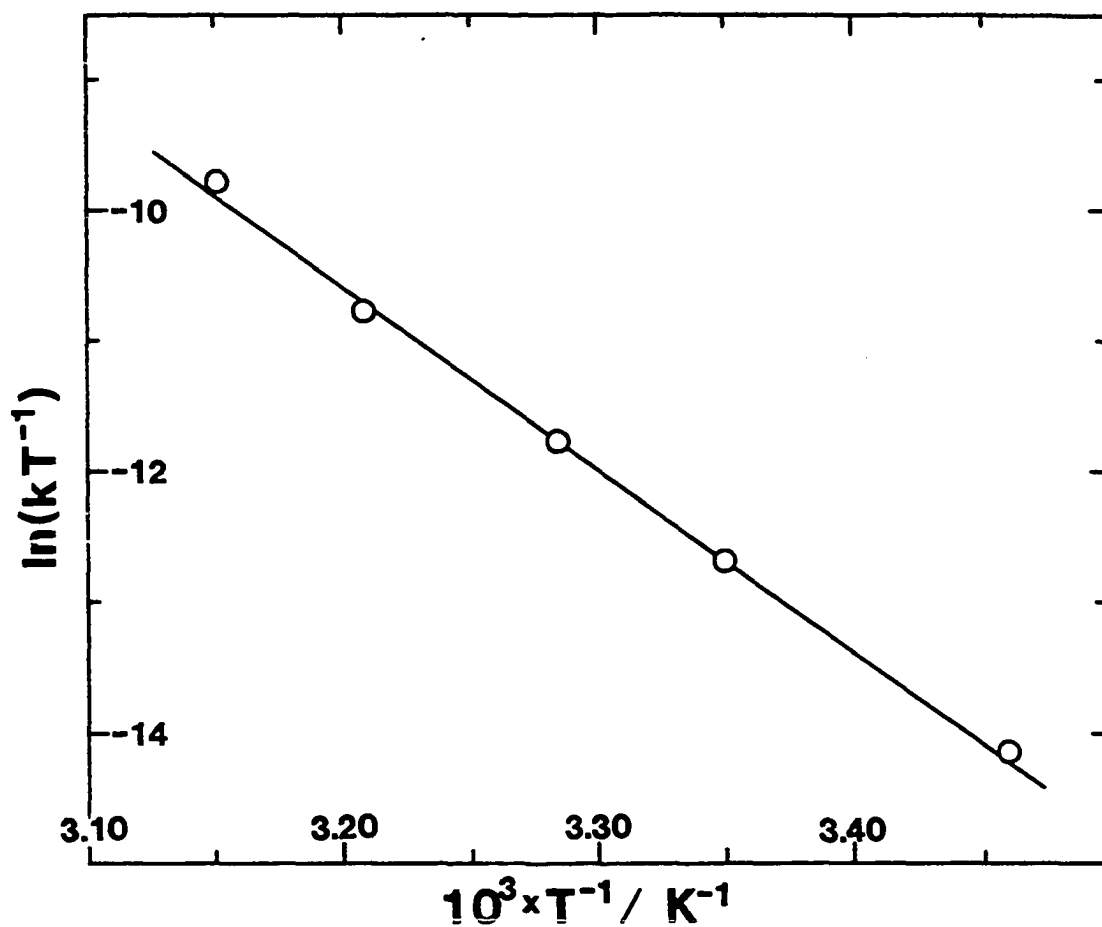the reactions except the aquo, which decomposes much more rapidly.

Figure II-17. Illustrating the temperature dependence of k for the reaction of $(CH_3)(C_2H_5)CHOOCo(dmgH)_2Py$ with $HClO_4$ in a plot of $\ln(k/T)$ vs. $(1/T)$. The rate constant k represents the sum of the rate constants for independent reactions and as such the slight upward curvature may be a real effect (see pg. 131).
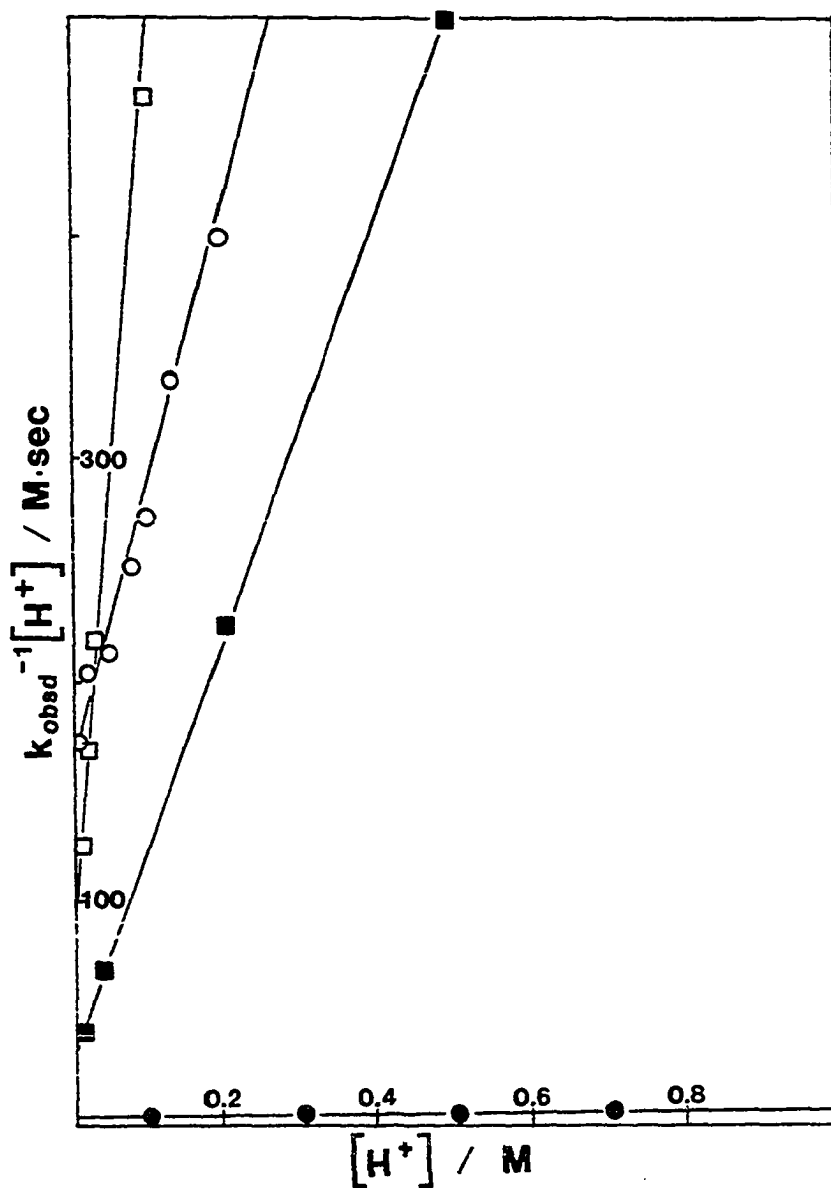
Figure II-18. The kinetic plots illustrating Equation II-30 for the
reactions of $(CH_3)_2CHOOCo(dmgH)_2L$ with $HClO_4$ at $25^{\circ}C$,
$\mu = 1.0M$. L = NH_3 (□); Py (○); Pip (■); and H_2O (●).

Table II-22. Kinetic parameters[a] for the overall disappearance of
isopropylperoxycobaloximes with different axial
ligands L

| L | Kinetic parameters at 25.0°C | |
	k/s^{-1}	K_H/M^{-1}
Pyridine	$(8.00 \pm 0.20) \times 10^{-4}$	7.63 ± 0.29
Pyridine[b]	$(4.7 \pm 0.2) \times 10^{-4}$	8.6 ± 0.8
Piperidine	$(10.6 \pm 0.2) \times 10^{-4}$	28.8 ± 1.0
Ammonia	$(2.59 \pm 0.06) \times 10^{-4}$	41.4 ± 2.4
Water	0.254 ± 0.010	1.01 ± 0.05

[a]The parameters are those of Equation II-30; conditions: aqueous
solution, 1.00M ionic strength.

[b]For $(CD_3)_2CDOOCo(dmgH)_2Py$.

Gas chromatography

The formation of ketone was monitored by GLC with time. The examination of alkyl hydroperoxides was impossible at 100°C, which was the temperature employed for the column. The reaction solution of 2-propyl system was prepared with $8.6 \times 10^{-3}M$ $(CH_3)_2CHOOCo(dmgH)_2Py$, 0.20M $HClO_4$, 80 ng/μl 2-butanol as internal standard and fixing the ionic strength at 1.0 by $LiClO_4$. The ratios of the peak heights corresponding to the forming acetone vs. 2-butanol with time are shown in Table II-23. The ratio values at zero time and the completion of the reaction were estimated by extrapolation. With these values and the half-life of the reaction at 25°C, which was determined by spectrophotometrically monitoring the disappearance of $(CH_3)_2CHOOCo(dmgH)_2Py$, a calculated curve was graphed. The experimental data plotted on the same graph are in good agreement with the calculated

Table II-23.   The gas chromatographic kinetic data for the formation
of acetone of the reaction $(CH_3)_2CHOOCo(dmgH)_2Py + HClO_4$,
$\mu = 1.0M$, $T = 23 \pm 2^oC$

Time (min.)	Peak height of acetone / Peak height of 2-butanol
0	0.43^a
2	0.46
10	0.54
20	0.70
30	0.78
40	0.85
50	0.85
60	0.90
70	0.94
80	1.07
90	1.11
100	1.12
110	1.03
120	1.11
130	1.01
140	0.96
150	1.15
160	1.17
∞	1.05^a

[a]Values were estimated by extrapolation.

kinetic curve, Figure II-19.

A similar analysis for the cyclopentyl system was done. Two runs with each containing 3 x 10^{-4}M c-C_5H_9OOCo(dmgH)$_2$Py, 0.10M HClO$_4$, 79.5 ng/μL acetone, and μ = 1.0 were recorded. Their data and the corresponding graph are shown in Table II-24 and Figure II-20, respectively. The apparent rates of the formation of the cyclopentanone also agree with the apparent rate of the disappearance of c-C_5H_9OOCo(dmgH)$_2$Py.
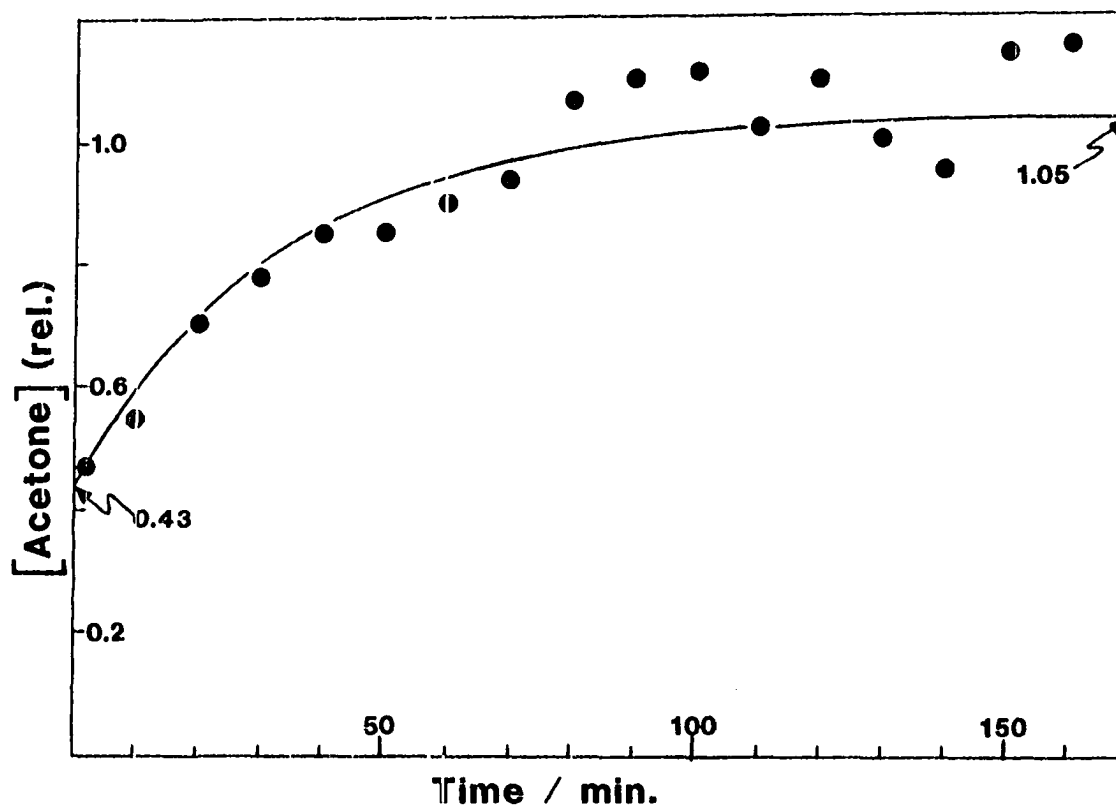
Figure II-19. GC analysis of acetone formed in the reaction of $(CH_3)_2CHOOCo(dmgH)_2Py$ with 0.200M HClO$_4$, plotted as (peak height of acetone)/(peak height of internal standard) vs. time. The data are shown in Table II-23. The solid curve is calculated from the rate constant (4.99 x $10^{-4}S^{-1}$) as determined spectrophotometrically and from the extrapolated data: [Acetone]$_o$ = 0.43, [Acetone]$_\infty$ = 1.05.

Table II-24. The gas chromatographed kinetic data of the formation
of cyclopentanone of the reaction $c-C_5H_9OOCo(dmgH)_2Py$
+ $HClO_4$, $\mu = 1.0$; $T = 23 \pm 3^oC$

Run 1		Run 2	
Time (min.)	$\dfrac{\text{Peak height of } \square\!=\!O}{\text{Peak height of acetone}}$	Time (min.)	$\dfrac{\text{Peak height of } \square\!=\!O}{\text{Peak height of acetone}}$
0	0.0 [a]	0	0.0 [a]
1	0.028	6	0.064
19	0.096	20	0.0987
27	0.11	33	0.126
36	0.14	47	0.177
47	0.15	60	0.164
56	0.15	72	0.180
67	0.17	87	0.196
87	0.19	100	0.189
97	0.19	∞	0.200[a]
107	0.20		
∞	0.21[a]		

[a]Values estimated by extrapolation.
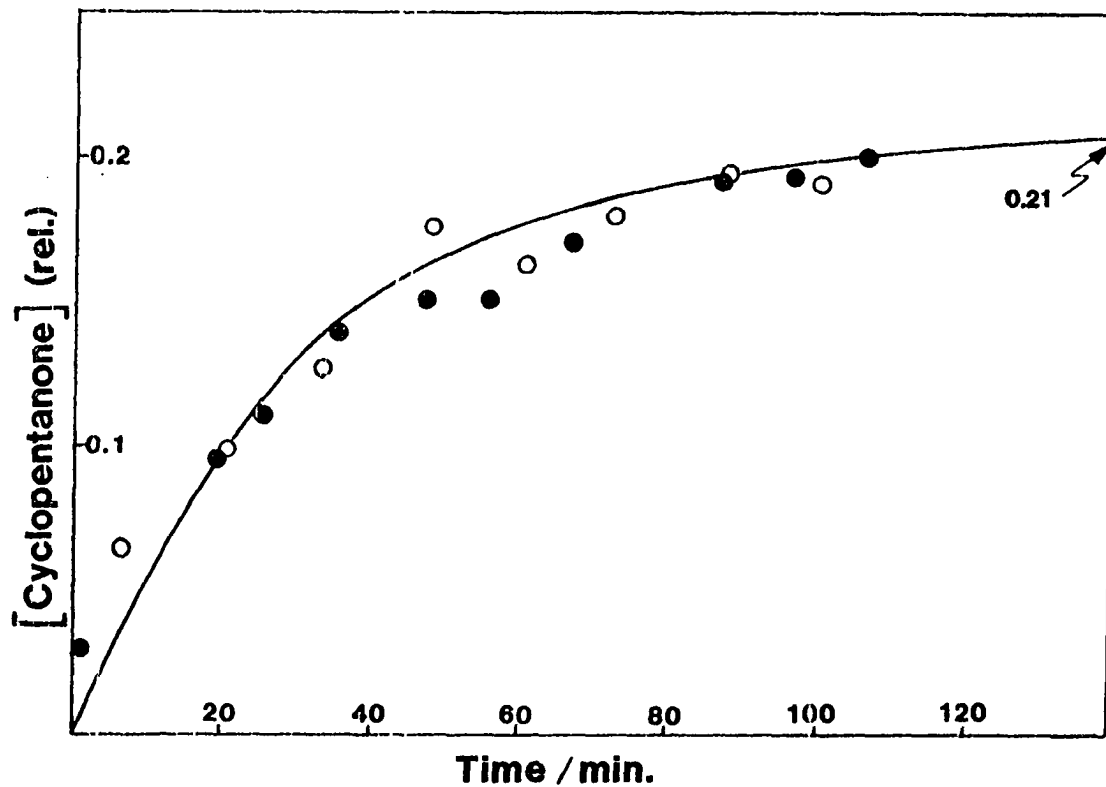
Figure II-20. GC analysis of cyclopentanone formed in the reaction of c-C$_5$H$_9$Co(dmgH)$_2$Py with 0.100M HClO$_4$, plotted as (peak height of cyclopentanone)/(peak height of internal standard) vs. time. The data of Run 1 (●), and Run 2 (○) are shown in Table II-24. The solid curve is calculated from the rate constant (5.07 x 10^{-4}s^{-1}) as determined spectrophotometrically and from the extrapolated data: [c-Pentanone]$_0$ = 0.00 and [c-Pentanone]$_\infty$ = 0.21.

INTERPRETATION AND DISCUSSION

Protonation of the Oxime Oxygen Atom

The rapid equilibrium protonation of one of the oxime oxygen atoms for alkyl(aquo)cobaloximes is well-known (82, 83). Values of K_H^R increase monotonically with the size

$$RCo(dmgH)_2H_2O + H^+ \xrightleftharpoons{K_H^R} RCo(dmg_2H_3)H_2O \qquad (II-32)$$
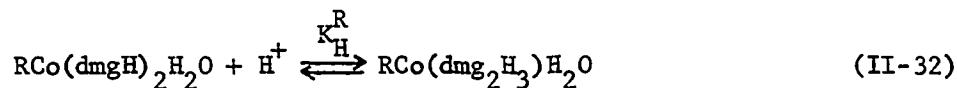
of the alkyl group within a range of 1-4 M^{-1}. It indicates that a better electron-donating group will inductively transmit a larger part of its basicity to the oxime oxygen. The dependence of the axial ligand L trans to R was not studied, owing to the extreme lability of L in aqueous solutions.

In this study, the analogous equilibria for $ROOCo(dmgH)_2L$ were also observed. Not only do the kinetic data suggest a protonation equilibrium, but also the instantaneous spectral change which occurs upon acidification, as shown in Figure II-13, supports it. Equation II-25 has expressed this process.

$$R_1R_2CHOOCo(dmgH)_2L + H^+ \xrightleftharpoons{K_H} R_1R_2CHOOCo(dmg_2H_3)L^+ \qquad (II-25)$$
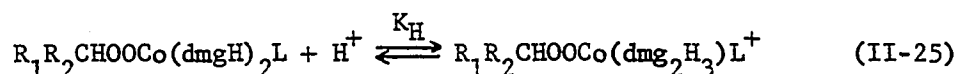
The value of K_H for $(CH_3)_2CHOOCo(dmgH)_2H_2O$ was determined as 1.01 M^{-1} which is smaller than $K_H = 4.2 \pm 0.3$ M^{-1} for $(CH_3)_2CHCo(dmgH)_2H_2O$, reflecting the 2-propyl peroxy group to be less electron-donating compared with the 2-propyl group, as expected.

The size of the alkyl group is relatively unimportant in determining the basicity of the peroxy compound. This is not surprising

since it is two atoms further from the cobalt center than in alkyl-

cobaloximes. Various ROOCo(dmgH)$_2$Py have the values of K_H lying in

a narrow range and without significant correlation: R = i-C$_3$H$_7$(K$_H$ =

7.6 $\pm$ 0.3 M^{-1}), i-C$_3$D$_7$(8.6 $\pm$ 0.8 M^{-1}), sec-C$_4$H$_9$(8.1 $\pm$ 1.0 M^{-1}),

Cy-C$_5$H$_9$(6.60 $\pm$ 0.23 M^{-1}). However, in the case of PhCH$_2$OOCo(dmgH)$_2$Py,

the electron-withdrawing effect of the benzyl group indeed lowers the

K_H value to ca. 1.9 M^{-1} which is smaller than that for all n-alkyl-

(aquo)cobaloximes.

The substitution inertness of axial ligand L in ROOCo(dmgH)$_2$L

permits the measurement of K_H for various axial ligands. A series of

(CH$_3$)$_2$CHOOCo(dmgH)$_2$L with increasing basicity of L show this tendency:

L = H$_2$O (K$_H$=1.0 $\pm$ 0.5 M^{-1}), L = Py (7.6 $\pm$ 0.3), L = NH$_3$ (44.4 $\pm$ 2.4).

Again, the better electron-donating ligand leads to a greater value

of K_H. The piperidine complex is an exception: although piperidine

is the strongest base of all, it possesses a value of K_H, 28.8 $\pm$ 1.0,

smaller than that for (CH$_3$)$_2$CHOOCo(dmgH)$_2$NH$_3$. The relatively rigid

and bulky structure of piperidine may cause steric hindrance to

limit the efficiency of its coordination to the macrocyclic cobalt.

Even though it is a stronger base than ammonia, it contributes a

poorer electron donation and causes a smaller K_H.

Concurrent Pathways for the Formation of Ketone and Hydroperoxide

The consecutive mechanism given in Equation II-7 could be true

only if the alkyl hydroperoxide decomposed to ketone as soon as it was

formed from the decomposition of alkylperoxycobaloxime, since the forma-

tion of the ketone and the disappearance of the peroxy complex were found to occur at the same apparent rate. This induction clearly disagrees with the NMR results, which show that both ketone and hydroperoxide coexisted in the reacted solution and were stable for more than 24 hours.

The concurrent pathways through which both ketone and alkyl hydroperoxide are established to be primary products are proposed as Scheme II-2. Its rate law is formulated in Equation II-34, wherein $[ROOCo]_T$ represents the sum of the concentrations of $ROOCo(dmgH)_2L$

Scheme II-2
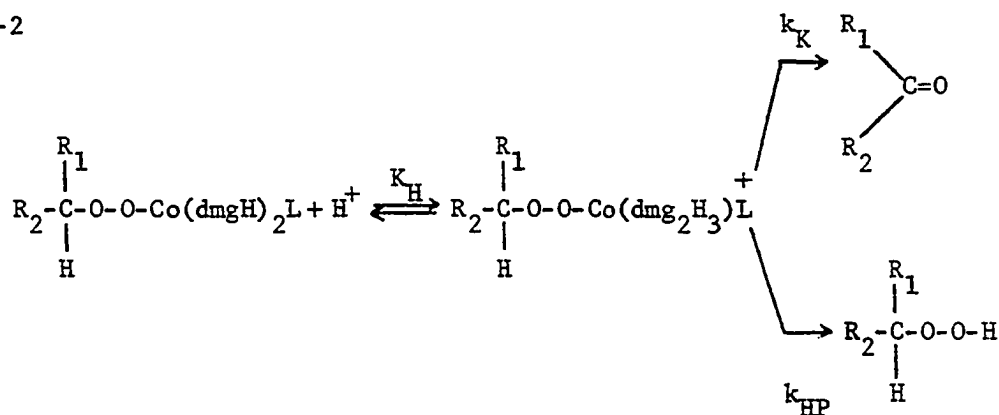
$$-\frac{d[ROOCo(dmgH)_2L]}{dt} = (\frac{(k_K + k_{HP})K_H[H^+]}{1 + K_H[H^+]})[ROOCo]_T \qquad (II\text{-}33)$$

and $ROOCo(dmg_2H_3)L^+$ at a given time t. In addition to the evidence from the NMR experiments, the kinetic studies of the ketone formation using the GLC technique also support this mechanism. It may be mathematically rationalized as follows. Integration of Equation II-33 gives Equation II-34.

$$[ROOCo(dmgH)_2L] = [ROOCo]_T \exp(- k_{obsd}t) \qquad (II\text{-}34)$$

The rate law with regard to the formation of ketone is in the form of Equation II-35.

$$\frac{d[\text{ketone}]}{dt} = (\frac{k_K K_H [H^+]}{1 + K_H[H^+]})[\text{ROOCo}]_T \exp(-k_{obsd}t) \qquad (II-35)$$

Integration of Equation II-35 yields the equation

$$[\text{ketone}] = (\frac{k_K}{k_K + k_{HP}})(\frac{K_H[H^+]}{1 + K_H[H^+]})[\text{ROOCo}]_T\left\{1 - \exp(-k_{obsd}t)\right\} \qquad (II-36)$$

Plotting [ROOCo(dmgH)$_2$L] vs. time and [ketone] vs. time according to Equations II-34 and II-36, respectively, gives graphs which are exponential curves changing with the same half life: $t_{1/2} = \ln 2/k_{obsd}$. Therefore, Scheme II-2 indeed agrees with the observation that the peroxy reactant is consumed with the same apparent rate constant as ketone grows.

The parameter k designated for the decomposition step in Scheme II-1 now is a composite of $k_K + k_{HP}$. The Eyring relationship thus has to be rewritten.

$$k = k_K + k_{HP} = \frac{RT}{Nh}[\exp(\frac{-\Delta H_K^{\ddagger}}{RT})\exp(\frac{\Delta S_K^{\ddagger}}{R}) + \exp(\frac{-\Delta H_{HP}^{\ddagger}}{RT})\exp(\frac{\Delta S_{HP}^{\ddagger}}{R})] \qquad (II-37)$$

Since the right-hand side of Equation II-37 is a sum of exponential terms, the plot of ln (k/T) vs. (1/T) is not necessarily linear anymore. In Figure II-17, the data indeed exhibit a slightly upward curvature but may be represented as a straight line within experimental error. The calculated $\Delta H^{\ddagger}$, 118 kJ·mole^{-1}, and $\Delta S^{\ddagger}$, 93 J·mole^{-1}°K^{-1}, though have only limited physical meaning; the very positive $\Delta S^{\ddagger}$, however, implies that the decomposition undergoes a dissociative process.

Reaction Mechanisms

Several alternative mechanisms leading to the same kinetic equation are considered. The common features possessed by these mechanisms are: (1) a preequilibrium of protonation on the oxime oxygen preceding the decomposition of the peroxy complex(es); (2) the formation of ketone and alkyl hydroperoxide by parallel and independent pathways; and (3) a unique cobaloxime(III) product with the retention of the axial ligand. Since both of the protonated and unprotonated peroxy complexes could be subjected to decomposition, a general form of four possible routes is illustrated in Scheme II-3 using the 2-propyl system as the representative.

Scheme II-3
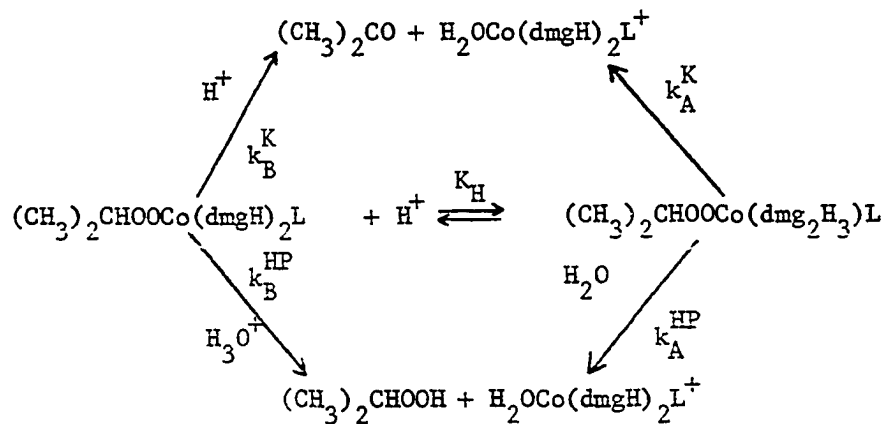
If the four processes are incapable of further distinction, the following equations apply:

$$k_{obsd} = \frac{(k_A^K + k_A^{HP}) + K_H^{-1}(k_B^K + k_B^{HP})\ [H^+]}{K_H^{-1} + [H^+]} \qquad (II\text{-}38)$$

$$\frac{[\text{Ketone}]_\infty}{[\text{Hydroperoxide}]_\infty} = \frac{k_A^K + k_B^K K_H^{-1}}{k_A^{HP} + k_B^{HP} K_H^{-1}} \qquad \text{(II-39)}$$

The relative yields of the organic products were determined by nmr spectroscopy and/or iodometric titrations. Values of both the numerator and denominator of Equation II-39 thus can be evaluated by the combination of Equations II-38 and II-39. For the 2-propylperoxy complex, $k_A^K + k_B^K K_H^{-1} = 3.3 \times 10^{-4}\,\text{s}^{-1}$ 3.3 $\times 10^{-4}\text{s}^{-1}$ and $k_A^{HP} + k_B^{HP} K_H^{-1} = 4.7 \times 10^{-4}\text{s}^{-1}$ and its deuterated analogue, 3.8 $\times 10^{-5}\text{s}^{-1}$ and $4.3 \times 10^{-4}\text{s}^{-1}$, respectively, are acquired. The significant isotope effect for the ketone pathway(s) shown by the data will be discussed later. These values for several other peroxy complexes are summarized in Table II-25. They afford important information for further resolving possibilities suggested by Scheme II-3, which will also be discussed in the following sections.

Table II-25. Kinetic parameters for the individual pathways from Scheme II-3 for $\text{ROOCo(dmgH)}_2\text{L}$

R	L	$\dfrac{k_A^K + k_B^K K_H^{-1}}{s^{-1}}$	$\dfrac{k_A^{HP} + k_B^{HP} K_H^{-1}}{s^{-1}}$
2-Propyl	Pyridine	$(3.4 \pm 0.2) \times 10^{-4}$	$(4.6 \pm 0.2) \times 10^{-4}$
d_7-2-Propyl	Pyridine	$(3.8 \pm 0.4) \times 10^{-5}$	$(4.3 \pm 0.3) \times 10^{-4}$
2-Butyl	Pyridine	$(3.3 \pm 0.3) \times 10^{-4}$	$(6.0 \pm 0.3) \times 10^{-4}$
2-Propyl	Water	$< 5 \times 10^{-3}$	0.25 ± 0.01
2-Propyl	Peperidine	$(3.1 \pm 0.4) \times 10^{-4}$	$(7.5 \pm 0.5) \times 10^{-4}$

Mechanism of Ketone Formation

The discrepant values of $k_A^K + k_B^K K_H^{-1}$ for the 2-propyl and the

d_7-2-propyl analogous systems, shown in Table II-25, manifest a

substantial deuterium kinetic isotope effect for the ketone pathway.

Expressed as a ratio, $k_K(H)/k_K(D) = 8.9 \pm 1.5$. This result indicates

that the breaking of the C-H bond in the alkyl group must be important

in the rate-limiting step. The main feature in the decomposition of

the peroxy complex leading to ketone is the O-O bond cleavage. Since

the axial ligand on the cobalt complex affords little effect in this

process according to the kinetic data in Table II-25, a solvent proton-

assisted mechanism is proposed, and the activated complex is depicted

below:
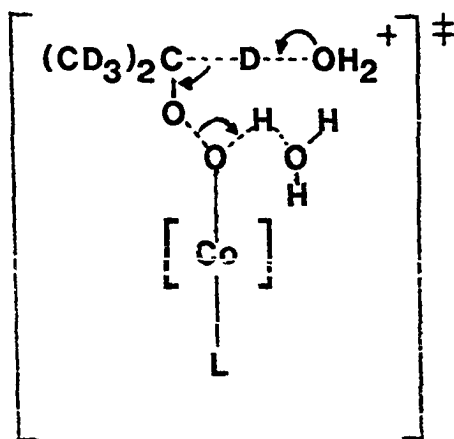
On the basis of this formulation, the bimolecular reaction of the un-

protonated peroxy complex with H_3O^+ is believed to be the dominant

pathway in forming ketone, and thus $k_K = k_B^K K_H^{-1}$. With known values of

K_H for each peroxy complex, k_B^K can be compared: 2.55×10^{-3} $M^{-1}s^{-1}$

$(2\text{-}C_3H_7OOCo(dmgH)_2Py)$, 2.39×10^{-3} $(2\text{-}C_4H_9OOCo(dmgH)_2Py)$, 3.2×10^{-4}

$(2\text{-}C_3D_7OOCo(dmgH)_2Py)$, 8.9×10^{-3} $(2\text{-}C_3H_7OOCo(dmgH)_2pip)$, and $< 5 \times 10^{-3}$ $(2\text{-}C_3H_7OOCo(dmgH)_2OH_2)$.

Mechanism of Hydroperoxide Formation

In contrast to the ketone pathway, the kinetic parameter, $k_{HP} = k_A^{HP} + k_B^{HP}K_H^{-1}$, for the hydroperoxide formation demonstrates absolutely no isotope effect. The k_{HP} values for R = 2-propyl, $(4.6 \pm 0.2) \times 10^{-4}s^{-1}$; and d_7-2-propyl, $(4.3 \pm 0.3) \times 10^{-4}s^{-1}$ are virtually the same. The ratio of $k_{HP}(H)/k_{HP}(D)$ thus being 1.07 is hardly surprising, since no C-H bond is broken during the forming of hydroperoxide.

The values of k_{HP} listed in Table II-25 increase with the bulky alkyl group and strongly basic ligand except that the aquo complex, which reacts extraordinarily rapidly. Without considering this exceptional case of L = H_2O temporarily, this reaction may be again explained by the attack of solvent proton at the peroxide oxygen bound to cobalt. The inductive electronic effect caused by both the electron-donating group R and the basic ligand L may give a higher rate.

The values of k_B^{HP} also can be estimated by neglecting k_A^{HP}, being $3.51 \times 10^{-3}s^{-1}$ $(2\text{-}C_3H_7OOCo(dmgH)_2Py)$, $3.70 \times 10^{-3}s^{-1}$ $(2\text{-}C_3D_7OOCo(dmgH)_2Py)$, $4.41 \times 10^{-3}s^{-1}$ $(2\text{-}C_4H_9OOCo(dmgH)_2Py)$, and $2.16 \times 10^{-2}s^{-1}$ $(2\text{-}C_3H_7OOCo(dmgH)_2Pip)$. The axial ligand effect is much more severe than that in the process of ketone formation. This is because now the Co-O bond which is closer to the axial ligand is cleaved in this pathway.

The reaction for the aquo derivative evidently involves a different mechanism. Since water is a very weak base compared to other nitrogen-coordinated ligands, it transmits very little basicity to the macrocyclic ring. Consequently, the hydroxyl group of oxime for the aquo complex is more acidic and capable of transferring the proton intramolecularly to the peroxide oxygen to motivate the cleavage of the Co-O bond and then the hydroperoxide formation. The following activated complex is proposed for this process.
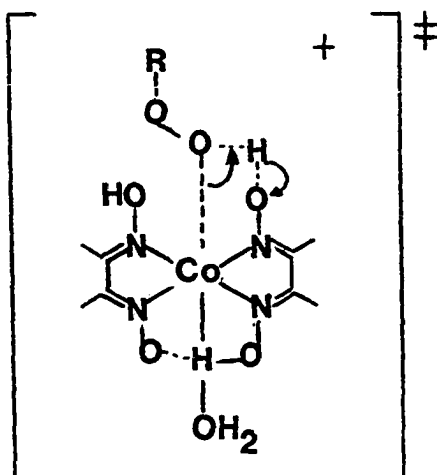
On the basis of this consideration, the pathway of k_A^{HP} and not k_B^{HP} is suggested to be predominant for the hydroperoxide formation, and $k_{HP} = k_A^{HP}$ is $0.25 \pm 0.01 \ S^{-1}$.

GENERAL SUMMARY

The method of chemical competition, based on the homolytic decomposition of organo(pentaaquo)chromium(III) complexes, has been proven to be suitable for the kinetic studies of the chemistry of highly reactive radicals, particularly the novel reactions which occur too slowly to be studied using radiation techniques.

A quite unusual reaction between $V(H_2O)_6^{2+}$ and the free radical, $\cdot C(CH_3)_2OH$, in which the latter functions as an oxidizing agent rather than in its more customary reducing role, has been discovered. The same radical also reacts with $Co^{II}([14]aneN_4)^{2+}$ to form the organocobalt species.

The secondary-alkylperoxycobaloxime is decomposed to ketone and alkyl hydroperoxide by parallel pathways in aqueous perchloric acid.

BIBLIOGRAPHY

1. Kochi, J. K. "Organometallic Mechanisms and Catalysis," Academic Press: New York, 1978.

2. Sheldon, R. A.; Kochi, J. K. "Metal-Catalyzed Oxidations of Organic Compounds," Academic Press: New York, 1981.

3. Parshall, G. W. "Homogeneous Catalysis," Wiley & Sons: New York, 1980.

4. Espenson, J. H.; Chen, J.-T. J. Am. Chem. Soc. 1981, 103, 2036.

5. Neta, P. Adv. Phys. Org. Chem. 1976, 12, 223.

6. Swallow, A. J. Prog. Reaction Kinetics 1978, 9, 195.

7. Espenson, J. H.; Shimura, M.; Bakac, A. Inorg. Chem. 1982, 21, 2537.

8. Espenson, J. H. Adv. Inorg. and Bioinorg. Reaction Mechanisms 1982, 1, 1.

9. Espenson, J. H. Submitted for publication in Prog. in Inorg. Chem.

10. Kirker, G. W.; Bakac, A.; Espenson, J. H. J. Am. Chem. Soc. 1982, 104, 1249.

11. Ross, A. B.; Neta, P. "Rate Constants for Reactions of Aliphatic Carbon-Centered Radicals in Aqueous Solution," Radiation Chemistry Data Center, Radiation Laboratory, University of Notre Dame, 1981.

12. Natarajan, P.; Endicott, J. F. J. Phys. Chem. 1973, 77, 1823.

13. Cohen, H.; Meyerstein, D. J. Chem. Soc. Dalton, 1977, 1056.

14. Endicott, J. F. "Concepts of Inorganic Photochemistry," Adamsom, A. W.; Fleishauer, P. D. (Eds.); Wiley, Interscience, 1975, pp. 90-92.

15. McHatton, R. C.; Espenson, J. H.; Bakac, A. J. Am. Chem. Soc. 1982, 104, 3531.

16. McHatton, R. C.; Espenson, J. H. Unpublished results, Ames Laboratory, Iowa State University, Ames, Iowa, 1982.

17. Pribush, A. C.; Brusentseva, S. A.; Shubin, V. N.; Dobin, P. I. High Energy Chem. 1975, 9, 206.

18. Rabani, J.; Mulac, W. A.; Matheson, M. S. *J. Phys. Chem.* 1977, <u>81</u>, 99.

19. Kelm, M.; Lilie, J.; Henglein, A.; Janata, E. *J. Phys. Chem.* 1974, <u>78</u>, 882.

20. Kelm, M.; Lilie, J.; Henglein, A. *J. Chem. Soc. Faraday, Trans. I* 1975, <u>5</u>, 1132.

21. Breitenkamp, M.; Henglein, A.; Lilie, J. *Ber Bunsenges. Phys. Chem.* 1976, <u>80</u>, 973.

22. Buxton, G. V.; Green, J. C. *J. Chem. Soc. Faraday Trans. I* 1978, <u>74</u>, 697.

23. Gold, V.; Wood, D. L. *J. Chem. Soc. Dalton*, 1982, 2462.

24. Cooper, T. A. *J. Am. Chem. Soc.* 1973, <u>95</u>, 4158.

25. Dodd, D.; Johnson, M. D. *Organomet. Chem. Rev.* 1973, <u>52</u>, 1.

26. Espenson, J. H.; Martin, A. H. *J. Am. Chem. Soc.* 1977, <u>99</u>, 5953.

27. Elroi, H.; Meyerstein, D. *J. Am. Chem. Soc.* 1978, <u>100</u>, 5540.

28. Herrman, W. A. "Organometallic Aspects of the Fischer-Tropsch Synthesis," *Angew. Chem. Int. Ed. Engl.* 1982, <u>21</u>, 117.

29. Tait, A. M.; Hoffman, M. Z.; Hayon, E. *J. Am. Chem. Soc.* 1978, <u>100</u>, 5540.

30. March, J. "Advanced Organic Chemistry: Reactions, Mechanisms, and Structure," McGraw-Hill Series in Advanced Chemistry, 1968.

31. Bakac, A.; Espenson, J. H. *Inorg. Chem.* 1982, <u>21</u>, 0000.

32. Cohen, H.; Meyerstein, D. *Inorg. Chem.* 1974, <u>13</u>, 2434.

33. Ryan, D. A.; Espenson, J. H. *Inorg. Chem.* 1982, <u>21</u>, 527.

34. Farhataziz; Ross, A. B. "Selected Specific Rates of Reactions of Transients from Water in Aqueous Solutions. III. Hydroxyl Radical and Perhydroxyl Radical and Their Radical Ions." National Bureau of Standards Report No. NSRDS, NBS59, 1977.

35. Kochi, J. K.; Rust, F. F. *J. Am. Chem. Soc.* 1961, <u>83</u>, 2017.

36. Espenson, J. H.; Sheveima, J. S. *J. Am. Chem. Soc.* 1973, <u>95</u>, 4469.

37. Heckman, R. A.; Espenson, J. H. *Inorg. Chem.* 1979, <u>18</u>, 38.

38. Hedja, E.; Winstein, S. J. Am. Chem. Soc. 1969, 89, 1661.

39. Kochi, J. K.; Davis, D. D. J. Am. Chem. Soc. 1964, 86, 5264.

40. Schmidt, W.; Swinehart, J. H.; Taube, H. J. Am. Chem. Soc. 1971, 93, 1117.

41. King, W. R., Jr.; Garner, C. S. J. Phys. Chem. 1954, 58, 29.

42. Swinehart, J. H. Inorg. Chem. 1965, 4, 1069.

43. Furman, S. C.; Garner, C. S. J. Am. Chem. Soc. 1950, 72, 1785.

44. Heckman, R. A. Ph.D. Dissertation, Iowa State University, Ames, Iowa, 1978.

45. Tateda, A.; Fritz, J. S. J. Chromatogr. 1978, 152, 329.

46. Espenson, J. H. Inorg. Chem. 1965, 4, 1025.

47. Bakac, A. Unpublished observations, Ames Laboratory, Iowa State University, Ames, Iowa, 1981.

48. Roche, T. S.; Endicott, J. F. Inorg. Chem. 1974, 13, 1575.

49. Redpath, J. L.; Willson, R. L. Int. J. Radiat. Biol. 1973, 23, 51.

50. Schrauzer, G. N.; Windgassen, R. J. J. Am. Chem. Soc. 1967, 89, 1999.

51. Johnson, M. D.; Tobe, M. L.; Wong, L. Y. J. Chem. Soc. A, 1968, 929.

52. Schrauzer, G. N.; Deutsch, E.; Windgassen, R. J. J. Am. Chem. Soc. 1968, 90, 2441.

53. Tackett, S. L.; Collat, J. W.; Abott, J. C. Biochem. 1963, 2, 919.

54. DeVries, B. J. Catal. 1962, 1, 489.

55. Chao, T.-H.; Espenson, J. H. J. Am. Chem. Soc. 1978, 100, 129.

56. Davison, J. M. "Catalysis," Vol. 2, Specialist Report, Chemical Society, 1978.

57. a) Basolo, F.; Hoffman, B. M.; Ibers, J. A. Accounts Chem. Res. 1975, 8, 384. b) Collman, J. P. Accounts Chem. Res. 1976, 10, 265. c) Ochiai, Z. I. "Bioinorganic Chemistry," Allyn and Bacon, Boston, 1977.

58. Lyons, J. E. "Aspects of Homogeneous Catalysis," Vol. 3, Uzo, R. Ed., Reidel, 1977.

59. Vaska, L. Accounts Chem. Res. 1976, 9, 175.

60. Valentine, J. S. Chem. Rev. 1973, 73, 235.

61. Haim, A.; Wilmarth, W. K. J. Am. Chem. Soc. 1961, 83, 509.

62. a) Winfield, M. E.; Bayston, J. H. J. Catalysis, 1964, 3, 123. b) Bayston, J. H.; Beale, R. N.; King, N. K.; Winfield, M. E. Aust. J. Chem. 1963, 16, 954.

63. Savatskii, A. J. General Chem. U.S.S.R. 1974, 44, 1518.

64. King, N. K.; Winfield, M. E. Aust. J. Chem. 1959, 12, 47.

65. Brilkina, T. G.; Shushunov, V. A. "Reactions of Organometallic Compounds with Oxygen and Peroxides." Eng. Ed. Davis, A. G. London, 1969.

66. a) Gianotti, C.; Gaudemer, A.; Fontaine, C. Tetrahedron Lett. 1970, 3209. b) Fontaine, C.; Duong, K. N. V.; Merienne, C.; Gaudemer, A.; Giannotti, C. J. Organomet. Chem. 1972, 38, 167. c) Giannotti, C.; Fontaine, C.; Gaudemer, A. J. Organomet. Chem. 1972, 39, 381. d) Giannotti, C.; Septe, B. J. Organomet. Chem. 1973, 52, C45. e) Merinne, C.; Giannotti, C.; Gaudemer, A. J. Organomet. Chem. 1977, 54, 281. f) Giannotti, C.; Fontaine, C.; Septe, B. J. Organomet. Chem. 1974, 71, 107.

67. a) Chiaroni, A.; Pascard-Billy, C. Bull. Soc. Chim. Fr. 1973, 781. b) Giannotti, C.; Fontaine, C.; Chiaroni, A.; Riche, C. J. Organomet. Chem. 1976, 113, 57.

68. Giannotti, C.; Fontaine, C. J. Organomet. Chem. 1973, 52, C41.

69. Bied-Charreton, C.; Gaudemer, A. Tetrahedron Lett. 1976, 4153.

70. Ryan, D. A.; Espenson, J. H. J. Am. Chem. Soc. 1982, 104, 704.

71. Schrauzer, G. N. Inorg. Synth. XI, 1968, 65.

72. Yamazaki, N.; Hohokabe, Y. Bull. Chem. Soc. Japan 1971, 44, 63.

73. Kasha, M. J. Opt. Soc. Am. 1949, 38, 929.

74. Nishinaga, A.; Nishizana, K.; Nakayama, Y.; Matsuura, T. Tetrahedron Lett. 1977, 85.

75. Ablov , V.; Samus, N. M. Russ. J. Inorg. Chem. 1960, 4, 410.

76. Heckman, R. A.; Espenson, J. H. Inorg. Chem. 1979, 18, 38.

77. Fritz, H. L.; Espenson, J. H.; Williams, D. A.; Molander, G. A. J. Am. Chem. Soc. 1974, 96, 2378.

78. Ablov., V.; Bouykin, B. A.; Samus, N. M. Dokl. Akad. Nauk U.S.S.R. 1965, 163, 635. (Chem. Abstr. 1965, 63, 1582.)

79. a) Williams, H. R.; Mosher, H. S. J. Am. Chem. Soc. 1954, 76, 2984. b) Sekera, V. C.; Marvel, C. S. J. Am. Chem. Soc. 1933, 55, 345.

80. a) Williams, H. R.; Mosher, H. S. J. Am. Chem. Soc. 1954, 76, 2990. b) Medweden, S. S.; Alexejewa, E. N. Ber. 1932, 65B, 133.

81. Hiatt, R. In "Organic Peroxides," Swern, D., Ed.; Wiley Interscience: New York, 1971; Vol. II, Chapter I.

82. Adin, A.; Espenson, J. H. Chem. Commun. 1971, 653.

83. Espenson, J. H.; Chao, T.-H. Inorg. Chem. 1977, 16, 2553.

ACKNOWLEDGMENTS

First of all, my gratitude is due to my major professor, Dr. James H. Espenson, for his guidance and advice throughout the course of this work. His deliberate and diligent attitude toward his work is definitely a successful model which will cause lasting influence in my life. I would also like to appreciate the help of the Analytical Service Group of the Ames Laboratory and the Instrumental Service Group. John J. Richard, Min-Fu Hsu, Michael D. Gaul helped with the GLC analysis.

I am grateful to the members of the research group. Many interesting discussions and unforgettable friendships will remain in my memory. Special thanks are due to Dr. Andreja Bakač for providing many valuable ideas. Brenda Smith has been a great help in typing work.

I am greatly indebted to my parents for their everlasting and un-changeable love. I am especially thankful to my wife, Chieu-Yueh. She has been sharing my life with considerate understanding and encouragement.

At last, my sincere thankfulness and praise are due to God and the Lord Jesus Christ. He is the ultimate source of my life and makes my years in Ames precious.